Elsevier Editorial System(tm) for Lithos
Manuscript Draft

Manuscript Number: LITHOS7846R2

Title: The coupling of high-pressure oceanic and continental units in Alpine Corsica: evidence for syn- exhumation tectonic erosion at the roof of the plate interface.

Article Type: VSI:Subd. Interface

Keywords: Plate interface; Continental subduction; HP-LT oceanic and continental units, Tectonic erosion; Alpine Corsica;

Corresponding Author: Dr. Francesca Meneghini,

Corresponding Author's Institution: University of Pisa

First Author: Maria Di Rosa

Order of Authors: Maria Di Rosa; Francesca Meneghini; Michele Marroni; Chiara Frassi; Luca Pandolfi

Abstract: The subduction of continental crust is now a matter of fact but which are the mechanisms and the factors controlling the exhumation of continental units and their coupling with oceanic units are still a matter of debate. We herein present the tectono-metamorphic study of selected continental units belonging to the Alpine Corsica (Corte area, Central Corsica, France). The tectonic pile in the study area features thin slices of oceanic units (i.e. Schistes Lustrés Complex) tectonically stacked between the continental units (i.e. the Lower Units), which record a pressure-temperature-deformation (P-T-d) evolution related to their burial, down to P-T-peak conditions in the blueschist facies and subsequent exhumation during the Late Cretaceous - Early Oligocene time span. The metamorphic conditions were calculated crossing the results of three different thermobarometers based on the HP-LT metapelites. The continental units only recorded the P-peak conditions of 1.2 GPa-250°C, up to the T-peak conditions of 0.8 GPa-400°C, and the retrograde path up to LP-LT conditions. The metamorphic record of the oceanic units includes part of the prograde path occurring before the peak conditions reached at 1.0 GPa-250°C followed by the last metamorphic event related to LP-LT conditions. The results indicate that each unit experienced a multistage independent pressure-temperature-deformation (P-T-d) evolution and suggest that the oceanic and continental units were coupled during the rising of the last ones at about 10 km of depth, where the oceanic units were stored at the base of the wedge. Subsequently they were deformed together by the last ductile deformation event during exhumation. We propose a mechanism of tectonic erosion at the base of the wedge, by which slices of Schistes Lustrés Complex were removed at the roof of the plate interface during the exhumation of the Lower Units.

ABSTRACT

The subduction of continental crust is now a matter of fact but which are the mechanisms and the factors controlling the exhumation of continental units and their coupling with oceanic units are still a matter of debate. We herein present the tectono-metamorphic study of selected continental units belonging to the Alpine Corsica (Corte area, Central Corsica, France). The tectonic pile in the study area features thin slices of oceanic units (i.e. Schistes Lustrés Complex) tectonically stacked between the continental units (i.e. the Lower Units), which record a pressure–temperature-deformation (P-T-d) evolution related to their burial, down to P-T-peak conditions in the blueschist facies and subsequent exhumation during the Late Cretaceous – Early Oligocene time span. The metamorphic conditions were calculated crossing the results of three different thermobarometers based on the HP-LT metapelites. The continental units only recorded the P-peak conditions of 1.2 GPa-250°C, up to the T-peak conditions of 0.8 GPa-400°C, and the retrograde path up to LP-LT conditions. The metamorphic record of the oceanic units includes part of the prograde path occurring before the peak conditions reached at 1.0 GPa-250°C followed by the last metamorphic event related to LP-LT conditions. The results indicate that each unit experienced a multistage independent pressure–temperature-deformation (P-T-d) evolution and suggest that the oceanic and continental units were coupled during the rising of the last ones at about 10 km of depth, where the oceanic units were stored at the base of the wedge. Subsequently they were deformed together by the last ductile deformation event during exhumation. We propose a mechanism of tectonic erosion at the base of the wedge, by which slices of Schistes Lustrés Complex were removed at the roof of the plate interface during the exhumation of the Lower Units.

***Highlights (for review)**

- Alpine Corsica features intimately associated HP-LT oceanic and continental units

- Exhumation-related mechanical coupling is a, polyphased, possibly punctuated process

- Mechanical coupling promotes tectonic erosion at the roof of the plate interface

The coupling of high-pressure oceanic and continental units in Alpine Corsica: evidence for syn- exhumation tectonic erosion at the roof of the plate interface.

Maria Di Rosa[1,2], Francesca Meneghini[1], Michele Marroni[1,3], Chiara Frassi[1] and Luca Pandolfi[1,3]

[1]*Dipartimento di Scienze della Terra, Università di Pisa, Via Santa Maria 53, 56126 Pisa, Italy.*

[2]*Dipartimento di Scienze della Terra, Università di Firenze, Via La Pira 4, 50121 Firenze, Italy.*

[2]*Istituto di Geoscienze e Georisorse, IGG-CNR, Via Moruzzi, 50124 Pisa, Italy.*

***

CORRESPONDING AUTHOR:
Francesca Meneghini
Dipartimento di Scienze della Terra,
Università di Pisa,
Via Santa Maria 53, 56126 Pisa, Italy.

ABSTRACT

The subduction of continental crust is now a matter of fact but which are the mechanisms and the factors controlling the exhumation of continental units and their coupling with oceanic units are still a matter of debate. We herein present the tectono-metamorphic study of selected continental units belonging to the Alpine Corsica (Corte area, Central Corsica, France). The tectonic pile in the study area features thin slices of oceanic units (i.e. Schistes Lustrés Complex) tectonically stacked between the continental units (i.e. the Lower Units), which record a pressure–temperature-deformation (P-T-d) evolution related to their burial, down to P-T-peak conditions in the blueschist facies and subsequent exhumation during the Late Cretaceous – Early Oligocene time span. The metamorphic conditions were calculated crossing the results of three different thermobarometers based on the HP-LT metapelites. The continental units only recorded the P-peak conditions of 1.2 GPa-250°C, up to the T-peak conditions of 0.8 GPa-400°C, and the retrograde path up to LP-LT conditions. The metamorphic record of the oceanic units includes part of the prograde path occurring before the peak conditions reached at 1.0 GPa-250°C followed by the last metamorphic event related to LP-LT conditions. The results indicate that each unit experienced a multistage independent pressure–temperature-deformation (P-T-d) evolution and suggest that the oceanic and continental units were coupled during the rising of the last ones at about 10 km of depth, where the oceanic units were stored at the base of the wedge. Subsequently they were deformed together by the last ductile deformation event during exhumation. We propose a mechanism of tectonic erosion at the base of the wedge, by which slices of Schistes Lustrés Complex were removed at the roof of the plate interface during the exhumation of the Lower Units.

1. Introduction

Material transfer across the plate interface of subduction margins occurs spatially along an ever-increasing range of pressure-temperature-strain conditions. As recently reviewed by Agard et al. (2018), this mass movement also develops on a wide range of temporal scales, from the short timescales of the seismic cycle, to longer, million year scales as that accounting for the exhumation and return of subducted rocks in fossil orogenic belts. The ability of rock recovery during the long-term evolution of a subduction boundary depends on the entity and distribution of mechanical coupling along the plate interface (i.e. to the ability of slicing of units and the net addition of them to the interface), which is in turn controlled by the nature and structure of the plate interface itself: lithology, topography and age/thermal state of the incoming plate, thickness and rheology of the incoming sedimentary sequence, geometry of the subduction plane, and their evolution with depth are some of the factors that control the long-term mechanical coupling (Agard et al., 2018 and references therein).

The subduction and exhumation of crustal fragments from continental plates is also now commonly accepted as a frequent step in the evolution of convergent margins. Several studies of exhumed HP-LT units, numerical models and review papers, also, indicate that the processes of continental subduction and exhumation can be envisaged as occurring through a multistage evolution of burial, slicing and stacking of units similarly, to what classically described for oceanic units in accretionary prisms, and then exhumed though buoyancy-aided processes (Raimbourg et al., 2007; Yamato et al. 2007; 2008; Li and Gerya, 2009; Beaumont et al., 2009; Guillot et al., 2009; Burov et al., 2012; 2014; Strzerzynski et al., 2012; Agard and Vitale Brovarone, 2013; Vitale Brovarone et al., 2012; Plunder et al., 2015; Di Rosa et al., 2019a).

The impossibility of directly accessing the entire plate interface in active margins impedes unraveling the mechanisms and conditions for subduction and exhumation of continental rocks, so that the study of recovered, high-pressure and low-temperature (HP-LT) rock slices in fossil orogenic belts remains the only way to understand the structure and P-T evolution along the plate interface at resolution ranging from the regional- to the micro-scale.

We report here a tectono-metamorphic study of several, juxtaposed HP-LT units with continental as well as oceanic affinities cropping out at the boundary between Alpine Corsica and the basement of Hercynian Corsica. The detailed structural study coupled with the definition of the P-T-t evolution of the units allowed us to make assumption on the mechanisms of their coupling and exhumation along the plate interface.

2. Tectonic background of Alpine Corsica

Corsica Island is a lithospheric continental fragment bounded westward and eastward by two extensional basins, respectively, the Liguro-Provencal and Tyrrhenian basins (e.g. Gueguen et al., 1998). This fragment bears the remnants of a collisional belt, referred to as Alpine Corsica, that is regarded as the southern branch of the Western Alps with which it shares a common history up to Early Oligocene. This history can be summarized in four main steps (Boccaletti et al., 1971; Durand-Delga, 1984; Jolivet et al. 1990; 1998; Malavieille et al., 1998; Brunet et al., 2000; Marroni et al., 2010; Handy et al., 2010; Malusà et al., 2015): 1) the Middle to Late Jurassic opening of the Ligure-Piemontese oceanic basin between the Europe and Adria margins, 2) its closure by the Upper Cretaceous-Lower Eocene Alpine (east-dipping) subduction, 3) the subsequent Middle Eocene to Lower Oligocene continental collision and, finally, 4) the extensional collapse of the orogenic wedge as a consequence of the back-arc extensional regime generated in the upper-plate of the Apennine (west-dipping) subduction.

As in the Alps, both oceanic and continental units were deformed and metamorphosed during the Upper Cretaceous - Early Oligocene time span to build the actual Alpine Corsica unit stack, that was thrust onto the external domain, here referred as to Hercynian Corsica, and composed of a Variscan basement topped by a Upper Carboniferous-upper Eocene sedimentary cover (Gibbons and Horak, 1984; Lahondére and Guerrot, 1997; Malavieille et al., 1998; Tribuzio and Giacomini, 2002; Molli, 2008; Vitale Brovarone and Herwartz, 2013; Rossetti et al., 2015; Di Rosa et al., 2017a). From Early Oligocene onward, Corsica underwent two major extensional stages, both related to the rollback of the Apennine slab (Gueguen et al., 1998; Chamot-Rooke et al., 1999; Faccenna et al., 2004). The first event is related to the opening of the Liguro-Provençal ocean that in the Early Oligocene isolated the Corso-Sardinian block from the European plate and, consequently, from the active deformation of the Western Alps. The breakup leading to the formation of the Liguro-Provençal oceanic basin whose spreading, that spanned from Aquitanian to Langhian, was coupled to a counterclockwise rotation of around 55° of the Corso-Sardinian block (Gattacceca et al., 2007). The second event consists in the Late Miocene opening of the Tyrrhenian Sea that, in turn, isolated the Corso-Sardinian block from the Adria plate.

The present-day Corsica, then, preserves two different domains, the Alpine and Hercynian Corsica, built during two different orogenies. In Alpine Corsica, the ocean-derived rocks, the so-called Schistes Lustrés Complex, registered a subduction-exhumation cycle with a metamorphic peak dated between 80 Ma and 35 Ma, similar to that reconstructed in the Western Alps (Agard et al., 2002 and references therein). The contact between these units of the Alpine Corsica and the Hercynian Corsica is marked by a stack of slices of highly deformed and metamorphosed units of continental affinity derived from the European margin that is referred to as Lower Units (Bezert and Caby, 1988; Malasoma et al., 2006; Malasoma and Marroni, 2007; Di Rosa et al., 2017a; 2019a) or to as Tenda Massif (Gibbons and Horak, 1984; Jolivet et al., 1990, 1998; Molli et al., 2006; Maggi et al., 2012; Rossetti et al., 2015)

The Lower Units show a polyphase deformation history associated with a metamorphic imprint whose peak occurs in the blueschist facies P/T conditions (Bezert and Caby, 1988; Malasoma et al., 2006; Maggi et al., 2012; Molli et al., 2017; Di Rosa et al., 2019a). The units consist of a Paleozoic basement (i.e. Carboniferous metagranites and their host rock), covered by a Permian meta-volcanosedimentary complex and a Triassic-Jurassic, mainly carbonate, a sequence unconformably covered by metabreccias and siliciclastic metarenites of Eocene age (Durand-Delga, 1984; Rossi et al., 1994; Michard and Martinotti, 2002; Di Rosa et al., 2017b).

The Lower Units stack is bounded at its base by an east-dipping shear zone that is now almost completely reworked by the wide, sinistral strike-slip fault zone system known as the Central Corsica Shear Zone (Maluski et al., 1973; Jourdan, 1988; Waters, 1990; Molli and Tribuzio, 2004; Lacombe and Jolivet, 2005). Where preserved, the primary basal boundary of the Lower Units is represented by a ductile shear zone with a top-to-the-west sense of shear (Di Rosa et al., 2017a; 2017b). The Lower Units are in turn overthrust to the E by the units belonging to the Schistes Lustrés Complex of the Alpine orogenic wedge. The boundary between the Lower Units and the orogenic wedge is an east-dipping shear zone showing a syntectonic metamorphic paragenesis indicating lower P-T conditions than those estimated for the neighboring Lower Units (Di Rosa et al., 2019a). Based on this observation, Di Rosa et al., (2019a) have proposed an interpretation of this shear zone as a ductile normal fault.

3. Materials and methods

The 1:50,000 scale geological maps published by BRGM, France (Rossi et al., 1994) were used as a first cartographic base for the geology of the Corte area objects of this study (modified after Di Rosa et al., 2017b, Di Rosa, 2019). The detailed geologic mapping (scale 1:5000) was coupled with mesoscopic structural analyses that were conducted in the area (Figs. 2-3). Four tectonic units of the Corte area were sampled for a total of seven samples (Figs. 3-4): 4 samples from the middle to upper Eocene metasandstones of the Lower Units (Castiglione-Popolasca Unit: CM22b, and CM29a; Piedigriggio-Prato Unit: CM21 and CM32C, already published in Di Rosa et al., 2017a; 2019b) and 3 samples from the middle Cretaceous (?) calc-schists of different slices of the Schistes Lustrés Complex (CMD121a and CMD121b from IZU-Buttinacce, and CMD118 from IZU-Botro, new data exclusive of this work). On all the samples, a detailed study of the microdeformation history were performed and quantitative compositional maps and spot analyses were acquired in order to estimate the P-T conditions of the four tectonic units using the chlorite-phengite multi-equilibrium thermodynamic technique (Vidal and Parra, 2000). The electron probe micro analysis (EPMA) data have been acquired using a JEOL-JXA 8230 electron microprobe apparatus of the IsTerre (Grenoble, France) equipped with five wavelength-dispersive spectrometers and calibrated with the following standards (Tab. 2): wollastonite (Ca, Si), orthoclase (K), albite (Al), periclase (Mg), rhodonite (Mn), TiO_2 (Ti), Al_2O_3 (Al), Fe_2O_3 (Fe) and Cr_2O_3 (Cr). The operating conditions were 15 keV accelerating voltage, 12 nA sample current and 200 to 300 ms per grid point counting time. Compositional maps and spot analysis were acquired for each sample; the X-ray maps resolution and the analytical spot size were set at 1 μm, as recommended by Lanari et al. (2014b), to detect any zoning in phengites (Fig. 5, Tab. 1). The compositional maps were calibrated with the spot analysis (De Andrade et al., 2006) using XMapTools 2.1.3 software (Lanari et al., 2014b), in order to obtain quantitative maps of oxide (Wt%). Chl and Ph structural formulas were calculated on

14 and 11 anhydrous oxygens, respectively. The chemical analysis of Chl and Ph obtained were processed through three different thermodynamic methods including water (wt) and Qz (i.e. Chl-Qz-wt, Ph-Qz-wt and Chl-Ph-Qz-wt methods) using ChlMicaEqui software (Lanari et al., 2012). These results (Tab. 3) were compared with those obtained through classical thermobarometry. Mineral abbreviations are from Whitney and Evans (2010).

3.1 The chlorite and phengite thermobarometry methods applied in this study

For each sample, we selected the micro-areas where the mutual relationships between all the identified generations of foliations were clearly and unambiguously identified. Among these sites, only those where the generations of foliations are associated to different mineral paragenesis were considered: particularly, the image analysis was performed with XMapTools in order to include any chemical heterogeneities of Chl and Ph within the same foliation and between different foliations (Tab. 2). Through this operation, performed on each of the 7 samples, at least 50 analyses for each mineral phase (Chl and Ph) were selected along each foliation.

The data obtained were processed through three different methods, based on the activity of the chlorite and mica end-members (Mg- and Fe-Ame, Clc, Dph, Sud for chlorite, Mg-Cel, Ms, Prl, Prl(H) and Php for mica) as well as the activity of water: the Chl-Qz-wt, Ph-Qz-wt and Chl-Ph-Qz-wt methods.

The Chl-Qz-wt method (Vidal et al., 2006), is a thermometer based on the equilibria

$$4Clc + 5Fe\text{-}Ame = 4Dph + 5Mg\text{-}Ame$$

$$4Dph + 6Sud = 5Fe\text{-}Ame + 3Mg\text{-}Ame + 14Qz + 8H2O$$

and allows the T range to be calculated with an equilibrium tolerance of 30°C and the percentage of Fe^{3+} for each Chl analysis fixing the pressure value (Lanari and Duesterhoeft, 2019). This method was employed to estimate the temperature conditions of the chlorites grown during different metamorphic phases, at given pressure (in this case was set at 0.8 GPa) and water activity (fixed at 1 unit, see Supplementary materials). This method is based on the convergence of the reactions involving the Chl end-members (Mg- and Fe-Ame, Clc, Dph, Sud), in presence of Qz and water (Vidal et al., 2006). The temperature location depends on the activity of water and the Chl end-members, that is in turn controlled by the Fe^{3+} content; this latter can be estimated following the recommendation of Vidal et al. (2006). T values were considered only when the scatter between T values achieved by the four reactions was less than 30°C.

The Ph-Qz-wt method (Dubacq et al., 2010) is a geobarometer based on the reactions:

$$\mathrm{Prl(H) = Prl + H2O}$$

$$\mathrm{3Mg\text{-}Cel + 2Prl = 2Ms + Phl + 11Qz + 2H2O}$$

where Prl(H) is hydrated Prl. The T range of stability is set on the base of the Chl-Qz-wt method results, as well as the Fe^{3+}, calculating an average of the values obtained with the Chl-Qz-wt method. Thus, the Ph-Qz-wt method allows calculating the P range for each group of Ph at fixed T and Fe^{3+}, with an absolute uncertainty of 0.2 GPa.

The variability of the Ph composition depends on the relative proportion of the end-members Cel, Ms and Prl that is mainly controlled by the activation of Tschermak and Phyrophyllite substitutions (e.g. Guidotti and Sassi, 1998). Each Ph analysis is represented in the P-T path with a line: in this work we considered only the P values corresponding to the T values previously estimated with the Chl-Qz-wt method.

Combining the values obtained from Chl-Qz-wt method with those of the Ph-Qz-wt method, i.e. considering Chl and Ph grown in the same microstructure, the P-T equilibrium conditions were calculated with the Chl-Ph-Qz-wt multi-equilibrium approach (Vidal and Parra, 2000; Vidal et al., 2006; Dubacq et al., 2010) using ChlMicaEqui software (Lanari et al., 2012). Only the couples whose P-T equilibrium shows T conditions similar to those obtained with classical thermometry were considered. On this selected group of P-T equilibrium conditions, an additional equilibrium tolerance was set in order to consider only the P-T values to which is related the minimum Gibbs free energy (i.e. < 1000 J).

The uncertainty associated to the Chl-Ph-Qz-wt multiequilibrium approach is 30°C and 0.2 GPa (Vidal and Parra, 2000).

Classical geothermometers (Cathelinau and Nieva, 1985; Cathelinau, 1988; Lanari et al., 2014a) and the geobarometer of Massonne and Schreyer, (1987) were applied on micro-areas within single Chl and Ph crystals showing homogeneous composition, in order to compare the results obtained with the multi-equilibrium techniques with other methods related to the Al^{IV} and Si contents in Chl and Ph, respectively.

4. The association of oceanic and continental units North of the Corte area

The area around the town of Corte (Figs. 1, 2) exposes a stack of deformed units of both continental and oceanic affinities affected by HP metamorphism. The three continental units ascribable to the Lower Units (i.e. Castiglione-Popolasca, Croce d'Arbitro and Piedigriggio-Prato, hereafter CPU, CDU and PPU, respectively) are made of a Paleozoic basement intruded by the Permo-Carboniferous metagranitoids and covered by a upper Permian-Middle to upper Eocene metasedimentary succession (Rossi et al., 1994). They crop out continuously as north-south elongated units with a lateral extension ranging from ca. 12 km (Castiglione-Popolasca Unit), to about 5 km (Croce d'Arbitro Unit) and ca. 7.5 km (Piedigriggio-Prato Unit), and an estimated average volume of 2-3 km^3: given the polyphase deformation affecting these units, their original thickness is hard to estimate.

The oceanic units of the Schistes Lustrés Complex are exposed through several thin slices whose lateral extension varies from 0.1 km^2 to 0.6 km^2, for an approximate volume ranging from 0.05 to 0.2 km^3. They are made up of Jurassic – middle Cretaceous (?)

ophiolitic-bearing lithotypes such as dominant metabasalts and calc-schists, and rarer metaserpentinites and metagabbros (Durand-Delga, 1984). In the present study, we focused on the slices cropping out around the localities of Buttinacce and Botro (here after referred to as IZU-Buttinacce and IZU-Botro tectonic slices, Figs. 1, 2).

Despite the Schistes Lustrés Complex crops out at the top of the Lower Units everywhere in the Alpine Corsica nappe stack, the Corte area is the only place where thin slices of the Schistes Lustrés Complex are found either sandwiched between the Lower Units or at the base of them along the Lower Units - Hercynian Corsica boundary zone (Figs. 1, 2) Therefore, Corte is a privileged area to reconstruct the pre- and post-coupling evolution of the Lower Units and the slices of the Schistes Lustrés Complex in the context of the evolution of the whole Alpine tectonic stack.

4.1 Map-scale relationships

The area between Buttinacce and Botro (top-east: 42°38’45.35’’N 9°18’91.17’’E, bottom-west: 42°28’56.41”N 9°16’31.42”E) is characterized by a N-S trending stack of metamorphic units belonging to both the Lower Units and the Schistes Lustrés Complex, respectively, that are thrust westward onto the domain of Hercynian Corsica (Fig. 2A and B). Toward the east/southeast, around Botro, this pile of units is separated from the rest of Alpine Corsica (e.g. Caporalino and Santa Lucia Units and other units of the Schistes Lustrés Complex) by the CCSZ (Di Rosa et al., 2017b). The detailed field mapping of the area allows a first order characterization of the progressive deformation experienced by the continental and oceanic units, as well as an estimation of the relative chronology.

The boundaries between the Lower Units, and those juxtaposing the Lower Units and the slices of Schistes Lustrés Complex, are marked by meter-scale ductile shear zones roughly N-S striking, E-dipping and with a top-to-the-west sense of shear (Di Rosa et al., 2017b, Fig. 4C), locally overprinted by later cataclastic deformation.

At map-scale, the ductile deformation in the Lower Units mainly consists of decimeter-scale isoclinal folds with axes plunging less than 35° towards N-NW and S-SE, with E/NE-dipping axial plane foliation. They are confined to each unit and cut by the units-bounding thrusts, as shown by the axial plane trace reported in Fig. 2A and B (see sections 4.2.1 and 4.2.2). In the Schistes Lustrés Complex slices the most dominant structures at mesoscale are isoclinal folds, with N-S trending, sub-horizontal axes. The subsequent folding event visible at map-scale is characterized by open to closed megafolds with an axial plane foliation gently dipping toward the W (Fig.2). The top to W shear zones bounding the mapped units, and responsible for their internal imbrication are all folded by this ductile event, suggesting that it postdates both the deformation described in each group of units as well as the stacking of the Lower Units and their coupling with Schistes Lustrés Complex slices (Fig. 2A and B, see sections 4.2.1 and 4.2.2). The units pile is subsequently reworked by the brittle deformation, the structures of which are all ascribable to the poorly constrained activity of the CCSZ.

In the following section, we describe in details the meso- and micro-scale features of the multiphase deformation events recorded by the oceanic and continental units prior to coupling, the deformation they shared together after coupling, and, for each group of units, we provide a brief description of the samples selected for the structural and petrological study.

4.2 The deformation until the coupling of continental and oceanic units

As introduced above, the oceanic and continental units are both characterized by a multiphase deformation evolution. Both the oceanic and the continental units, during their independent subduction/exhumation paths, registered two ductile deformation phases before the last ductile event that is common to all units. For the seek of clarity, we have named D1 and D2 with the subscript “c” and “o” for the independent deformation path of continental and oceanic units, respectively (see Figs. 3, 4). Then the third deformation event, shared by all units, is referred to as simply D3 (see also Bezert and Caby, 1988; Malasoma et al., 2006; Malasoma and Marroni, 2007; Di Rosa et al., 2017a). As we will show in the following sections, and described already elsewhere in Corsica (Di Rosa et al., 2017a; Di Rosa et al., 2019 a; b), the D1c-o and D2c-o occurred before the stacking of the units, and are therefore interpreted as related to the subduction/exhumation path followed by each single unit at the plate interface, from different depths (i.e. under different P-T conditions, see Di Rosa et al., 2019 a; b).

4.2.1 Deformation fabrics of the continental units

The deformation history recognized in the Lower Units is therefore schematized in the D1c, D2c and D3 phases (Bezert and Caby, 1988; Malasoma et al., 2006; Malasoma and Marroni, 2007; Di Rosa et al., 2017a, Figs. 3, 4).

The D1c phase. In the CPU, CDU and PPU the D1c phase is characterized by rarely preserved isoclinal F1c folds with acute to sub-acute hinges. Rare F1c non-cylindrical folds are observed in CPU and PPU (Fig. 3A-D). The F1c folds are associated with S1c axial plane foliation, occasionally preserved at meso-scale in the F2c hinge zones, where it is crenulated by the S2c foliation (Fig. 3A-D). At microscale, the S1c foliation is a continuous cleavage constituted by a Chl+Ph+Qz+Cal metamorphic assemblage (Fig. 3C-D). well preserved in the metapelites (e.g. in the matrix of the Permian metavolcaniclastics and of the Tertiary metabreccias and metasandstones).

The D2c phase. The D2c phase is characterized by W-verging, close to isoclinal F2c folds with NNE/SSW-trending A2c axes (Fig. 3A-D). F2 folds show typically necked and boudinaged limbs and are associated with a well-developed NNE/SSW-striking S2c foliation that represents the main planar anisotropy at the scale of the outcrop (Fig. 3B). ESE-WNW trending L2c mineral and mineral stretching lineations are widespread everywhere in the Corte area. In the metapelites, the L2c mineral stretching lineation is represented by elongated Chl, Qz and Ph grains, whereas in the metalimestones and in the metadolomites are dominated by boudinaged millimetric Py and Qz grains. At the microscale, the metagranitoids show protomylonitic to ultramylonitic S2c foliation marked by discontinuous lepidoblastic layers of recrystallized Ph, Chl, Bt and granoblastic layers of fine-grained recrystallized Qz, wrapping weakly elongated Fsp grains and Qz grains. Relicts of Qz, characterized by bulging recrystallization and subgrain rotation, are affected by cataclastic flow, and the fractures are filled by Ph, Chl and thin-grained Qz. S2c foliation in metapelites, is a crenulation cleavage characterized by a new generation of Chl+Ph+Qz+Ab+Cal.

Following is a brief description of the selected samples analyzed in this study (see Fig. 1B for sample location).

Sample CM22b (CPU) is a matrix-supported metasandstone. Qz and Ab porphyroclasts ranging in size from 200 µm to 2 mm are immersed in a foliated matrix composed of layers of Qz, Ab and K-Fsp smaller than 30 µm alternated to Chl- and Ph-rich layers. This foliation, ascribable to the D2c deformation phase, is associated with F2c microfolds at the hinge of which are typically preserved relicts of the S1c foliation. The Chl and Ph grown along the S1 foliation are bigger than those aligned along the S2 foliation, despite being always smaller than 200 µm. Zones of localized deformation with mylonitic to ultramylonitic fabric are a common feature of this sample.

Sample CM29a (CPU) is a matrix-supported coarse-grained metasandstone with 200 µm- to 8 mm- sized deformed porphyroclasts of Qz, K-Fsp, Chl and Ab in a fine-grained matrix comparable to that of sample CM22b. The S1c foliation is detectable only as a relict in rare microlithons of the S2c foliation. The S2c foliation is a penetrative foliation marked by a preferred orientation of deformed Qz and Ab porphyroclasts. Particularly, the D2c phase produces high-strained bands with stretched clasts: the measurement of 25 clasts resulted in an average major/minor axis ratio (Rxz) of 13:1 (S.D.=0.055, Dunnet, 1969).

Samples CM21 and CM32c (CPU) are metasandstones with clasts of Qz, Cal, metamorphic rocks (i.e. the Roches Brunes Fm.) and metagranitoids immersed in a pelitic matrix of phyllosilicates, Qz and Ab. Relicts of the D1c phase are preserved within mm-thick metapelites layers in the D2 microlithons. These relicts are represented by a S1c continuous foliation marked by syn-kinematic grown of Chl, Ph, Ab and Qz. The S2c foliation is a continuous and pervasive foliation highlighted by the growth of new Chl, Ph, Ab, K-Fsp and Qz minerals. The S2 represents a composite layering given by the superimposition of the S2 on the S1 foliation. In the F2 hinge zones, the S2 foliation can be instead classified as a crenulation cleavage. The S3 foliation is classifiable as crenulation cleavage, to which no recrystallization is associated.

4.2.2 Deformation fabrics of the oceanic units

As for the Lower Units, the slices of the Schistes Lustrés Complex outcropping in the Corte area also show a polyphase deformation history comprising pre-coupling phases (D1o-D2o phases), and post-coupling D3 deformation (Figs. 3, 4).

The D1o phase. The D1o phase structures at the meso-scale have been completely transposed by the subsequent D2o phase. In the metabasalts the S1o foliation is the main anisotropy defined by layers of Cpx, Pl and Ep, and layers of Pl, Chl and opaque oxides. D1o-related veins filled by Qz affected by grain boundary migration recrystallization are abundant (sample CMD123a’). In the calc-schists, at the microscale, the S1o foliation is superimposed on the primary layering of phyllosilicates, Cal and Qz. Relicts of the S1o foliation can be documented only in the F2o folds hinges, where thin crystals of Chl and Ph are preserved in the microlithons of the S2 foliation (Fig. 3G).

The D2o phase. In the Schistes Lustrés Complex slices the most dominant structures at mesoscale are F2o isoclinal folds, with N-S trending, sub-horizontal A2o axes. They are associated with a pervasive S2o, N-S trending axial plane foliation (Fig. 3E). An L2o mineral lineation is well visible in the calc-schist (Fig. 2B), marked by preferred alignment of synkinematic Cal and Ph.

At the microscale, F2o folds and S2o foliation are well developed in both metabasalts calc-schists (Fig. 3F-H). In the calc-schists, the relations between the S1o and the S2o foliation are well visible within the hinge zones of centimeter-scale F2o folds (Fig. 3G). Locally, in the calc-schists, σ-type porphyroclasts made by Qz aggregates, with asymmetric tales of re-crystallized Qz and/or Ph, together with bookshelf structures in Fsp, suggest a sinixtral, top-to-W sense of shear.

A later foliation arranged at low-angle with respect to the S2o and defined by re-crystallization of a new generation of Chl and Ph, is visible exclusively at microscale (Fig. 3H). This foliation is clearly subsequent to the S2o foliation, but, given the lack of mesoscale evidence of a foliation between the S2o and the S3, this anisotropy has been assigned to the late stages of the D2o phase. In the metabasalts Qz veins are arranged parallel to the S2o foliation, whereas Cal veins are set parallel to this late S2o foliation.

Here again we report a brief description of the selected samples analyzed in this study (see Fig. 1B for sample location).

Samples CMD121a and CMD121b (IZU-Buttinacce) are calc-schists made by a millimeter-scale alternation of granoblastic layers of Qz and lepidoblastic layers of Chl+Ph+Ab+Qz+Cal. This planar anisotropy is a composite S0+S1o+S2o foliation. Only in the hinge zone of the centimetric F2 folds, in which relicts of the S1o foliation are preserved, is possible to distinguish the S1o foliation to the S2o foliation, both characterized by the recrystallization of Chl, Ph, Ab Qz and minor Cal. The late S2o, to which are associated late-F2o microfolds, is accompanied by recrystallization of Chl, Ph and Cal.

Sample CMD118 (IZU-Botro*)* is a calc-schist characterized by Cal-rich layers less than 1 mm thick alternating with thinner lepidoblastic layers of phyllosilicates and Qz. Similarly, to the samples CMD121a and CMD121b, the main foliation is the composite S0+S1o+S2o foliation, made by metamorphic Chl, Ph, Ab, Qz and folded by F3o folds. Opaque oxides oriented along the S2o foliation have been also found. At the thin section scale, the S1o/S2o interference pattern has been rarely observed: if present, relicts of Chl and Ph were observed within the microlithons of the S2o foliation in the F2o hinge zones. The S3o is classifiable as disjunctive cleavage and no recrystallization seems to be associated to it.

4.2.3 The tectonic imbrication of the continental and oceanic units

As said in section 4.1, after the folding events that deformed independently the Lower Units and the slices of Schistes Lustrès Complex, these units are tectonically juxtaposed by N-S trending shear zones bounding the mapped units and responsible for their internal imbrication (see Figs. 2, 3C and 4). The shear zones are characterized by protomylonitic to mylonitic fabric with S-C fabric, σ-type porphyroclast of Fsp and bookshelf structures (with synthetic and antithetic fractures) in Fsp, all indicating a top-to-W sense of shear.

These shear zones cut the axial planes of the F2c and F2o folds (Fig. 2A and B), and are in turn deformed by the following phase, which is traditionally referred in literature as D3 (e.g. Di Rosa et al., 2019a). Therefore, in this paper, we will refer to these shear zones as late-D2.

4.3 The deformation after the coupling between continental and oceanic units

The D3 phase recorded in the Lower Units has the same features of the D3 phase documented in the slices of the Schistes Lustrés Complex. The F3 folds rework the S1 and S2 foliations registered independently by the two groups of units, and they also deform the tectonic contacts between them (Figs. 1, 2 and 4). Therefore, the D3 phase occurred after the coupling of the Lower Units with the slices of the Schistes Lustrés Complex, uniformly deforming the entire stack of units (Di Rosa et a., 2017b), and can be considered as the last ductile event affecting the units.

At the mesoscale, the D3 phase produces F3 open to close, gently inclined to recumbent folds with eastward/southeastward vergence and a NNE-SSW trending S3 axial plane foliation (Fig. 4A-C). A type-3 interference pattern (Ramsay, 1967) describes the relationship with the F2 generation of folds both in the Lower Units and in the slices of the Schistes Lustrés Complex.

Microscale F3 open folds are visible in calc-schists samples (e.g. CMD120), associated with an axial plane S3 disjunctive cleavage marked by recrystallizations of Cal and Qz (Fig. 3D-E). The morphology of the S3 foliation and the sole recrystallization of Cal and Qz suggest development of the D3 phase at shallow structural levels. Microfractures, averagely 300 μm to several mm in thickness, commonly mimic the S3 foliation.

After the D3 phase, the main deformation event affecting Corsica is the brittle deformation related to the activity of the Central Corsica Shear Zone system (i.e. CCSZ, Figs.

1, 2). In the study area CCSZ develops as a km-wide, N-S trending sinistral strike slip fault, associated with sinistral and dextral syntethic, and dextral antythetic strike-slip faults (Di Rosa et al., 2017b).

5. Petrography and phase equilibria

5.1 Mineral chemistry and P-T results

5.1.1 Chlorite

The Chl and Ph thermobarometry of the Lower Units is reconstructed in detail in Di Rosa et al., (2019b). The analyzed samples (CM22b and CM29a from CPU and CM21 and CM32c from PPU) are characterized by different generations of Chl grown along both the S1c and S2c foliations (Di Rosa et al., 2019b). All of them show XMg content ranging between 0.15 and 0.55 and Si content between 2.58 and 3.00 apfu (atom per formula unit, see Fig. 5 and Tab.1); they have a minimum Clc + Dph content of 54 %, with higher values for CM22b (CPU). The Chl along the S1c foliation are distinguishable from those grown along the S2c because of a slightly lower Si content. In addition, the Chl related to the S1 have lower content in Sud, that never reaches the 35 %, and their composition varies between Ame and Clc+Dph (Fig. 5, Tab.1).

In the samples from the slices of Schistes Lustrés Complex analyzed in this paper (CMD118 for IZU-Botro and CMD121a and CMD121b for IZU-Buttinacce), the Chl are arranged on the relicts of the S1o foliation, on the S2o main foliation and on the late S2o foliation, which is set at a low angle to the main one. XMg content varies between 0.43-0.47 in the sample CMD118 and between 0.47-0.55 in the samples CMD121a and CMD121b, without showing appreciable differences among the S1o, S2o and late S2o foliations (Fig. 5, Tab.1). The Si content ranges from 2.53 and 2.98 apfu with higher values for the samples

CMD121a and CMD121b. All the samples are characterized by Clc+Dph end-members proportion between 55 and 90 % (Fig. 5, Tab.1). In the sample CMD118, the S1o foliation contains Chl enriched in Clc+Dph, whereas in the S2o foliation the Ame (main S2o foliation) and Sud (late S2o foliation) contents increase. The samples CMD121a and CMD121b show a more homogeneous composition (Clc+Dph between 65 and 90 %), with small-scale differences between the S1o and the S2o foliations similar to those observed for the sample CMD118 (Fig. 5, Tab.1).

5.1.2 Phengite

For the samples from the Lower Units (CM22b and CM29a for CPU and CM21 and CM32c for PPU), Di Rosa et al., (2019b) report that the Ph are located along the S1c and the S2c foliations and have Si and Al content that vary between 3.20 and 3.80 apfu and between 1.55 and 2.45 apfu, respectively (Fig.5, Tab.1). The end-members proportion is always intermediate between Cel and Ms, with a Prl content always lower than 40 %. The composition of the Ph grown along the S1c shows slightly higher Si content with respect to the S2c-related phases, which are instead characterized by higher Al contents. More in general, small-scale differences show that the composition of the S2c-related Ph is more homogeneous that the composition of those grown along the S1c (Di Rosa et al., 2019b). The end-members composition related to the Ph of the S1c foliation ranges between the Cel and Ms end-members of 25-60 % and 30-65 % respectively. Ph grown along the S2c foliation are instead characterized by an increasing Prl content observable in all the units (Tab.1).

Different generations of Ph have been observed in the samples from slices of the Schistes Lustrés Complex (CMD118 for IZU-Botro and CMD121a and CMD121b for IZU-Buttinacce). Si content varies from 3.15 to 3.53 apfu in all the samples: in this range, the S1o foliation is characterized by an homogeneous Si content of 3.20-3.49 apfu (Fig. 5, Tab.1).

The K-content in the S1o-related Ph is generally higher in sample CMD121a (0.74-0.84 apfu) than in sample CMD118 (0.34-0.92 apfu), but tends to decrease in the Ph related to the late S2o of all the samples (Tab.1). End-member proportions of phengite change in the three samples: CMD118 records only small differences for Cel, slightly increasing in the S2o foliation compared to the S1o foliation, and an increase in Prl content (up to ~30 %) associated to the late S2o foliation (Fig. 5, Tab.1). The Ph of the sample CMD121b have a fairly homogeneous composition (5-20 % Prl, 35-60 % Ms and 35-60 % Cel). In the sample CMD121a the Cel proportion is lower than 40 % in the S1o foliation and higher than 30 % in the S2 foliation; a Prl content between 10 and 25 % characterizes the late S2o (Tab.1).

5.1.3 Estimation of the P-T conditions

For all the samples, each homogeneity of Chl and Ph recognized in the compositional map has been considered, in order to have a dataset in which every different mineral phase is represented by at least 50 wt% analysis (Fig. 6A, C). The results obtained with the Chl-Qz-wt and Ph-Qz-wt methods (listed Tab. 3) allowed the P-T conditions to be identified from chlorite and white-mica local equilibra (Fig. 6B, D).

The Chl-Qz-wt method (Vidal et al., 2006) applied to the selected samples, indicate that chlorite formation temperatures span three different ranges of temperatures (histograms of Fig. 6B, D): in the Lower Units, two of them are related to the mineral phases grown along the S1c foliation and one is related to the S2c foliation; in the Schistes Lustrés Complex the three T ranges correspond to the Chl related to the S1o, S2o and late S2o foliations, respectively. Then, the P conditions have been estimated through the Ph-Qz-wt method (Dubacq et al., 2010) considering only the Ph analysis (in Fig. 6B, D, each colored lines represents one single Ph analyses) contained in the T range defined with the Chl-Qz-wt method. For the metabreccias and metasandstones (Lower Units) the P conditions of the D1c phase have been estimated through the two groups of Ph related to the S1c foliation, and those of the D2c through the single group of Ph related to the S2c foliation, fixing the T conditions at the values calculated with the Chl-Qz-wt method. Similarly, for the calc-schists of the Schistes Lustrés Complex, the P conditions of the D1o phase was estimated through the first generation of Ph grown along the S1o foliation, while those related to the D2o phase have been calculated on the base of the second and third generations of Ph recrystallized along the S2o and the late S2o foliations, respectively.

The P-T estimates obtained with the Chl-Ph-Qz-wt multi-equilibrium approach (Vidal and Parra, 2000) were compared with the T and P ranges defined with the Chl-Qz-wt and Ph-Qz-wt methods (stars and P/T diagrams of Fig. 6B, D). Accordingly, data have confirmed that for all units, the different deformation events where accompanied by a multistage metamorphic history.

Three clusters of data have been recognized within the microstructures of each sample collected from the CPU and PPU Lower Units (Di Rosa et al., 2019b): the first set of data related to the S1c foliation (i.e. firsts Chl-Ph generations) is associated to HP/LT (P-peak), the second data set, still aligned along the S1c foliation (i.e. seconds Chl- Ph generations) is stable at LP/HT (T-peak) and the third set, related to the Chl-Ph couples grown along the S2c foliation (i.e. thirds Chl-Ph generations) is stable at LP/LT conditions. These three P-T conditions are reached at slightly different pressures and temperatures in the two tectonic units (Tab. 3). If we take together these two P and T ranges (samples CM22B and CM29A for CPU and CM21 and CM32C for PPU), the maximum variability of P-T conditions for all the continental units, calculated with the Chl-Ph-Qz-wt multi-equilibrium are (for details see Di Rosa et al., 2019b):

- P-peak (HP/LT) event: 1.22-0.75 GPa/250-330°C for CPU and 1.10-0.75 GPa/200-270°C for PPU;

- T-peak (LP/HT) event: 0.80-0.50 GPa/320-350°C for CPU and at 0.80-0.50 GPa/280-400°C for PPU;

- the LP/LT event: 0.45-0.25 GPa/230-310°C for CPU and 0.45-0.25 GPa/230-300°C, for PPU

Similarly, the Chl-Ph-Qz-wt multi-equilibrium method applied in this study to the samples from the Schistes Lustrés Complex (IZU-Botro and IZU-Buttinacce), allowed identifying 3 clusters representative of 3 different P-T conditions during the D1o, D2o and late-D2o deformation events (Tab. 3):

- D1o phase: the Chl-Ph couples are in equilibrium at mP/Ht conditions of 0.75-0.65 GPa/220-245°C for IZU-Botro (sample CMD118) and 0.70-0.50 GPa/265-310°C for IZU-Buttinacce (widest T and P ranges considering the samples CMD121A and CMD121B);

- D2o phase: the samples reached HP/mT conditions of at 1.00-0.85 GPa/200-250°C for IZU-Botro and at 0.90-0.70 GPa/ 240-300°C for IZU-Buttinacce;

- late-D2o event: the Chl-Ph couples are stable at LP/LT conditions of equilibrium, at 0.60-0.50 GPa/ 150-190°C for IZU-Botro and at 0.60-0.40 GPa/ 140-275°C for IZU-Buttinacce.

Similar T values related to the S1o and to the S2o suggest that the transition between the D1o and the D2o phases occurs in almost isothermic conditions in the studied samples of the Schistes Lustrés Complex.

6. Discussion: evidence for syn-collisional processes

6.1 Critical aspects about the method and related P-T estimates

Thermobarometry showed that the metapelites from the Lower Units and the slices of Schistes Lustrés Complex have recorded contrasted P-T conditions. Particularly, three Chl+Ph+Ab+Qz+wt assemblages were documented on the base of chemical (i.e. chlorite and phengite composition) and microstructural (i.e. the foliation along which the mineral grown) criteria in each group of units. For the Lower Units, two of these paragenesis grew along the S1c foliation, and are related to the P- and T-peak, while a third one, along the S2c foliation, at lower P-T conditions. In the samples from the slices of the Schistes Lustrés Complex, the first paragenesis records the prograde path along the S1o foliation, while the other two parageneses are related to the peak conditions and to the retrograde path (early and late S2o foliations). Partial re-equilibration of the phyllosilicates during a multi-stepped history of deformation and metamorphism cannot be excluded a priori (e.g., Sheffer et al., 2016; Airaghi et al., 2017; Lanari and Duesterhoeft, 2019), but it is not observed in the samples studied for this work.

Every P-T estimate is affected by a relative uncertainty of 0.2 GPa and 30°C that includes the uncertainties of the Chl-Qz-wt and Ph-Qz-wt methods. To give strength to the final data, the local equilibrium of the chlorite-phengite pairs have been tested in all the samples for at least 50 couples grew in each microstructure. Only when the scatter between the data is lower than the uncertainty of each single estimates the local equilibrium was considered as achieved.

Another choice made while processing the data is the water activity settled to 1 unit (see Supplementary materials). Water activity can vary in calcite bearing metapelites and affect the P-T estimates obtained via fluid-buffered equilibria. In this work, applying the Chl-Qz-wt, Ph-Qz-wt and the Chl-Ph-Qz-wt methods, the water activity has been set to 0.8 and 1.0 unit in each calculation in order to catch any differences in the results (see Supplementary materials). Our results show that the scatter between the two sets of calculations (i.e. considering the water activity to 1 and 0.8 unit) is lower than the uncertainty of the methods (0.2 GPa and 30°C) and therefore we present the data with the higher water activity (i.e. 1 unit).

6.2 Structural setting of the coupling between oceanic and continental units

The processes allowing the tectonic coupling of oceanic and continental units during the exhumation of high grade units in the subduction setting have been the object of many studies in the last decade (Brun and Faccenna, 2008; Lapen et al., 2007; Angiboust et al., 2012; Agard and Vitale-Brovarone, 2013; Plunder et al., 2012; 2015). Most of these studies provided a detailed reconstruction of the tectono-metamorphic evolution of the continental and oceanic units to decipher how slices of oceanic units, previously subducted and accreted at the base of the orogenic wedge, are then coupled with the continental units that are rising up within the plate interface.

The structural setting of the Corte area at map scale clearly indicates that the oceanic units of the Schistes Lustrés Complex not only occupy the uppermost structural levels of the Alpine Corsica unit stack, but occur also as fragments tectonically sandwiched between the Lower Units, i.e. the units of continental crust that underwent subduction and slicing within the plate interface (Figs. 2, 4). In addition, the structural analysis at meso- and microscale indicate that the oceanic and continental units experienced a polyphase and independent deformation history before their coupling. This polyphase deformation includes two generations of isoclinal folds (D1c/o and D2c/o) showing axial plane foliations developed during the highest metamorphic conditions: none of these sets of folds (F1c/o and F2c/o) deform the tectonic boundaries between oceanic and continental units. The juxtaposition of continental and oceanic units develops through N-S trending top-to-W shear zones (Fig. 4C and section 4.1). These shear zones truncate the F2c fold structures and are in turn deformed by the F3 folds and the associated S3 foliation: therefore they can be consequently considered as occurring at the late stages of the D2 phase (e.g. Molli et al., 2006; Malasoma and Marroni, 2007; Di Rosa et al., 2017a; 2019b). From a structural point of view, the units coupling is therefore defined by the late stage of the D2 phase. In this picture, we can envision the D3 phase as originated from vertical shortening and folding of preexisting non-horizontal layers during the extensional tectonics due to the collapse of the Alpine orogenic wedge, similarly to what recognized in several areas of the Alpine Corsica as, for instance, in the Tenda Massif (e.g., Jolivet et al., 1998; Molli et al., 2006; Maggi et al., 2012; Rossetti et al., 2015) or in the Corte area (e.g. Malasoma et al., 2006; Di Rosa et al., 2017a; 2019a).

Additional constraints to the coupling processes are provided by the metamorphic study of the oceanic and continental units. For the Lower Units, the Chl-Ph couples grown along the S1c foliation recorded the P-peak and T-peak conditions, whereas the same minerals grown along the S2c foliation are in equilibrium at LP-LT conditions. Since no evidence of older foliations occur, and thus no trace of prograde relicts is preserved, we can assume that the P-T history reconstructed in this study is related to the retrograde path of CPU and PPU, recording a multiphase history of exhumation after the P-peak conditions (Di Rosa et al., 2017a; 2017b; 2019b). Moreover, the estimated P-T paths in the two continental units are different: the different absolute P and T values reached during the D1c phase in the CPU and PPU, allowed Di Rosa et al., (2019b) identifying two different paths during exhumation, isothermic for CPU and warmer for PPU. Given a geobaric gradient for a "normal" crust of 27 MPa/km (Best, 2003) and considering that the lithostatic pressure exerted on the Lower Units is given by metamorphic rocks of both oceanic and continental affinities, we have used an average crustal geobaric gradient of 30 MPa/km for every calculation The P–T estimates related to the P-peak suggest a steady thermal regime of 5-6 °C/km for these units, lower than what suggested by Agard and Vitale-Brovarone (2013) for the continental subduction in Oman and New Caledonia, and for other continental units of Alpine Corsica. The proposed lower thermal regime could better fit the subduction of a continental margin after the underthrusting of an old and cool oceanic lithosphere, below an upper plate dominantly made of a continental crust without arc-related magmatism (Marroni et al., 2010 and references therein).

In the Schistes Lustrés Complex, the P-peak conditions are reached during the D2o phase. The P-T differences between the investigated samples indicates that each oceanic tectonic slice moved along independent paths until the end of the D2o phase. The maximum P-T burial conditions for these oceanic slices span roughly between 6 and 11 °C/km, approximately in the range of the subduction gradient estimated for the Schistes Lustrés in the Western Alps (5-10 °C/km, Agard et al., 2001; Plunder et al., 2012).

On the whole, the P-T data confirm these observations. Oceanic and continental units followed different P-T paths until the end of the D2 phase, when they were coupled along what we have defined the late-D2 N-S trending top-to-W shear zones at ~10 km of depth, before being deformed by the F3 folds during the final stages of exhumation. The reconstructed P-T paths for the subduction evolution of the continental units can be compared to what proposed for other sectors of Alpine Corsica by Agard and Vitale-Brovarone (2013) in their “scenario 3” model of burial and slicing of continental units. In this scenario the authors depict early slicing and continued underthrusting of the continental units with HP conditions reached late in the burial evolution. Most importantly, they suggest that this scenario, might be representative of a mechanical coupling concentrated at the bottom of the upper plate. Similar reconstructions of the evolution of both continental and oceanic units of Alpine Corsica have been proposed in literature by Molli et al. (2006), Molli (2008), Maggi et al. (2012) and Rossetti et al. (2015).

A similar P-T evolution has been observed in the Alps by Berger and Bousquet, (2008), which described exhumation of oceanic units occurring through cold geothermic gradients, while that of the continental units as requiring an increasing in temperature during their retrograde path. In the case of Corsica, in particular, the continental units show between them relevant differences during their exhumation, being subjected to isothermic as well as warm paths.

6.3 Timing of the exhumation for the oceanic and continental units

The convergence between the Europe and Adria plates induced the closure of the Ligure-Piemontese oceanic basin during Upper Cretaceous-Early Eocene that was followed in the Middle to Late Eocene by the continental subduction of the European margin (Schmid et al., 1996; Malavieille et al., 1998; Handy et al., 2010; Malusà et al., 2015; Marroni et al., 2017). Coherently with this picture, a progressive younging trend of the deformation and metamorphism from the oceanic and ocean/continent transition (i.e. the Schistes Lustrés Complex) to the continental margin (i.e. the Lower Units) is expected, in accordance with what proposed in literature (Strerzynski et al., 2012, Lanari et al., 2012; 2014a).

For the Lower Units of the study area, no recent and reliable radiogenic data about the metamorphism are available. The age of the deformation and the related metamorphism can be constrained only by stratigraphic relations between the youngest rocks involved in the deformation and the oldest sediments that unconformably seal the stack of the tectonic units. The depositional age of the youngest deformed rocks is attributed to the Late Eocene (Bartonian) for the occurrence of *Nummulites sp.* in the Metabreccia and Metasandstone Fms. of CPU (Bezert and Caby, 1988). The deposits unconformably found at the top of the stack of the Lower Units are represented by the continental sedimentary succession of the Francardo Basin (Ferrandini et al., 2003), whose base has been assigned to the Burdigalian (Alessandri et al., 1977). Therefore, the progressive, multiphase deformation recorded in the Lower Units can be bracketed between 37.8, i.e. the age of the Metabreccia and Metasandstone Fms., and 20.4 Ma, i.e. the age of the base of the Francardo Basin. More accurate constraints are provided by Rossetti et al. (2015) that have studied the East Tenda Shear Zone located at the eastern side of the Tenda Massif (Fig. 1), an European-derived continental crust slice correlated with the Lower Units (Bezert and Caby, 1988; Malasoma and Marroni, 2007; Di Rosa et al., 2017a). The Rb–Sr geochronological data provided by Rossetti et al. (2015) documented that the deformations related to the continental subduction in Alpine Corsica, including our D1c and D2c phase, occurred during the ~27-32 Ma time span, corresponding to Rupelian (Early Oligocene; Walker et al. 2018). In addition, these authors suggested that the extensional tectonic connected to the orogenic collapse occurred after ~27 Ma, with a final exhumation of the continental units of Alpine Corsica during the Early Miocene (~20-21 Ma). These constraints are in agreement with the $^{40}Ar/^{39}Ar$ dating of the Alpine deformations performed in the Hercynian Corsica by Di Vincenzo et al. (2016). These authors have provided the evidence of the syn-kinematic growth of white micas in the strike-slip shear zones between 37-35 Ma and 33-32 Ma, i.e. in the Late Eocene–Early Oligocene time span.

As for the Lower Units, no radiogenic data are available for the metamorphism of the slices Schistes Lustrés Complex cropping out around Corte. Elsewhere in the Alpine Corsica, the ages of the prograde and retrogarde metamorphism in the oceanic and transitional units span a wide range from Upper Cretaceous (Lahondére and Guerrot, 1997) to Late Eocene (Lahondère, 1996; Brunet et al., 2000; Martin et al., 2011; Vitale Brovarone et al., 2012). For the oceanic units correlated with the Lento Unit (e.g. Levi et al., 2007) i.e. the unit to which the slices of the studied area can be correlated, Vitale Brovarone and Hewartz (2013) provided an age for the peak metamorphism of 37.5 Ma. Considering the time span necessary for the subducted oceanic crust to reach the depths of 33 and 28 km, i.e. the estimated depth of peak metamorphism (e.g. Levi et al. 2007 and this study), the inception of subduction of these units must have occurred before the Middle Eocene.

To summarize, the oceanic units of the study area where already subducted and incorporated in the accretionary wedge in the Late Eocene, when the continental margin, represented by the Lower Units of the study area, was still undeformed and characterized by the foredeep sedimentation of the Bartonian Metabreccia and Metasandstone Fms. (CPU unit). This picture is therefore coherent with the progressive younging trend of the deformation and metamorphism from the oceanic and transitional units to the continental units mentioned above (Strerzynski et al., 2012, Lanari et al., 2012; 2014a), and provides further evidence that the continental and oceanic units of the study area have followed an independent tectono-metamorphic history before their coupling.

6.4 In search for a possible model for the coupling

Even if the exhumation record is incomplete, the available data provide evidence that the continental and oceanic rocks of the study area have been exhumed as tectonic units that have followed an independent tectono-metamorphic history before their mechanical coupling. According to what suggested by several tectono-metamorphic studies and thermo-mechanical modeling, these independent histories have in common a multiphased evolution made of several, distinct deformation phases (Raimbourg et al., 2007; Yamato et al. 2007; 2008; Li and Gerya, 2009; Beaumont et al., 2009; Guillot et al., 2009; Burov et al., 2012; 2014; Strerzynski et al., 2012; Agard and Vitale-Brovarone, 2013; Vitale-Brovarone et al., 2013; Plunder et al., 2015; Di Rosa et al., 2019a; 2019b). The structural data indicate that the coupling has occurred in the late stage of the D2o-c deformation phases, so that after this stage, the two groups of units all share the same deformation history, recorded by the D3 structures which also deform all the previous structures in all units. The P-T data about the metamorphism confirm this observation showing that the oceanic and continental units followed different P-T paths until the end of the D2 phase. All these data indicate that coupling occurred at about 10 km of depth. Afterwards, during post-D3, latest stage of exhumation along the plate interface, a possible brittle re-activation of these shear zones responsible for coupling can be hypothesized on the base of the meso-scale observation. However, not much can be said about these tardive, brittle phases, because of the poor-constrained activity of the CCSZ system in the area.

The mechanical coupling thus produced an association of continental and oceanic units, with the latter located both at the top and tectonically sliced inside the continental units. This evidence indicates that the continental units during their exhumation are able to drag slices of the orogenic wedge that are subsequently displaced upward inside the continental rocks (Fig. 8). Therefore, the tectonic erosion of the orogenic wedge, i.e. the removal of materials at the roof of the plate interface, might be envisioned as an effective process active also during the continental subduction.

The contrasting P-T paths recorded in the Lower Units indicate that the CPU and PPU were exhumed at different metamorphic gradients. Whereas the CPU is characterized by isothermal decompression, the PPU is affected during the exhumation by a warming with a small increase of temperature, not higher than 200°C (Fig. 7). Variable factors may influence the thermal structure of plate interface during the oceanic and continental subduction, including not only the effects of shear heating and radioactive heating but also the thermal conditions of the subducting and the overriding plates as well as the plate convergence rate (e.g. Faccenna et al., 2008; Gerya et al., 2008; Maierová et al., 2012; Syracuse et al., 2010; Warren et al., 2008; Zheng and Chen, 2016). Particularly, Gerya et al. (2008) have proposed possible transient episodes of anomalously high temperature along the plate interface during incipient continental collision. These episodes seem to be primarily controlled by changes in the intensity of viscous and radioactive heating in subducted crustal rocks, and are generally associated with partial melting (Burg and Gerya, 2005). In addition, focused pulses of dehydration during subduction have been proposed in literature as contributing to the rapid heating during the early stages of exhumation within the plate interface (Camacho et al., 2005; John et al., 2012; Dragovic et al., 2015). Therefore, we could postulate the occurrence of transient episodes of anomalously high temperature during the exhumation of the Lower Units, to explain the difference in temperature observed in the exhumation paths of CPU and PPU. A possible explanation to these episodes for the PPU case can derive from the P-T path estimated for this unit, where the warming during the exhumation seems to be connected with a break or a slowing in the exhumation process resulting in a stationing at a depth of ca. 17-25 km.

We could simply comment that in the reported study we see no evidence of the melting described by Burg and Gerya, (2005) because the supposed increase of temperature during the exhumation of the PPU was not so relevant to produce the partial melting of subducted crustal rocks. However, this hypothesis is at present only a speculation and will deserve more attention in future investigations on the subducted continental rocks in Alpine Corsica.

In the proposed model we envision a flow of material that is dragged and translated upward through a mechanism that can be regarded as similar to the basal tectonic erosion, when fragments of the wedge are dragged and translated downward during the oceanic subduction (von Huene and Scholl, 1991; Clift and Vannucchi, 2004; Sallares and Ranero, 2005, see also re-definition by Agard et al., 2018). Analogously to what described for basal erosion, specific weak lithological horizons within the orogenic wedge, characterized by rheological contrasts, can be re-activated as shear zones during exhumation, allowing mass dragging along the plate interface/orogenic wedge boundary. Then, the oceanic fragments detached from the base of the orogenic wedge are subsequently incorporated within the continental units and translated upward along the roof of the plate interface. In their model of burial of continental units suggested for Corsica, Agard and Vitale-Brovarone (2013) propose a correlation between the proposed model and a mechanical coupling (i.e. strain) preferentially concentrated at the base of the upper plate. Accordingly, this could facilitate the possibility of removing previously underplated material from the bottom of the wedge as tectonic slices to be incorporated in the rising continental units. Moreover, if we take into account the large volumes of the studied continental units, compared to the small volumes of the Schistes Lustrés slices, we could speculate, in accordance with what observed and proposed for the continental subduction in W. Turkey (Plunder et al., 2015), and in the Western Alps (Angiboust et al., 2009; Plunder et al., 2012), that the buoyancy-driven exhumation of the large Lower Units units may have contributed to scrapping off the slices of oceanic units on its way up the plate interface.

A similar occurrence of oceanic fragments intimately associated with and deformed within the continental rocks has been described by Molli et al. (2006) at the eastern border of the Tenda Massif. The Tenda Massif is regarded as a fragment of the European continental margin involved into subduction during Middle Eocene. As a consequence, the Tenda Massif is strongly deformed and is affected by HP/LT metamorphism and bounded at its roof by the Schistes Lustrés Complex (Waters, 1990; Daniel et al., 1996; Gueydan et al., 2003; Molli et al., 2006; Maggi et al., 2012). In the area studied by Molli et al. (2006), slices of oceanic rocks are recognized inside the orthogneisses of the Tenda Massif, at the core of strongly non-cylindric recumbent F1 fold developed in association with epidote-blueschist facies metamorphism (peak metamorphism at about 1.0 GPa and 450°C). The oceanic and continental rocks show a common retrograde structural and metamorphic history during exhumation that is recorded by the D2 ductile fabrics described in the Tenda Massif and developed under greenschist facies P-T metamorphic conditions. On the whole, the eastern border of the Tenda Massif provides the evidence that the slices of the orogenic wedge are dragged in a ductile way and exhumed with the continental rocks also at a depth of 30-35 km.

If we integrate the information derived from the study area with those from the Tenda Massif, the mechanical coupling between continental and oceanic rocks seems to be effective at two different depths, i.e. at 30-35 km and at about 10 km, where small volumes of rocks are eroded at the roof of the subduction channel and incorporated within. According to Agard et al. (2009), the buoyant continental crust seems to be exhumed during continental subduction with velocities comparable with those of plate tectonics at mantle depths (1–5 cm/yr) and later decelerates (ca. 1 mm/yr) in the upper crust. As a first approximation, the available data for the Lower Units seems to be coherent with this picture, indicating a mean velocity of ∼ 1 cm/yr for their burial and exhumation.

The presented data are insufficient to assess whether the coupling between continental and oceanic rocks and their basal erosion occur along the entire plate interface, or if they show a punctuated character and/or a connection with large-scale, lithospheric-scale geodynamic events (Agard et al., 2009; Penniston-Dorland et al., 2015). However, we could tentatively favor a more punctuated process, according to several studies of rock recovery from literature, that point to a mechanical coupling effective only at precise depths (for an exhaustive review, see Agard et al., 2018). The hypothesized stationing at ca. 17-25 km of the PPU during exhumation could support this option. Thus, if the exhumation is punctuated, also the coupling between continental and oceanic fragments can be hypothesized as punctuated and connected with main geodynamic events. Assuming a correlation between the D2c phase in the Lower Units with the D2-phase in the Tenda Massif dated by Rossetti et al. (2015), we can constrain the D2c phase between ~27 and 32 Ma. In this time span also the activation of the shear zones that developed in the Lower Units at the late stage of the D2c phase occurred. This age is highly critical for the geodynamics of the Alpine-Apennine system (e.g. Malusà et al., 2015) since it records: 1) the inception of rifting phase leading to the opening of the Ligure-Provençal oceanic basin (e.g. Chamot-Rooke et al., 1999); 2) the slab-break off of the alpine subducted slab (Handy et al., 2010) and 3) development of the strike slip tectonics connected to the indenter of the Adria plate within the Alpine-Apennine collisional system (Marroni et al. 2019). According to Vignaroli et al (2010) and Agard et al. (2002), all these geodynamic events occurred during the switch from syn-to-post-orogenic extensional deformation in the Alpine-Apennine system. A direct link between these geodynamic events with the erosion at the roof of the plate interface and the final exhumation of the continental and oceanic units requires, however, more data to be assessed.

7. Conclusions

The study of the Corte area (Corsica) presented in his work has revealed a complex tectonic setting with intimately associated oceanic and continental units, both affected by HP metamorphism. In this area the oceanic units, belonging to the Schistes Lustrés Complex, not only occupy the uppermost structural levels of the tectonic stack as in the other areas of the Alpine Corsica, but occur also as thin slices tectonically sandwiched between the Lower Units, i.e. the units of European continental margin that underwent to subduction. This area enables studying the mechanisms of coupling between oceanic and continental units during their exhumation along the plate interface in the frame of continental subduction.

The data collected show that the units experienced different tectono-metamorphic histories, occurred at different time, that represent the oceanic (D1o and D2o) and continental (D1c and D2c) subduction stages until their coupling (late D2o and D2c), after which they were deformed together (D3). The tectono-metamorphic study highlighted that (i) each tectonic unit has a different P-T history, which implies that they followed independent exhumation path until their coupling and (ii) the coupling of the tectonic units occurred at about 10 km of depth through top-to-W ductile shear zones and thus in a still compressive tectonic regime.

Considering the different time in which the oceanic and the continental units were exhumed, we provided the evidence that the processes of exhumation of the continental units were able to drag oceanic slices from the orogenic wedge and displace them upward in intimate association with the continental rocks. This picture suggests that the tectonic erosion of the orogenic wedge, i.e. the removal of materials at the roof of the subduction channel, might be an effective process also during the continental subduction. Moreover, if we take into account the large volumes of the studied continental units, compared to the small volumes of the Schistes Lustrés slices, we could speculate that the buoyancy-driven exhumation of the large Lower Units may have contributed to the scrapping off the slices of oceanic units on its way up the plate interface.

Even if the exhumation record is incomplete, all the available data for the continental units from Alpine Corsica tentatively favor a punctuated process, where the mechanical coupling is effective only at specific depths. The possible link between the main geodynamic events of the Alpine-Apennine system with the erosion at the roof of the plate interface and the final exhumation of the continental and oceanic units should be investigated in the future.

ACKNOWLEDGMENTS

We are thankful to the editor Philippe Agard and the reviewers Gianluca Vignaroli and Pierre Lanari for the critical, stimulating and constructive reviews that allowed us to improve this work. Olivier Vidal, Valentina Batanova and Valerie Magnin (IsTerre, Grenoble) are also thanked for the EPMA analysis. This work was possible thanks to the financial support from Italian societies SIMP, SGI, SOGEI and AIV, and the PRA grant from University of Pisa.

REFERENCES CITED

Agard, P., Vitale Brovarone, A., 2013. Thermal regime of continental subduction: the record from exhumed HP-LT terranes (New Caledonia, Oman, Corsica). Tectonophysics 601, 206-215.

Agard, P., Plunder, A., Angiboust, S., Bonnet, G., Ruh, J., 2018. The subduction plate interference: rock record and mechanical coupling (from long to short timescales). Lithos 320-321, 537-566.

Agard, P., Jolivet, L., Goffé, B., 2001. Tectonometamorphic evolution of the Schistes Lustrés complex: implications for the exhumation of HP and UHP rocks in the Western Alps. Bulletin de la Société Géologique de France 175(5), 617-636.

Agard, P., Monié, P., Jolivet, L., Goffé, B., 2002. In situ laser probe 40Ar/39Ar dating of the Schistes Lustrés complex: implications for the exhumation of the Western Alps. Journal of Metamorphic Geology 20, 599-618.

Agard, P., Yamato, P., Jolivet, L., Burov, E., 2009. Exhumation of oceanic blueschists and eclogites in the subduction channel: timing and mechanisms. Earth Science Reviews 92, 53-79.

Airaghi, L., Lanari, P., de Sigoyer, J., Guillot, S., 2017. Microstructural vs compositional preservation and pseudomorphic replacement of muscovite in deformed metapelites from the Longmen Shan (Sichuan, China). Lithos 282-283, 262-280.

Alessandri, J.A., Magné, J., Pilot, M.D., Samuel, E., 1977. Le Miocène de la région de Corte-Francardo. Bulletin Société Sciences Historiques Naturelles Corse 622, 51-54.

Angiboust, S., Agard, P., Jolivet, L., Beyssac, O., 2009. The Zermatt–Saas ophiolite: the largest (60-km wide) and deepest (c. 70–80 km) continuous slice of oceanic lithosphere detached from a subduction zone? Terra Nova 21, 171–180.

Angiboust, S., Wolf, S., Burov, E., Agard, P., Yamato, P., 2012. Effect of fluid circulation on subduction interface tectonic processes: insights from thermo-mechanical numerical modelling. Earth and Planetary Science Letters 357-358, 238-248.

Beaumont, C., Jamieson, R.A., Butler, J.P., Warren, C.J., 2009. Crustal structure: a key constraint on the mechanism of ultra-high-pressure rock exhumation. Earth and Planetary Science Letters 287, 116-129.

Berger, A., Bousquet, R., 2008. Subduction-related metamorphism in the Alps: review of isotopic ages based on petrology and their geodynamic consequences, in: Sigesmund, S., Fugenschuh, B., Froitzheim, N. (Eds.), Tectonic Aspects of the Alpine-Dinaride-Carpathian system. Geological Society, London, Special Publications 298, pp. 117-144.

Best, M.G. 2003. Igneous and metamorphic petrology. Brigham Young University, Blackwell Publishing, 2nd edition, 758 p.

Bezert P., Caby R., 1988. Sur l'age post-bartonien des événements tectonométamorphiques alpins en bordure orientale de la Corse cristalline (Nord de Corte). Bulletin de la Société Géologique de France 4(6), 965-971.

Boccaletti M., Elter P., Guazzone, G., 1971. Plate tectonic models for the development of the western Alps and northern Apennines. Nature 234, 108-111.

Brun, J.P., Faccenna, C., 2008. Exhumation of high-pressure rocks driven by slab rollback. Earth and Planetary Science Letters 272(1), 1-7.

Brunet, C., Monié, P., Jolivet, L., Cadet J.P. 2000. Migration of compression and extension in the Tyrrhenian Sea, insights from 40Ar/39Ar ages on micas along a transect from Corsica to Tuscany. Tectonophysics 321, 127-155.

Burg, J.P., Gerya, T.V., 2005. The role of viscous heating in Barrovian metamorphism of collisional orogens: thermomechanical models and application to the Lepontine Dome in Central Alps. Journal of Metamorphic Geology 23, 75-95.

Burov, E., Francois, T., Yamato, P., Wolf, S., 2012. Mechanisms of continental subduction and exhumation of HP and UHP rocks. Gondwana Research 25, 464-493.

Burov, E., Francois, T., Agard, P., Le Pourhiet, L., Meyer, B., Tirel, C., Lebedev, S., Yamato, P., Brun, J-P., 2014. Rheological and geodynamic controls on the mechanisms of subduction and HP/UHP exhumation of crustal rocks during continental collision: Insights from numerical models. Tectonophysics 631, 212-250.

Camacho, A., Lee, J.K., Hensen, B.J. and Braun, J., 2005. Short-lived orogenic cycles and the eclogitization of cold crust by spasmodic hot fluids. Nature, 435(7046), p.1191.

Cathelineau, M., 1988. Cation site occupancy in chlorites and illites as a function of temperature. Clay Minerals 23, 471-485.

Cathelineau, M., Nieva, D., 1985. A chlorite solid solution geothermometer. The Los Azufres (Mexico) geothermal system. Contributions to Mineralogy and Petrology 91, 235-224.

Chamot-Rooke, N., Gaulier, J.M., Jestin, F., 1999. Constraints on Moho depth and crustal thickness in the Liguro-Provencal basin from a 3D gravity inversion: geodynamic implications, in: Durand, B., Jolivet, L., Horvath, F., Sérranne, M., (Eds.), The Mediterranean basin: Tertiary extenson within the Alpine Orogen. Geological Society, London, Special Publications 156, pp. 37-61.

Clift, P., Vannucchi, P., 2004. Controls on tectonic accretion versus erosion in subduction zones: implications for the origin and recycling of the continental crust. Reviews of Geophysics 42, RG2001.

Daniel, J.M., Jolivet, L., Goffé, B., Poinssot, C., 1996. Crustal-scale strain partitioning: footwall deformation below the Alpine Oligo-Miocene detachment of Corsica. Journal of Structural Geology 18(1), 41–59.

De Andrade, V., Vidal, O., Lewin, E., O'Brien, P., Agard, P., 2006. Quantification of electron microprobe compositional maps of rock thin sections: an optimized method and examples. Journal of metamorphic Geology 24, 655-668.

Di Rosa, M., De Giorgi, A., Marroni, M., Vidal, O., 2017a. Syn-convergence exhumation of continental crust: evidence from structural and metamorphic analysis of the Monte Cecu area, Alpine Corsica (Northern Corsica, France). Geological Journal 52, 919-937.

Di Rosa, M., De Giorgi, A., Marroni, M., Pandolfi, L., 2017b. Geology of the area between Golo and Tavignano Valleys (Central Corsica): a snapshot of the continental metamorphic units of Alpine Corsica. Journal of Maps 13, 644-653.

Di Rosa, M., Meneghini, F., Marroni, M., Hobbs, N., Vidal, O., (2019a). The exhumation of continental crust in collisional belts: insights from the deep structure of Alpine Corsica in the Cima Pedani area. The Journal of Geology (in press).

Di Rosa, M., Frassi, C., Meneghini, F., Marroni, M., Pandolfi, L., De Giorgi, A., (2019b). Tectono-metamorphic evolution in the European continental margin involved in the Alpine subduction: new insights from the Alpine Corsica, France. Comptes Rendus – Geosciences (in press).

Di Vincenzo, G., Grande, A., Prosser, G., Cavazza, W., DeCelles, P.G., 2016. 40Ar/39Ar laser dating of ductile shear zones from central Corsica (France): Evidence of Alpine (middle to late Eocene) syn-burial shearing in Variscan granitoids. Lithos 262, 369-383.

Dragovic, B., Baxter, E.F., Caddick, M.J., 2015. Pulsed dehydratation and garnet growth during subduction revealed by zoned garnet geochronology and thermodynamic modeling, Sifnos, Greece. Earth and Planetary Science Letters 413, 111-122.

Dubacq, B., Vidal, O., De Andrade, V., 2010. Dehydration of dioctahedral aluminous phyllosilicates: thermodynamic modelling and implications for thermobarometric estimates. Contributions to Mineralogy and Petrology 159, 159–174.

Dunnet, D., 1969. A technique of finite strain analysis using particles. Tectonophysics 7, 117-136.

Durand-Delga, M., 1984. Principaux traits de la Corse Alpine et correlations avec les Alpes Ligures. Memorie della Società Geologica Italiana 28, 285-329.

Faccenna, C., Priomallo, C., Crespo-Blanc, L., Jolivet, L., Rossetti, F., 2004. Lateral slab deformation and the origin of Western Mediterranean arcs. Tectonics 23, TC1012.

Ferrandini, J., Gattacceca, J., Ferrandini, M., Deino, A., Janin, M.C., 2003. Chronostratigraphie et paléomagnétisme des dépots oligo-miocènes de Corse: implications géodynamiques pour l’ouverture du bassin liguro-provencal, Bulletin de la Société Géologique de France 174 (4), 357–371.

Gattacceca, J., Deino, A., Rizzo, R., Jones, D.S., Henry, B., Beaudoin, B., Vedeboin, F., 2007. Miocene rotation of Sardinia: new paleomagnetic and geochronological constraints and geodynamic implications. Earth and Planetary Science Letters 258, 359-377.

Gerya, T.V., Perchuk, L.L., Burg J.P., 2008. Transient hot channels: perpetrating and regurgitating ultrahigh-pressure, high temperature crust-mantle associations in collision belts. Lithos 103, 236-256.

Gibbons, W., Horak, J., 1984. Alpine metamorphism of Hercynian hornblende granodiorite beneath the blueschist facies Schistes Lustrés nappe of NE Corsica. Journal of Metamorphic Geology 2, 95-113.

Gueguen, E., Doglioni, C., Fernandez, M., 1998. On the post-25 Ma geodynamic evolution of the western Mediterranean. Tectonophysics 298, 259–269.

Gueydan, F., Leroy, Y.M., Jolivet, L., Agard, P., 2003. Analyses of continental midcrustal strain localization induced by microfaultinf and reactionsoftening. Journal of Geophysical Research 108, 2064-2081.

Guidotti, C.V., Sassi, F.P. 1998. Miscellaneous isomorphus substitution in Na-K white mica: a review, with special emphasis to metamorphic micas. Rendiconti Lincei. Scienze Fisiche e Naturali 9(9), 57-78.

Guillot S., Hattori K., Agard P., Schwartz S., Vidal O., 2009. Exhumation Processes in Oceanic and Continental Subduction Contexts: A Review, in: Lallemand, S., Funiciello, F., (Eds.), Subduction Zone Geodynamics. Springer-Verlag, Berlin, pp. 175-205.

Handy, M.R., Schmid, S.M., Bousquet, R., Kissling, E., Bernoulli, D., 2010. Reconciling plate–tectonic reconstructions of Alpine Tethys with the geological–geophysical record of spreading and subduction in the Alps. Earth Science Reviews 102, 121–158.

John, T., Gussone, N., Podladchikov, Y.Y., Bebout, G.E., Dohmen, R., Halama, R., Klemd, R., Magna, T. and Seitz, H.M., 2012. Volcanic arcs fed by rapid pulsed fluid flow through subducting slabs. Nature Geoscience, 5(7), p.489.Jolivet, L., Dubois, R., Fournier, M., Goffé, B., Michard, A., Jourdan, C., 1990. Ductile extension in alpine Corsica. Geology, 18, 1007-1010.

Jolivet, L., Dubois, R., Fournier, M., Goffé, B., Michard, A., Jourdan, C., 1990. Ductile extension in alpine Corsica. Geology, 18, 1007-1010.

Jolivet, L., Faccenna, C., Goffé, B., Mattei, M., Rossetti, F., Brunet, C., Parra, T., 1998. Midcrustal shear zones in postorogenic extension: example from the northern Tyrrhenian Sea. Journal of Geophysical Research: Solid Earth, 103, 12123-12160.

Jourdan, C., 1988. Balagne orientale et massif du Tenda (Corse septentrionale): etude structural, interpretation des accidents et des deformation reconstructions géodynamiques. Ph.D. thesis, Paris, Université Paris-Sud.

Lacombe, O., Jolivet, L., 2005. Structural and kinematic relationships between Corsica and the Pyrenees–Provence domain at the time of the Pyrenean orogeny. Tectonics 24, TC1003. doi:10.1029/2004TC001673.

Lahondère, D., Guerrot, C., 1997. Datation Sm-Nd du métamorphisme éclogitique en Corse alpine: un argument pour l'existence au Crétacé supérieur d'une zone de subduction active localisée sous le bloc corso-sarde. Géologie de la France 3, 3-11.

Lahondère, D., 1996. Les schistes blues et les éclogites à lawsonite des unités continentals et océanique de la Corse alpine: Nouvelles donnée pétrologique et structurales (Corse). Documents du BRGM, 240.

Lanari, P., Duesterhoeft, E., 2019. Modeling Metamorphic Rocks using Equilibrium Thermodynamics and Internally Consistent Databases: Past Achievements, Problems and Perspectives. Journal of Petrology 60, 19-56.

Lanari, P., 2012. Micro-cartgraphie P-T-‘d’ dans les roches métamorphiques. Applications aux Alpes et à l’Himalaya. Thèse de doctorat Sciences de la Terre, Université de Grenoble.

Lanari, P., Wagner, T., Vidal, O., 2014a. A thermodynamic model for di-trioctahedral chlorite from experimental and natural data in the system MgO-FeO-Al2O3-SiO2-H2O: applications to P-T sections and geothermometry. Contributions to Mineralogy and Petrology 167. doi:10.1007/s00410-014-0968-8.

Lanari, P., Vidal, O., De Andrade, V., Dubacq, B., Lewin, E., Grosch, E., Schwartz, S., 2014b. XMAPTOOLS: a MATLAB c -based program for electron microprobe X-ray image processing and geothermobarometry. Computers and Geosciences 62, 227-240.

Lapen, T.J., Johnson, C.M., Baumgartner, L.P., Dal Piaz, G.V., Skora, S., Beard, B., 2007. Coupling of oceanic and continental crust during Eocene eclogite-facies metamorphism: evidence from Monte Rosa nappe, Western Alps. Contributions to Mineralogy and Petrology 153, 139-157.

Levi, N., Malasoma, A., Marroni, M., Pandolfi, L., Paperini, M., 2007. Tectono-metamorphic history of the ophiolitic Lento unit (northern Corsica): evidences for the complexity of accretion-exhumation processes in a fossil subduction system. Geodinamica Acta 20(1), 99-118.

Li, Z., Gerya, T.V., 2009. Polyphase formation and exhumation of HP-UHP rocks in continental subduction zone: numerical modelling and application to the Sulu UHP terrane in eastern Cina. Journal of Geophysical Research 114, B09406.

Maggi, M., Rossetti, F., Corfu, F., Theye, T., Andersen, T.B., Faccenna, C., 2012. Clinopyroxene-rutile phyllonites from East Tenda Shear Zone (Alpine Corsica, France): pressure-temperature-time constraints to the Alpine reworking of Variscan Corsica. Journal of the Geological Society of London 169, 723–732.

Maierová, P., Schulmann, K., Lexa, O., Guillot, S., Štípská, P., Janoušek, V. and Čadek, O., 2016. European Variscan orogenic evolution as an analogue of Tibetan- Himalayan orogen: Insights from petrology and numerical modeling. Tectonics, 35(7), pp.1760-1780.

Malasoma, A., Marroni, M., 2007. HP/LT metamorphism in the Volparone Breccia (Northern Corsica, France): evidence for involvement of the Europe/Corsica continental margin in the Alpine subduction zone. Journal of Metamorphic Geology 25, 529-545.

Malasoma, A., Marroni, M., Musumeci, G., Pandolfi, L., 2006. High pressure mineral assemblage in granitic rocks from continental units, Alpine Corsica, France. Geological Journal 41, 49-59.

Malavieille, J., Chemenda, A., Larroque, C., 1998. Evolutionary model for the Alpine Corsica: mechanism for ophiolite emplacement and exhumation of high-pressure rocks. Terra Nova 10, 317–322.

Malusà, M.G., Faccenna, C., Baldwin, S.L., Fitzgerald, P.G., Rossetti, F., Balestrieri, M.L., Danisik., M., Ellero, A., Ottria, G., Piromallo, C., 2015. Contrasting styles of (U)HP rock exhumation along the Cenozoic Adria-europe plate boundary (Western Alps, Calabria, Corsica). Geochemistry, Geophysics, Geosystems 16, 1786-1824.

Maluski, H., Mattauer, M., Matte, P.H., 1973. Sur la presence de decrochement alpins en Corse: Comptes Rendue de l'Académie Science 276, 709-712.

Marroni, M., Meneghini, F., Pandolfi, L., Hobbs, N., Luvisi, E., 2019. The Ottone-Levanto Line of Eastern Liguria (Italy) uncovered: a Late Eocene-Early Oligocene snapshot of Northern Apennine geodynamics at the Alps/Apennines Junction. Episodes (In press)

Marroni, M., Meneghini, F., Pandolfi, L., 2010. Anatomy of the Ligure-Piemontese subduction system: evidence from Late Cretaceous-Middle Eocene convergent margin deposits from Northern Apennines (Italy). International Geological Reviews 10-12, 1160-1192.

Marroni, M., Meneghini, F., Pandolfi, L., 2017. A revised subduction inception model to explain the Late Cretaceous, double-vergent orogen in the pre-collisional Western Tethys: evidence from the Northern Apennines. Tectonics 36, 2227-2249.

Martin, A.J., Rubatto, D., Vitale Brovarone, A., Hermann, J., 2011. Late Eocene lawsonite-eclogite facies metasomatism of a granulite sliver associated to ophiolites in Alpine Corsica. Lithos 125, 620-640.

Massonne, H.J., Schreyer, W., 1987. Phengite geobarometry based on the limiting assemblage with K-feldspar, phlogopite, and quartz. Contributions to Mineralogy and Petrology 96, 212–224.

Michard, A., Martinotti, G., 2002. The Eocene unconformity of the Brianconnais domain in the French-Italian Alps, revisited (Marguareis massif, Cuneo); a hint for a Late Cretaceous-Middle Eocene frontal bulge setting. Geodinamica Acta 15, 289-301.

Molli, G., Tribuzio, R., 2004. Shear zones and metamorphic signature of subducted continental crust as tracers of the evolution of the Corsica/Northern Apennine orogenic system, in: Alsop, G.I., Holdsworth, R.E., McCaffrey, K.J.W., Handy, M., (Eds.) Flow processes in faults and shear zones. Geological Society, London, Special Publications 224, pp. 321-335.

Molli, G., Tribuzio, R., Marquer, D., 2006. Deformation and metamorphism at the eastern border of Tenda Massif (NE Corsica): a record of subduction and exhumation of continental crust. Journal of Structural Geology 28, 1748–1766.

Molli, G., Menegon, L., Malasoma, A., 2017. Switching deformation mode and mechanisms during subduction of continental crust: a case study from Alpine Corsica. Solid Earth Discussions doi:10.5194/se-2017-11.

Molli, G., 2008. Northern Apennine-Corsica orogenic system: an updated overview, in: Siegesmund S., Fugenschuh B., Froitzheim N., (Eds.), Tectonic Aspects of the Alpine-Dinaride-Carpathian System, Geological Society, London, Special Publications 298, 413–442.

Penniston-Dorland, S.C., Kohn, M.J., Manning, C.E., 2015. The global range of subduction zone thermal structures from exhumed blueschists and eclogites: rocks are hotter than models. Earth and Planetary Science Letters 428, 243-254.

Plunder, A., Agard, P., Dubacq, B., Chopin, C., Bellanger, M., 2012. How continuous and precise is the record of P-T paths? Insights from combined thermobarometry and thermodynamic modelling into subduction dynamics (Schistes Lustrés, Western Alps). Journal of Metamorphic Geology 30(3), 323-346.

Plunder, A., Agard, P., Chopin, C., Pourteau, A., Okay, A.I., 2015. Accretion, underplating and exhumation along subduction interface: from subduction initiation to continental subuction (Tavsanli zone, W Turkey). Lithos 226, 233-254.

Raimbourg, H., Jolivet, L., Leroy, Y., 2007. Consequences of progressive eclogitization on crustal exhumation, a mechanical study. Geophysical Journal International 168, 379-401.

Ramsay, J.G., 1967. Folding and fracturing of rocks. New York: McGraw-Hill.

Rossetti, F., Glodny, J., Theye, T., Maggi, M., 2015. Pressure temperature deformation-time of the ductile Alpine shearing in Corsica from orogenic construction to collapse. Lithos 218-219, 99-116.

Rossi, P., Durand-Delga, M., Caron, J.M., Guieu, G., Conchon, O., Libourel, G., Loye-Pilot, M., 1994. Carte Geologique de la France (1/50,000), feuille Corte (1110). BRGM, Orléans.

Sallares, V., Ranero, C.R., 2005. Structure and tectonics of the erosional convergent margin of Antofagasta, north Chile (23°30’S). Journal of Geophysical Research 110, B06101.

Schmid, S.M., Pfiffner, O.A., Froitzheim, N., Schönborn, G., Kissling, E., 1996. Geophysical–geological transect and tectonic evolution of the Swiss–Italian Alps. Tectonics 15(5), 1036–1064.

Sheffer, C., Vanderhaeghe, O., Lanari, P., Tarantola, A., Ponthus, L., Photiades, A., France, L., 2016. Syn- to post-orogenic exhumation of metamorphic nappes: Structure and thermobarometry of the western Attic-Cycladic metamorphic complex (Lavrion, Greece). Journal of Geodynamics 96, 174-193.

Strzerzynski, P., Guillot, S., Leloup, P.H., Arnaud, N., Vidal, O., Ledru, P., Corrioux, G., Darmendrail, X., 2012. Tectono-metamorphic evolution of Brianconnains zone (Modane-

Aussois and Southern Vanoise units, Lyon Turin transect, Western Alps). Journal of Geodynamics 56-57, 55-75.

Syracuse, E.M., van Keken, P.E. and Abers, G.A., 2010. The global range of subduction zone thermal models. Physics of the Earth and Planetary Interiors, 183(1-2), pp.73-90.

Tribuzio, R., Giacomini, F., 2002. Blueschist facies metamorphism of peralkaline rhyolites from Tenda crystalline massif (northern Corsica): evidence for involvement in the Alpine subduction event? Journal of Metamorphic Geology 20, 513-526.

Trincal, V., Lanari, P., 2016. Evidence of Al-free di-trioctahedral substitution in chlorite and a ferri-sudoite end-member. Clay Minerals 51, 675-689.

Vidal, O., Parra, T., 2000. Exhumation paths of high-pressure metapelites obtained from local equilibria for chlorite–phengite assemblage. Geological Journal 35, 139–161.

Vidal, O., De Andrade, V., Lewin, E., Munoz, M., Parra, T., Pascarelli, S., 2006. P–T-deformation-Fe2+/Fe3+ mapping at the thin section scale and comparison with XANES mapping: application to a garnet-bearing metapelite from the Sambagawa metamorphic belt (Japan). Journal of Metamorphic Geology 24, 669-683.

Vignaroli, G., Rossetti, F., Rubatto, D., Theye, T., Lisker, F., Phillips, D., 2010. Pressure-temperature-deformation-time (P-T-d-t) exhumation history of the Voltri Massif HP complex, Ligurian Alps, Italy. Tectonics 29(6), TC6009.

Vitale Brovarone, A., Herwartz, D., 2013. Timing of HP metamorphism in the Schistes Lustrés of Alpine Corsica: new Lu-Hf garnet and lawsonite ages. Lithos 172-173, 175–191.

Vitale Brovarone, A., Beyssac, O., Malavieille, J., Molli, G., Beltrando, M., Compagnoni, R., 2012. Stacking and metamorphism of continuous segments of subducted lithosphere in a high-pressure wedge: The example of Alpine Corsica (France). Earth Science Reviews 116, 35-56.

von Huene R, Scholl DW., 1991. Observations at convergent margins concerning sediment subduction, subduction erosion, and the growth of continental crust. Review of Geophysics 29, 279–316.

Walker, J.D., Geissman, J.W., Bowring, S.A., and Babcock, L.E., compilers, 2018, Geologic Time Scale v. 5.0: Geological Society of America, https://doi.org/10.1130/2018.CTS005R3C.

Warren, C.J., Beaumont, C., Jamieson, R.A., 2008. Modelling tectonic styles and ultra-high pressure (UHP) rock exhumation during the transition from oceanic subduction to continental collision. Earth and Planetary Science Letters 267, 129-145.

Waters, C.N., 1990. The Cenozoic tectonic evolution of Alpine Corsica. Journal of Geological Society of London 147, 811-824.

Whitney, D. L., Evans, B. W., 2010. Abbreviations for names of rock-forming minerals. American Mineralogist 95, 185-187.

Yamato, P., Agard, P., Burov, E., Le Pourhiet, L., Jolivet, L., Tiberi, C., 2007. Burial and exhumation in a subducting wedge: mutual constraints from thermomechanical modeling and natural P-T-t data (Sch.Lustrés, W. Alps). Journal of Geophysical Research 112, B07410.

Yamato, P., Burov, E., Agard, P., Le Pourhiet, L., Jolivet, L., 2008. HP-UHP exhumation during slow continental subduction: self-consistent thermodynamically and thermomechanically coupled model with application to the Western Alps. Earth and Planetary Science Letters 271, 63-74.

Zheng, Y., Chen, R., Xu, Z. and Zhang, S., 2016. The transport of water in subduction zones. Science China Earth Sciences, 59(4), pp.651-682.

FIGURE CAPTIONS

Figure 1. (A) Tectonic map of the north-eastern Corsica (modified after Vitale Brovarone et al., 2012) and schematic cross section (not to scale, after Di Rosa et al., 2017a). QtD: Quaternary deposits, SfB: Saint-Florent Basin, FcB: Francardo Basin, AlP: Aleria Plain, MaU: Macinaggio Unit, BoU: Bas-Ostriconi Unit, BaU: Balagne Unit, NeU: Nebbio Unit, SpU: Serra Debbione and Pineto Units, SlU: Santa Lucia Unit, CsU: Castagniccia Unit, MfU: Morteda-Farinole-Volpajola Unit, SoU: Serra di Pigno and Oletta Units, IZU: Inzecca and Lento Units, BrU: Bagliacone-Riventosa Unit, CeU: Centuri Unit, TeM: Tenda Massif, AnU: Annunciata Unit, EcU: External Continental Units, PdU: Cima Pedani Units, CoU: Caporalino Unit, HcY: Hercynian Corsica; the position of the Fig. 1B is marked in blue. (B) Tectonic sketch of the study area; the positions of the Fig. 2A, B are marked in black.

Figure 2. Geological map, cross section and stereographic projections of (A) Buttinacce (modified after Di Rosa et al., 2017b) and (B) IZU- Botro, where the relationships between the continental and oceanic units are highlighted. In the stereographic projections related to the D3 phase different colours are used for the data measured in the Lower Units (A3: blue, S3: red) and in the Schistes Lustrés Complex (A3: green; S3: yellow), to highlight that this deformation event affected uniformly the entire stack of units

Figure 3. D1-D2 phases (A-E) in the continental units and (F-H) in the oceanic units. (A) F1c sheath fold in the Metasandstone Fm., Piedigriggio-Prato Unit. (B) F2c isoclinal folds and related S2c axial plane foliation, Detritic Metalimestone Fm., Piedigriggio-Prato Unit. (C) S-C fabric in the Detritic Metalimestone Fm. in the Lower Units (CPU). (D) Relict of chlorite crystal grown during the D1c phase in the Metasandstone Fm., Castiglione-Popolasca Unit

(sample CM29A, parallel nicols); the S1c foliation is also shown. (E) S1c-S2c foliations interference pattern in the Metasandstone Fm., Castiglione-Popolasca Unit (sample CM29A, crossed nicols). (F) F2o subisoclinal folds in the calc-schists, Inzecca Unit; a subtle S3 foliation is also shown. (G) Relicts of S1o foliation within the S2o foliation in a pelitic layer in the calc-schists, Inzecca Unit (sample CMD121A, parallel nicols); the late S2o foliation is also shown. (H) Subgrain rotation (SR) recrystallization parallel to the S2 foliation in the F2o hinges zones, quartz veins in metabasalts, Inzecca Unit (sample CMD123A', crossed nicols).

Figure 4. Map-, meso and microphotographs of the D3 phase. (A) Landscape of Pietra Piana (NE of Monte Cecu): a slice of the Schistes Lustrés Complex (IZU) is sandwiched between the Lower Units (two subunits of PPU). Both the tectonic contacts are folded by the D3 phase. (B) Folded tectonic contact between the Lower Units (PPU) and the Schistes Lustrés Complex (IZU) in San Quilico hill, NE of Monte Cecu; the contact is cut by two post-D3 faults (CCSZ). (C) S2c-S3 foliations interference pattern in the Metasandstone Fm., PPU (sample CM23B, parallel nicols).

Figure 5. Binary and ternary diagrams showing the compositions of the Chl and Ph of the samples studied. The position of each colored rhombus in the diagrams is that of the average value calculated on 15 spot analysis. The position of the DT (di-trioctahedral) and TK (Tschermak) substitutions in the Al/Si diagram are calculated by Trincal and Lanari, 2016. Blue spots in the small ternary diagrams indicate the distribution of all the spot analysis acquired from the compositional map. Yellow triangles and DT and TK substitutions reported in the ternary diagrams are taken from Vidal and Parra, 2000.

Figure 6. Chemical analysis, compositional maps and the results of the analytical methods employed (Chl-Qz-wt, Ph-Qz-wt and Chl-Ph-Qz-wt multiequilibrium methods) for the study of the sample CM22B related to the Lower Units (A-B) and the sample CM121B related to the Schistes Lustrés Complex (C-D). In the binary plots and in the compositional maps (Si- and Al-content for Ph, Mg- and Al-content for Chl) of the samples (A) CM22B and (C) CMD121B, the Chl and the Ph types discussed in the text are noted by black arrows. The colored boxes in the P/T diagram represent the P-T equilibrium stability of the Chl-Ph couples (in (B): Early D1c, Late D1c and D2c; in (D): D1o, D2o and late D2o), tracked using the results of the Chl-Qz-wt method of Vidal et al., 2006 (histograms) and of the Ph-Qz-wt method of Dubacq et al., 2010 (blue, red and yellow lines). Black circles along the colored lines indicate the activity of the water (aH_2O). Stars indicate the P-T equilibria conditions of a single representative Chl-Ph couple (blue star for the early D1c and D1o, red star for the late D1c and D2o and yellow star for the D2c and late D2o) estimated with the Chl-Ph-Qz-wt multiequilibrium approach (Vidal and Parra, 2000). Details about the reactions related to these Chl-Ph couples are reported in the small P-T diagrams.

Figure 7. P-T paths of the samples studied. Colored boxes indicate the P-T ranges calculated with the Chl-Qz-wt and Ph-Qz-wt methods (average ranges were calculated in the case of more than one sample for the same unit). The paths (colored arrows) were drawn considering the best fit between the boxes and the P-T estimates obtained with the Chl-Ph-Qz-wt multiequilibrium method (average values were considered in the case of more than one sample for the same unit).

Figure 8. 2D sketch (not to scale) of a snapshot of the Corsica system at Late Eocene/Lower Oligocene time, showing the model proposed in this work for the mechanical coupling of the

Lower Units with the Schistes Lustrés Complex in the Corte area. In the main sketch the position the blue box evidences the position of the Lower Units as well as the Tenda massif at the plate interface; thick white and thin black arrows represent the last extensional event, thick black arrows indicate the kinematics at the boundaries of the plate interface and the blue box indicates the position of the zoom. The zoom shows a schematic representation of the path (i.e. the dotted orange line) made by the Lower Units at the plate interface and the geometry of the zone of mechanical coupling between the Lower Units and the slices of the Schistes Lustrés Complex (in the dotted box); black arrow indicates the subduction of the European crust. In the PT path, the three thick arrows represent three different stages of the unit deformation. Blue arrow indicates the underplating of the Lower Units up to the p-peak (i.e. early D1c). Green arrow indicates the first stage of exhumation from the early D1c phase to the D2c phase. During a later stage of exhumation (i.e. the late D2c phase), top-to-W shear zones are activated within the plate interface and along the roof decollement and produced the basal erosion of the Schistes Lustrés Complex that is exhumed as thin slices together with the Lower Units (yellow arrow). At the end of the D2 phase the Lower Units are located at the base of the Schistes Lustrés Complex (the tectonic contact is indicated by a thick black line in the zoom). The last stage of exhumation deformed this unit pile in an extensional regime (i.e. the D3 phase). In the PT diagram, the path of CPU (orange), PPU (red), IZU-Botro (green) and IZU-Buttinacce (blue) is drown (simplified version of Fig. 7).

Tab. 1 Chemical ranges and end-members proportions of Chl and Ph related to each metamorphic assemblage.

Tab. 2 Representative electron microprobe analysis of the Chl-Ph pairs selected in the samples of metapelites.

Tab. 3 P-T estimates for the three generations of Chl-Ph pairs in the 5 studied units. P-T estimates of CPU and PPU are after Di Rosa et al. (2019a). The results (Chl-Ph 1^{st}, 2^{nd} and 3^{rd} generation) obtained with the Chl-Ph-Qz-wt multiequilibrium approach (Vidal and Parra, 2000) are compared with those calculated with the Chl-Qz-wt (Vidal et al., 2006) and Ph-Qz-wt (Dubacq et al., 2010) methods (T and P range, respectively) and with classical geothermometers and geobarometers (P and T max).

The coupling of high-pressure oceanic and continental units in Alpine Corsica: evidence for syn- exhumation tectonic erosion at the roof of the plate interface.

Maria Di Rosa[1,2], Francesca Meneghini[1], Michele Marroni[1,3], Chiara Frassi[1] and Luca Pandolfi[1,3]

[1]*Dipartimento di Scienze della Terra, Università di Pisa, Via Santa Maria 53, 56126 Pisa, Italy.*

[2]*Dipartimento di Scienze della Terra, Università di Firenze, Via La Pira 4, 50121 Firenze, Italy.*

[2]*Istituto di Geoscienze e Georisorse, IGG-CNR, Via Moruzzi, 50124 Pisa, Italy.*

***

CORRESPONDING AUTHOR:

Francesca Meneghini

Dipartimento di Scienze della Terra,

Università di Pisa,

Via Santa Maria 53, 56126 Pisa, Italy.

ABSTRACT

The subduction of continental crust is now a matter of fact but which are the mechanisms and the factors controlling the exhumation of continental units and their coupling with oceanic units are still a matter of debate. We herein present the tectono-metamorphic study of selected continental units belonging to the Alpine Corsica (Corte area, Central Corsica, France). The tectonic pile in the study area features thin slices of oceanic units (i.e. Schistes Lustrés Complex) tectonically stacked between the continental units (i.e. the Lower Units), which record a pressure–temperature-deformation (P-T-d) evolution related to their burial, down to P-T-peak conditions in the blueschist facies and subsequent exhumation during the Late Cretaceous – Early Oligocene time span. The metamorphic conditions were calculated crossing the results of three different thermobarometers based on the HP-LT metapelites. The continental units only recorded the P-peak conditions of 1.2 GPa-250°C, up to the T-peak conditions of 0.8 GPa-400°C, and the retrograde path up to LP-LT conditions. The metamorphic record of the oceanic units includes part of the prograde path occurring before the peak conditions reached at 1.0 GPa-250°C followed by the last metamorphic event related to LP-LT conditions. The results indicate that each unit experienced a multistage independent pressure–temperature-deformation (P-T-d) evolution and suggest that the oceanic and continental units were coupled during the rising of the last ones at about 10 km of depth, where the oceanic units were stored at the base of the wedge. Subsequently they were deformed together by the last ductile deformation event during exhumation. We propose a mechanism of tectonic erosion at the base of the wedge, by which slices of Schistes Lustrés Complex were removed at the roof of the plate interface during the exhumation of the Lower Units.

1. Introduction

Material transfer across the plate interface of subduction margins occurs spatially along an ever-increasing range of pressure-temperature-strain conditions. As recently reviewed by Agard et al. (2018), this mass movement also develops on a wide range of temporal scales, from the short timescales of the seismic cycle, to longer, million year scales as that accounting for the exhumation and return of subducted rocks in fossil orogenic belts. The ability of rock recovery during the long-term evolution of a subduction boundary depends on the entity and distribution of mechanical coupling along the plate interface (i.e. to the ability of slicing of units and the net addition of them to the interface), which is in turn controlled by the nature and structure of the plate interface itself: lithology, topography and age/thermal state of the incoming plate, thickness and rheology of the incoming sedimentary sequence, geometry of the subduction plane, and their evolution with depth are some of the factors that control the long-term mechanical coupling (Agard et al., 2018 and references therein).

The subduction and exhumation of crustal fragments from continental plates is also now commonly accepted as a frequent step in the evolution of convergent margins. Several studies of exhumed HP-LT units, numerical models and review papers, also, indicate that the processes of continental subduction and exhumation can be envisaged as occurring through a multistage evolution of burial, slicing and stacking of units similarly, to what classically described for oceanic units in accretionary prisms, and then exhumed though buoyancy-aided processes (Raimbourg et al., 2007; Yamato et al. 2007; 2008; Li and Gerya, 2009; Beaumont et al., 2009; Guillot et al., 2009; Burov et al., 2012; 2014; Strzerzynski et al., 2012; Agard and Vitale Brovarone, 2013; Vitale Brovarone et al., 2012; Plunder et al., 2015; Di Rosa et al., 2019a).

The impossibility of directly accessing the entire plate interface in active margins impedes unraveling the mechanisms and conditions for subduction and exhumation of continental rocks, so that the study of recovered, high-pressure and low-temperature (HP-LT) rock slices in fossil orogenic belts remains the only way to understand the structure and P-T evolution along the plate interface at resolution ranging from the regional- to the micro-scale.

We report here a tectono-metamorphic study of several, juxtaposed HP-LT units with continental as well as oceanic affinities cropping out at the boundary between Alpine Corsica and the basement of Hercynian Corsica. The detailed structural study coupled with the definition of the P-T-t evolution of the units allowed us to make assumption on the mechanisms of their coupling and exhumation along the plate interface.

2. Tectonic background of Alpine Corsica

Corsica Island is a lithospheric continental fragment bounded westward and eastward by two extensional basins, respectively, the Liguro-Provencal and Tyrrhenian basins (e.g. Gueguen et al., 1998). This fragment bears the remnants of a collisional belt, referred to as Alpine Corsica, that is regarded as the southern branch of the Western Alps with which it shares a common history up to Early Oligocene. This history can be summarized in four main steps (Boccaletti et al., 1971; Durand-Delga, 1984; Jolivet et al. 1990; 1998; Malavieille et al., 1998; Brunet et al., 2000; Marroni et al., 2010; Handy et al., 2010; Malusà et al., 2015): 1) the Middle to Late Jurassic opening of the Ligure-Piemontese oceanic basin between the Europe and Adria margins, 2) its closure by the Upper Cretaceous-Lower Eocene Alpine (east-dipping) subduction, 3) the subsequent Middle Eocene to Lower Oligocene continental collision and, finally, 4) the extensional collapse of the orogenic wedge as a consequence of the back-arc extensional regime generated in the upper-plate of the Apennine (west-dipping) subduction.

As in the Alps, both oceanic and continental units were deformed and metamorphosed during the Upper Cretaceous - Early Oligocene time span to build the actual Alpine Corsica unit stack, that was thrust onto the external domain, here referred as to Hercynian Corsica, and composed of a Variscan basement topped by a Upper Carboniferous-upper Eocene sedimentary cover (Gibbons and Horak, 1984; Lahondére and Guerrot, 1997; Malavieille et al., 1998; Tribuzio and Giacomini, 2002; Molli, 2008; Vitale Brovarone and Herwartz, 2013; Rossetti et al., 2015; Di Rosa et al., 2017a). From Early Oligocene onward, Corsica underwent two major extensional stages, both related to the rollback of the Apennine slab (Gueguen et al., 1998; Chamot-Rooke et al., 1999; Faccenna et al., 2004). The first event is related to the opening of the Liguro-Provençal ocean that in the Early Oligocene isolated the Corso-Sardinian block from the European plate and, consequently, from the active deformation of the Western Alps. The breakup leading to the formation of the Liguro-Provençal oceanic basin whose spreading, that spanned from Aquitanian to Langhian, was coupled to a counterclockwise rotation of around 55° of the Corso-Sardinian block (Gattacceca et al., 2007). The second event consists in the Late Miocene opening of the Tyrrhenian Sea that, in turn, isolated the Corso-Sardinian block from the Adria plate.

The present-day Corsica, then, preserves two different domains, the Alpine and Hercynian Corsica, built during two different orogenies. In Alpine Corsica, the ocean-derived rocks, the so-called Schistes Lustrés Complex, registered a subduction-exhumation cycle with a metamorphic peak dated between 80 Ma and 35 Ma, similar to that reconstructed in the Western Alps (Agard et al., 2002 and references therein). The contact between these units of the Alpine Corsica and the Hercynian Corsica is marked by a stack of slices of highly deformed and metamorphosed units of continental affinity derived from the European margin that is referred to as Lower Units (Bezert and Caby, 1988; Malasoma et al., 2006; Malasoma and Marroni, 2007; Di Rosa et al., 2017a; 2019a) or to as Tenda Massif (Gibbons and Horak, 1984; Jolivet et al., 1990, 1998; Molli et al., 2006; Maggi et al., 2012; Rossetti et al., 2015)

The Lower Units show a polyphase deformation history associated with a metamorphic imprint whose peak occurs in the blueschist facies P/T conditions (Bezert and Caby, 1988; Malasoma et al., 2006; Maggi et al., 2012; Molli et al., 2017; Di Rosa et al., 2019a). The units consist of a Paleozoic basement (i.e. Carboniferous metagranites and their host rock), covered by a Permian meta-volcanosedimentary complex and a Triassic-Jurassic, mainly carbonate, a sequence unconformably covered by metabreccias and siliciclastic metarenites of Eocene age (Durand-Delga, 1984; Rossi et al., 1994; Michard and Martinotti, 2002; Di Rosa et al., 2017b).

The Lower Units stack is bounded at its base by an east-dipping shear zone that is now almost completely reworked by the wide, sinistral strike-slip fault zone system known as the Central Corsica Shear Zone (Maluski et al., 1973; Jourdan, 1988; Waters, 1990; Molli and Tribuzio, 2004; Lacombe and Jolivet, 2005). Where preserved, the primary basal boundary of the Lower Units is represented by a ductile shear zone with a top-to-the-west sense of shear (Di Rosa et al., 2017a; 2017b).

The Lower Units are in turn overthrust to the E by the units belonging to the Schistes Lustrés Complex of the Alpine orogenic wedge. The boundary between the Lower Units and the orogenic wedge is an east-dipping shear zone showing a syntectonic metamorphic paragenesis indicating lower P-T conditions than those estimated for the neighboring Lower Units (Di Rosa et al., 2019a). Based on this observation, Di Rosa et al., (2019a) have proposed an interpretation of this shear zone as a ductile normal fault.

3. Materials and methods

The 1:50,000 scale geological maps published by BRGM, France (Rossi et al., 1994) were used as a first cartographic base for the geology of the Corte area objects of this study (modified after Di Rosa et al., 2017b, Di Rosa, 2019). The detailed geologic mapping (scale 1:5000) was coupled with mesoscopic structural analyses that were conducted in the area (Figs. 2-3). Four tectonic units of the Corte area were sampled for a total of seven samples (Figs. 3-4): 4 samples from the middle to upper Eocene metasandstones of the Lower Units (Castiglione-Popolasca Unit: CM22b, and CM29a; Piedigriggio-Prato Unit: CM21 and CM32C, already published in Di Rosa et al., 2017a; 2019b) and 3 samples from the middle Cretaceous (?) calc-schists of different slices of the Schistes Lustrés Complex (CMD121a and CMD121b from IZU-Buttinacce, and CMD118 from IZU-Botro, new data exclusive of this work). On all the samples, a detailed study of the microdeformation history were performed and quantitative compositional maps and spot analyses were acquired in order to estimate the P-T conditions of the four tectonic units using the chlorite-phengite multi-equilibrium thermodynamic technique (Vidal and Parra, 2000). The electron probe micro analysis (EPMA) data have been acquired using a JEOL-JXA 8230 electron microprobe apparatus of the IsTerre (Grenoble, France) equipped with five wavelength-dispersive spectrometers and calibrated with the following standards (Tab. 2): wollastonite (Ca, Si), orthoclase (K), albite (Al), periclase (Mg), rhodonite (Mn), TiO_2 (Ti), Al_2O_3 (Al), Fe_2O_3 (Fe) and Cr_2O_3 (Cr). The operating conditions were 15 keV accelerating voltage, 12 nA sample current and 200 to 300 ms per grid point counting time. Compositional maps and spot analysis were acquired for each sample; the X-ray maps resolution and the analytical spot size were set at 1 μm, as recommended by Lanari et al. (2014b), to detect any zoning in phengites (Fig. 5, Tab. 1). The compositional maps were calibrated with the spot analysis (De Andrade et al., 2006) using XMapTools 2.1.3 software (Lanari et al., 2014b), in order to obtain quantitative maps of oxide (Wt%). Chl and Ph structural formulas were calculated on

14 and 11 anhydrous oxygens, respectively. The chemical analysis of Chl and Ph obtained were processed through three different thermodynamic methods including water (wt) and Qz (i.e. Chl-Qz-wt, Ph-Qz-wt and Chl-Ph-Qz-wt methods) using ChlMicaEqui software (Lanari et al., 2012). These results (Tab. 3) were compared with those obtained through classical thermobarometry. Mineral abbreviations are from Whitney and Evans (2010).

3.1 The chlorite and phengite thermobarometry methods applied in this study

For each sample, we selected the micro-areas where the mutual relationships between all the identified generations of foliations were clearly and unambiguously identified. Among these sites, only those where the generations of foliations are associated to different mineral paragenesis were considered: particularly, the image analysis was performed with XMapTools in order to include any chemical heterogeneities of Chl and Ph within the same foliation and between different foliations (Tab. 2). Through this operation, performed on each of the 7 samples, at least 50 analyses for each mineral phase (Chl and Ph) were selected along each foliation.

The data obtained were processed through three different methods, based on the activity of the chlorite and mica end-members (Mg- and Fe-Ame, Clc, Dph, Sud for chlorite, Mg-Cel, Ms, Prl, Prl(H) and Php for mica) as well as the activity of water: the Chl-Qz-wt, Ph-Qz-wt and Chl-Ph-Qz-wt methods.

The Chl-Qz-wt method (Vidal et al., 2006), is a thermometer based on the equilibria

$$4Clc + 5Fe\text{-}Ame = 4Dph + 5Mg\text{-}Ame$$

$$4Dph + 6Sud = 5Fe\text{-}Ame + 3Mg\text{-}Ame + 14Qz + 8H2O$$

and allows the T range to be calculated with an equilibrium tolerance of 30°C and the percentage of Fe^{3+} for each Chl analysis fixing the pressure value (Lanari and Duesterhoeft, 2019). This method was employed to estimate the temperature conditions of the chlorites grown during different metamorphic phases, at given pressure (in this case was set at 0.8 GPa) and water activity (fixed at 1 unit, see Supplementary materials). This method is based on the convergence of the reactions involving the Chl end-members (Mg- and Fe-Ame, Clc, Dph, Sud), in presence of Qz and water (Vidal et al., 2006). The temperature location depends on the activity of water and the Chl end-members, that is in turn controlled by the Fe^{3+} content; this latter can be estimated following the recommendation of Vidal et al. (2006). T values were considered only when the scatter between T values achieved by the four reactions was less than 30°C.

The Ph-Qz-wt method (Dubacq et al., 2010) is a geobarometer based on the reactions:

$$\text{Prl(H)} = \text{Prl} + \text{H2O}$$

$$\text{3Mg-Cel} + \text{2Prl} = \text{2Ms} + \text{Phl} + \text{11Qz} + \text{2H2O}$$

where Prl(H) is hydrated Prl. The T range of stability is set on the base of the Chl-Qz-wt method results, as well as the Fe^{3+}, calculating an average of the values obtained with the Chl-Qz-wt method. Thus, the Ph-Qz-wt method allows calculating the P range for each group of Ph at fixed T and Fe^{3+}, with an absolute uncertainty of 0.2 GPa.

The variability of the Ph composition depends on the relative proportion of the end-members Cel, Ms and Prl that is mainly controlled by the activation of Tschermak and Phyrophyllite substitutions (e.g. Guidotti and Sassi, 1998). Each Ph analysis is represented in the P-T path with a line: in this work we considered only the P values corresponding to the T values previously estimated with the Chl-Qz-wt method.

Combining the values obtained from Chl-Qz-wt method with those of the Ph-Qz-wt method, i.e. considering Chl and Ph grown in the same microstructure, the P-T equilibrium conditions were calculated with the Chl-Ph-Qz-wt multi-equilibrium approach (Vidal and Parra, 2000; Vidal et al., 2006; Dubacq et al., 2010) using ChlMicaEqui software (Lanari et al., 2012). Only the couples whose P-T equilibrium shows T conditions similar to those obtained with classical thermometry were considered. On this selected group of P-T equilibrium conditions, an additional equilibrium tolerance was set in order to consider only the P-T values to which is related the minimum Gibbs free energy (i.e. < 1000 J).

The uncertainty associated to the Chl-Ph-Qz-wt multiequilibrium approach is 30°C and 0.2 GPa (Vidal and Parra, 2000).

Classical geothermometers (Cathelinau and Nieva, 1985; Cathelinau, 1988; Lanari et al., 2014a) and the geobarometer of Massonne and Schreyer, (1987) were applied on micro-areas within single Chl and Ph crystals showing homogeneous composition, in order to compare the results obtained with the multi-equilibrium techniques with other methods related to the Al^{IV} and Si contents in Chl and Ph, respectively.

4. The association of oceanic and continental units North of the Corte area

The area around the town of Corte (Figs. 1, 2) exposes a stack of deformed units of both continental and oceanic affinities affected by HP metamorphism. The three continental units ascribable to the Lower Units (i.e. Castiglione-Popolasca, Croce d'Arbitro and Piedigriggio-Prato, hereafter CPU, CDU and PPU, respectively) are made of a Paleozoic basement intruded by the Permo-Carboniferous metagranitoids and covered by a upper Permian-Middle to upper Eocene metasedimentary succession (Rossi et al., 1994). They crop out continuously as north-south elongated units with a lateral extension ranging from ca. 12 km (Castiglione-Popolasca Unit), to about 5 km (Croce d'Arbitro Unit) and ca. 7.5 km (Piedigriggio-Prato Unit), and an estimated average volume of 2-3 km^3: given the polyphase deformation affecting these units, their original thickness is hard to estimate.

The oceanic units of the Schistes Lustrés Complex are exposed through several thin slices whose lateral extension varies from 0.1 km^2 to 0.6 km^2, for an approximate volume ranging from 0.05 to 0.2 km^3. They are made up of Jurassic – middle Cretaceous (?)

ophiolitic-bearing lithotypes such as dominant metabasalts and calc-schists, and rarer metaserpentinites and metagabbros (Durand-Delga, 1984). In the present study, we focused on the slices cropping out around the localities of Buttinacce and Botro (here after referred to as IZU-Buttinacce and IZU-Botro tectonic slices, Figs. 1, 2).

Despite the Schistes Lustrés Complex crops out at the top of the Lower Units everywhere in the Alpine Corsica nappe stack, the Corte area is the only place where thin slices of the Schistes Lustrés Complex are found either sandwiched between the Lower Units or at the base of them along the Lower Units - Hercynian Corsica boundary zone (Figs. 1, 2) Therefore, Corte is a privileged area to reconstruct the pre- and post-coupling evolution of the Lower Units and the slices of the Schistes Lustrés Complex in the context of the evolution of the whole Alpine tectonic stack.

4.1 Map-scale relationships

The area between Buttinacce and Botro (top-east: 42°38’45.35’’N 9°18’91.17’’E, bottom-west: 42°28’56.41”N 9°16’31.42”E) is characterized by a N-S trending stack of metamorphic units belonging to both the Lower Units and the Schistes Lustrés Complex, respectively, that are thrust westward onto the domain of Hercynian Corsica (Fig. 2A and B). Toward the east/southeast, around Botro, this pile of units is separated from the rest of Alpine Corsica (e.g. Caporalino and Santa Lucia Units and other units of the Schistes Lustrés Complex) by the CCSZ (Di Rosa et al., 2017b). The detailed field mapping of the area allows a first order characterization of the progressive deformation experienced by the continental and oceanic units, as well as an estimation of the relative chronology.

The boundaries between the Lower Units, and those juxtaposing the Lower Units and the slices of Schistes Lustrés Complex, are marked by meter-scale ductile shear zones roughly N-S striking, E-dipping and with a top-to-the-west sense of shear (Di Rosa et al., 2017b, Fig. 4C), locally overprinted by later cataclastic deformation.

At map-scale, the ductile deformation in the Lower Units mainly consists of decimeter-scale isoclinal folds with axes plunging less than 35° towards N-NW and S-SE, with E/NE-dipping axial plane foliation. They are confined to each unit and cut by the units-bounding thrusts, as shown by the axial plane trace reported in Fig. 2A and B (see sections 4.2.1 and 4.2.2). In the Schistes Lustrés Complex slices the most dominant structures at mesoscale are isoclinal folds, with N-S trending, sub-horizontal axes. The subsequent folding event visible at map-scale is characterized by open to closed megafolds with an axial plane foliation gently dipping toward the W (Fig.2). The top to W shear zones bounding the mapped units, and responsible for their internal imbrication are all folded by this ductile event, suggesting that it postdates both the deformation described in each group of units as well as the stacking of the Lower Units and their coupling with Schistes Lustrés Complex slices (Fig. 2A and B, see sections 4.2.1 and 4.2.2). The units pile is subsequently reworked by the brittle deformation, the structures of which are all ascribable to the poorly constrained activity of the CCSZ.

In the following section, we describe in details the meso- and micro-scale features of the multiphase deformation events recorded by the oceanic and continental units prior to coupling, the deformation they shared together after coupling, and, for each group of units, we provide a brief description of the samples selected for the structural and petrological study.

4.2 The deformation until the coupling of continental and oceanic units

As introduced above, the oceanic and continental units are both characterized by a multiphase deformation evolution. Both the oceanic and the continental units, during their independent subduction/exhumation paths, registered two ductile deformation phases before the last ductile event that is common to all units. For the seek of clarity, we have named D1 and D2 with the subscript “c” and “o” for the independent deformation path of continental and oceanic units, respectively (see Figs. 3, 4). Then the third deformation event, shared by all units, is referred to as simply D3 (see also Bezert and Caby, 1988; Malasoma et al., 2006; Malasoma and Marroni, 2007; Di Rosa et al., 2017a). As we will show in the following sections, and described already elsewhere in Corsica (Di Rosa et al., 2017a; Di Rosa et al., 2019 a; b), the D1c-o and D2c-o occurred before the stacking of the units, and are therefore interpreted as related to the subduction/exhumation path followed by each single unit at the plate interface, from different depths (i.e. under different P-T conditions, see Di Rosa et al., 2019 a; b).

4.2.1 Deformation fabrics of the continental units

The deformation history recognized in the Lower Units is therefore schematized in the D1c, D2c and D3 phases (Bezert and Caby, 1988; Malasoma et al., 2006; Malasoma and Marroni, 2007; Di Rosa et al., 2017a, Figs. 3, 4).

The D1c phase. In the CPU, CDU and PPU the D1c phase is characterized by rarely preserved isoclinal F1c folds with acute to sub-acute hinges. Rare F1c non-cylindrical folds are observed in CPU and PPU (Fig. 3A-D). The F1c folds are associated with S1c axial plane foliation, occasionally preserved at meso-scale in the F2c hinge zones, where it is crenulated by the S2c foliation (Fig. 3A-D). At microscale, the S1c foliation is a continuous cleavage constituted by a Chl+Ph+Qz+Cal metamorphic assemblage (Fig. 3C-D). well preserved in the metapelites (e.g. in the matrix of the Permian metavolcaniclastics and of the Tertiary metabreccias and metasandstones).

The D2c phase. The D2c phase is characterized by W-verging, close to isoclinal F2c folds with NNE/SSW-trending A2c axes (Fig. 3A-D). F2 folds show typically necked and boudinaged limbs and are associated with a well-developed NNE/SSW-striking S2c foliation that represents the main planar anisotropy at the scale of the outcrop (Fig. 3B). ESE-WNW trending L2c mineral and mineral stretching lineations are widespread everywhere in the Corte area. In the metapelites, the L2c mineral stretching lineation is represented by elongated Chl, Qz and Ph grains, whereas in the metalimestones and in the metadolomites are dominated by boudinaged millimetric Py and Qz grains. At the microscale, the metagranitoids show protomylonitic to ultramylonitic S2c foliation marked by discontinuous lepidoblastic layers of recrystallized Ph, Chl, Bt and granoblastic layers of fine-grained recrystallized Qz, wrapping weakly elongated Fsp grains and Qz grains. Relicts of Qz, characterized by bulging recrystallization and subgrain rotation, are affected by cataclastic flow, and the fractures are filled by Ph, Chl and thin-grained Qz. S2c foliation in metapelites, is a crenulation cleavage characterized by a new generation of Chl+Ph+Qz+Ab+Cal.

Following is a brief description of the selected samples analyzed in this study (see Fig. 1B for sample location).

Sample CM22b (CPU) is a matrix-supported metasandstone. Qz and Ab porphyroclasts ranging in size from 200 μm to 2 mm are immersed in a foliated matrix composed of layers of Qz, Ab and K-Fsp smaller than 30 μm alternated to Chl- and Ph-rich layers. This foliation, ascribable to the D2c deformation phase, is associated with F2c microfolds at the hinge of which are typically preserved relicts of the S1c foliation. The Chl and Ph grown along the S1 foliation are bigger than those aligned along the S2 foliation, despite being always smaller than 200 μm. Zones of localized deformation with mylonitic to ultramylonitic fabric are a common feature of this sample.

Sample CM29a (CPU) is a matrix-supported coarse-grained metasandstone with 200 µm- to 8 mm- sized deformed porphyroclasts of Qz, K-Fsp, Chl and Ab in a fine-grained matrix comparable to that of sample CM22b. The S1c foliation is detectable only as a relict in rare microlithons of the S2c foliation. The S2c foliation is a penetrative foliation marked by a preferred orientation of deformed Qz and Ab porphyroclasts. Particularly, the D2c phase produces high-strained bands with stretched clasts: the measurement of 25 clasts resulted in an average major/minor axis ratio (Rxz) of 13:1 (S.D.=0.055, Dunnet, 1969).

Samples CM21 and CM32c (CPU) are metasandstones with clasts of Qz, Cal, metamorphic rocks (i.e. the Roches Brunes Fm.) and metagranitoids immersed in a pelitic matrix of phyllosilicates, Qz and Ab. Relicts of the D1c phase are preserved within mm-thick metapelites layers in the D2 microlithons. These relicts are represented by a S1c continuous foliation marked by syn-kinematic grown of Chl, Ph, Ab and Qz. The S2c foliation is a continuous and pervasive foliation highlighted by the growth of new Chl, Ph, Ab, K-Fsp and Qz minerals. The S2 represents a composite layering given by the superimposition of the S2 on the S1 foliation. In the F2 hinge zones, the S2 foliation can be instead classified as a crenulation cleavage. The S3 foliation is classifiable as crenulation cleavage, to which no recrystallization is associated.

4.2.2 Deformation fabrics of the oceanic units

As for the Lower Units, the slices of the Schistes Lustrés Complex outcropping in the Corte area also show a polyphase deformation history comprising pre-coupling phases (D1o-D2o phases), and post-coupling D3 deformation (Figs. 3, 4).

The D1o phase. The D1o phase structures at the meso-scale have been completely transposed by the subsequent D2o phase. In the metabasalts the S1o foliation is the main anisotropy defined by layers of Cpx, Pl and Ep, and layers of Pl, Chl and opaque oxides. D1o-related veins filled by Qz affected by grain boundary migration recrystallization are abundant (sample CMD123a’). In the calc-schists, at the microscale, the S1o foliation is superimposed on the primary layering of phyllosilicates, Cal and Qz. Relicts of the S1o foliation can be documented only in the F2o folds hinges, where thin crystals of Chl and Ph are preserved in the microlithons of the S2 foliation (Fig. 3G).

The D2o phase. In the Schistes Lustrés Complex slices the most dominant structures at mesoscale are F2o isoclinal folds, with N-S trending, sub-horizontal A2o axes. They are associated with a pervasive S2o, N-S trending axial plane foliation (Fig. 3E). An L2o mineral lineation is well visible in the calc-schist (Fig. 2B), marked by preferred alignment of synkinematic Cal and Ph.

At the microscale, F2o folds and S2o foliation are well developed in both metabasalts calc-schists (Fig. 3F-H). In the calc-schists, the relations between the S1o and the S2o foliation are well visible within the hinge zones of centimeter-scale F2o folds (Fig. 3G). Locally, in the calc-schists, σ-type porphyroclasts made by Qz aggregates, with asymmetric tales of re-crystallized Qz and/or Ph, together with bookshelf structures in Fsp, suggest a sinixtral, top-to-W sense of shear.

A later foliation arranged at low-angle with respect to the S2o and defined by re-crystallization of a new generation of Chl and Ph, is visible exclusively at microscale (Fig. 3H). This foliation is clearly subsequent to the S2o foliation, but, given the lack of mesoscale evidence of a foliation between the S2o and the S3, this anisotropy has been assigned to the late stages of the D2o phase. In the metabasalts Qz veins are arranged parallel to the S2o foliation, whereas Cal veins are set parallel to this late S2o foliation.

Here again we report a brief description of the selected samples analyzed in this study (see Fig. 1B for sample location).

Samples CMD121a and CMD121b (IZU-Buttinacce) are calc-schists made by a millimeter-scale alternation of granoblastic layers of Qz and lepidoblastic layers of Chl+Ph+Ab+Qz+Cal. This planar anisotropy is a composite S0+S1o+S2o foliation. Only in the hinge zone of the centimetric F2 folds, in which relicts of the S1o foliation are preserved, is possible to distinguish the S1o foliation to the S2o foliation, both characterized by the recrystallization of Chl, Ph, Ab Qz and minor Cal. The late S2o, to which are associated late-F2o microfolds, is accompanied by recrystallization of Chl, Ph and Cal.

Sample CMD118 (IZU-Botro*)* is a calc-schist characterized by Cal-rich layers less than 1 mm thick alternating with thinner lepidoblastic layers of phyllosilicates and Qz. Similarly, to the samples CMD121a and CMD121b, the main foliation is the composite S0+S1o+S2o foliation, made by metamorphic Chl, Ph, Ab, Qz and folded by F3o folds. Opaque oxides oriented along the S2o foliation have been also found. At the thin section scale, the S1o/S2o interference pattern has been rarely observed: if present, relicts of Chl and Ph were observed within the microlithons of the S2o foliation in the F2o hinge zones. The S3o is classifiable as disjunctive cleavage and no recrystallization seems to be associated to it.

4.2.3 The tectonic imbrication of the continental and oceanic units

As said in section 4.1, after the folding events that deformed independently the Lower Units and the slices of Schistes Lustrès Complex, these units are tectonically juxtaposed by N-S trending shear zones bounding the mapped units and responsible for their internal imbrication (see Figs. 2, 3C and 4). The shear zones are characterized by protomylonitic to mylonitic fabric with S-C fabric, σ-type porphyroclast of Fsp and bookshelf structures (with synthetic and antithetic fractures) in Fsp, all indicating a top-to-W sense of shear.

These shear zones cut the axial planes of the F2c and F2o folds (Fig. 2A and B), and are in turn deformed by the following phase, which is traditionally referred in literature as D3 (e.g. Di Rosa et al., 2019a). Therefore, in this paper, we will refer to these shear zones as late-D2.

4.3 The deformation after the coupling between continental and oceanic units

The D3 phase recorded in the Lower Units has the same features of the D3 phase documented in the slices of the Schistes Lustrés Complex. The F3 folds rework the S1 and S2 foliations registered independently by the two groups of units, and they also deform the tectonic contacts between them (Figs. 1, 2 and 4). Therefore, the D3 phase occurred after the coupling of the Lower Units with the slices of the Schistes Lustrés Complex, uniformly deforming the entire stack of units (Di Rosa et a., 2017b), and can be considered as the last ductile event affecting the units.

At the mesoscale, the D3 phase produces F3 open to close, gently inclined to recumbent folds with eastward/southeastward vergence and a NNE-SSW trending S3 axial plane foliation (Fig. 4A-C). A type-3 interference pattern (Ramsay, 1967) describes the relationship with the F2 generation of folds both in the Lower Units and in the slices of the Schistes Lustrés Complex.

Microscale F3 open folds are visible in calc-schists samples (e.g. CMD120), associated with an axial plane S3 disjunctive cleavage marked by recrystallizations of Cal and Qz (Fig. 3D-E). The morphology of the S3 foliation and the sole recrystallization of Cal and Qz suggest development of the D3 phase at shallow structural levels. Microfractures, averagely 300 µm to several mm in thickness, commonly mimic the S3 foliation.

After the D3 phase, the main deformation event affecting Corsica is the brittle deformation related to the activity of the Central Corsica Shear Zone system (i.e. CCSZ, Figs.

1, 2). In the study area CCSZ develops as a km-wide, N-S trending sinistral strike slip fault, associated with sinistral and dextral syntethic, and dextral antythetic strike-slip faults (Di Rosa et al., 2017b).

5. Petrography and phase equilibria

5.1 Mineral chemistry and P-T results

5.1.1 Chlorite

The Chl and Ph thermobarometry of the Lower Units is reconstructed in detail in Di Rosa et al., (2019b). The analyzed samples (CM22b and CM29a from CPU and CM21 and CM32c from PPU) are characterized by different generations of Chl grown along both the S1c and S2c foliations (Di Rosa et al., 2019b). All of them show XMg content ranging between 0.15 and 0.55 and Si content between 2.58 and 3.00 apfu (atom per formula unit, see Fig. 5 and Tab.1); they have a minimum Clc + Dph content of 54 %, with higher values for CM22b (CPU). The Chl along the S1c foliation are distinguishable from those grown along the S2c because of a slightly lower Si content. In addition, the Chl related to the S1 have lower content in Sud, that never reaches the 35 %, and their composition varies between Ame and Clc+Dph (Fig. 5, Tab.1).

In the samples from the slices of Schistes Lustrés Complex analyzed in this paper (CMD118 for IZU-Botro and CMD121a and CMD121b for IZU-Buttinacce), the Chl are arranged on the relicts of the S1o foliation, on the S2o main foliation and on the late S2o foliation, which is set at a low angle to the main one. XMg content varies between 0.43-0.47 in the sample CMD118 and between 0.47-0.55 in the samples CMD121a and CMD121b, without showing appreciable differences among the S1o, S2o and late S2o foliations (Fig. 5, Tab.1). The Si content ranges from 2.53 and 2.98 apfu with higher values for the samples

CMD121a and CMD121b. All the samples are characterized by Clc+Dph end-members proportion between 55 and 90 % (Fig. 5, Tab.1). In the sample CMD118, the S1o foliation contains Chl enriched in Clc+Dph, whereas in the S2o foliation the Ame (main S2o foliation) and Sud (late S2o foliation) contents increase. The samples CMD121a and CMD121b show a more homogeneous composition (Clc+Dph between 65 and 90 %), with small-scale differences between the S1o and the S2o foliations similar to those observed for the sample CMD118 (Fig. 5, Tab.1).

5.1.2 Phengite

For the samples from the Lower Units (CM22b and CM29a for CPU and CM21 and CM32c for PPU), Di Rosa et al., (2019b) report that the Ph are located along the S1c and the S2c foliations and have Si and Al content that vary between 3.20 and 3.80 apfu and between 1.55 and 2.45 apfu, respectively (Fig.5, Tab.1). The end-members proportion is always intermediate between Cel and Ms, with a Prl content always lower than 40 %. The composition of the Ph grown along the S1c shows slightly higher Si content with respect to the S2c-related phases, which are instead characterized by higher Al contents. More in general, small-scale differences show that the composition of the S2c-related Ph is more homogeneous that the composition of those grown along the S1c (Di Rosa et al., 2019b). The end-members composition related to the Ph of the S1c foliation ranges between the Cel and Ms end-members of 25-60 % and 30-65 % respectively. Ph grown along the S2c foliation are instead characterized by an increasing Prl content observable in all the units (Tab.1).

Different generations of Ph have been observed in the samples from slices of the Schistes Lustrés Complex (CMD118 for IZU-Botro and CMD121a and CMD121b for IZU-Buttinacce). Si content varies from 3.15 to 3.53 apfu in all the samples: in this range, the S1o foliation is characterized by an homogeneous Si content of 3.20-3.49 apfu (Fig. 5, Tab.1).

The K-content in the S1o-related Ph is generally higher in sample CMD121a (0.74-0.84 apfu) than in sample CMD118 (0.34-0.92 apfu), but tends to decrease in the Ph related to the late S2o of all the samples (Tab.1). End-member proportions of phengite change in the three samples: CMD118 records only small differences for Cel, slightly increasing in the S2o foliation compared to the S1o foliation, and an increase in Prl content (up to ~30 %) associated to the late S2o foliation (Fig. 5, Tab.1). The Ph of the sample CMD121b have a fairly homogeneous composition (5-20 % Prl, 35-60 % Ms and 35-60 % Cel). In the sample CMD121a the Cel proportion is lower than 40 % in the S1o foliation and higher than 30 % in the S2 foliation; a Prl content between 10 and 25 % characterizes the late S2o (Tab.1).

5.1.3 Estimation of the P-T conditions

For all the samples, each homogeneity of Chl and Ph recognized in the compositional map has been considered, in order to have a dataset in which every different mineral phase is represented by at least 50 wt% analysis (Fig. 6A, C). The results obtained with the Chl-Qz-wt and Ph-Qz-wt methods (listed Tab. 3) allowed the P-T conditions to be identified from chlorite and white-mica local equilibra (Fig. 6B, D).

The Chl-Qz-wt method (Vidal et al., 2006) applied to the selected samples, indicate that chlorite formation temperatures span three different ranges of temperatures (histograms of Fig. 6B, D): in the Lower Units, two of them are related to the mineral phases grown along the S1c foliation and one is related to the S2c foliation; in the Schistes Lustrés Complex the three T ranges correspond to the Chl related to the S1o, S2o and late S2o foliations, respectively. Then, the P conditions have been estimated through the Ph-Qz-wt method (Dubacq et al., 2010) considering only the Ph analysis (in Fig. 6B, D, each colored lines represents one single Ph analyses) contained in the T range defined with the Chl-Qz-wt method. For the metabreccias and metasandstones (Lower Units) the P conditions of the D1c phase have been estimated through the two groups of Ph related to the S1c foliation, and those of the D2c through the single group of Ph related to the S2c foliation, fixing the T conditions at the values calculated with the Chl-Qz-wt method. Similarly, for the calc-schists of the Schistes Lustrés Complex, the P conditions of the D1o phase was estimated through the first generation of Ph grown along the S1o foliation, while those related to the D2o phase have been calculated on the base of the second and third generations of Ph recrystallized along the S2o and the late S2o foliations, respectively.

The P-T estimates obtained with the Chl-Ph-Qz-wt multi-equilibrium approach (Vidal and Parra, 2000) were compared with the T and P ranges defined with the Chl-Qz-wt and Ph-Qz-wt methods (stars and P/T diagrams of Fig. 6B, D). Accordingly, data have confirmed that for all units, the different deformation events where accompanied by a multistage metamorphic history.

Three clusters of data have been recognized within the microstructures of each sample collected from the CPU and PPU Lower Units (Di Rosa et al., 2019b): the first set of data related to the S1c foliation (i.e. firsts Chl-Ph generations) is associated to HP/LT (P-peak), the second data set, still aligned along the S1c foliation (i.e. seconds Chl- Ph generations) is stable at LP/HT (T-peak) and the third set, related to the Chl-Ph couples grown along the S2c foliation (i.e. thirds Chl-Ph generations) is stable at LP/LT conditions. These three P-T conditions are reached at slightly different pressures and temperatures in the two tectonic units (Tab. 3). If we take together these two P and T ranges (samples CM22B and CM29A for CPU and CM21 and CM32C for PPU), the maximum variability of P-T conditions for all the continental units, calculated with the Chl-Ph-Qz-wt multi-equilibrium are (for details see Di Rosa et al., 2019b):

- P-peak (HP/LT) event: 1.22-0.75 GPa/250-330°C for CPU and 1.10-0.75 GPa/200-270°C for PPU;

- T-peak (LP/HT) event: 0.80-0.50 GPa/320-350°C for CPU and at 0.80-0.50 GPa/280-400°C for PPU;

- the LP/LT event: 0.45-0.25 GPa/230-310°C for CPU and 0.45-0.25 GPa/230-300°C, for PPU

Similarly, the Chl-Ph-Qz-wt multi-equilibrium method applied in this study to the samples from the Schistes Lustrés Complex (IZU-Botro and IZU-Buttinacce), allowed identifying 3 clusters representative of 3 different P-T conditions during the D1o, D2o and late-D2o deformation events (Tab. 3):

- D1o phase: the Chl-Ph couples are in equilibrium at mP/Ht conditions of 0.75-0.65 GPa/220-245°C for IZU-Botro (sample CMD118) and 0.70-0.50 GPa/265-310°C for IZU-Buttinacce (widest T and P ranges considering the samples CMD121A and CMD121B);

- D2o phase: the samples reached HP/mT conditions of at 1.00-0.85 GPa/200-250°C for IZU-Botro and at 0.90-0.70 GPa/ 240-300°C for IZU-Buttinacce;

- late-D2o event: the Chl-Ph couples are stable at LP/LT conditions of equilibrium, at 0.60-0.50 GPa/ 150-190°C for IZU-Botro and at 0.60-0.40 GPa/ 140-275°C for IZU-Buttinacce.

Similar T values related to the S1o and to the S2o suggest that the transition between the D1o and the D2o phases occurs in almost isothermic conditions in the studied samples of the Schistes Lustrés Complex.

6. Discussion: evidence for syn-collisional processes

6.1 Critical aspects about the method and related P-T estimates

Thermobarometry showed that the metapelites from the Lower Units and the slices of Schistes Lustrés Complex have recorded contrasted P-T conditions. Particularly, three Chl+Ph+Ab+Qz+wt assemblages were documented on the base of chemical (i.e. chlorite and phengite composition) and microstructural (i.e. the foliation along which the mineral grown) criteria in each group of units. For the Lower Units, two of these paragenesis grew along the S1c foliation, and are related to the P- and T-peak, while a third one, along the S2c foliation, at lower P-T conditions. In the samples from the slices of the Schistes Lustrés Complex, the first paragenesis records the prograde path along the S1o foliation, while the other two parageneses are related to the peak conditions and to the retrograde path (early and late S2o foliations). Partial re-equilibration of the phyllosilicates during a multi-stepped history of deformation and metamorphism cannot be excluded a priori (e.g., Sheffer et al., 2016; Airaghi et al., 2017; Lanari and Duesterhoeft, 2019), but it is not observed in the samples studied for this work.

Every P-T estimate is affected by a relative uncertainty of 0.2 GPa and 30°C that includes the uncertainties of the Chl-Qz-wt and Ph-Qz-wt methods. To give strength to the final data, the local equilibrium of the chlorite-phengite pairs have been tested in all the samples for at least 50 couples grew in each microstructure. Only when the scatter between the data is lower than the uncertainty of each single estimates the local equilibrium was considered as achieved.

Another choice made while processing the data is the water activity settled to 1 unit (see Supplementary materials). Water activity can vary in calcite bearing metapelites and affect the P-T estimates obtained via fluid-buffered equilibria. In this work, applying the Chl-Qz-wt, Ph-Qz-wt and the Chl-Ph-Qz-wt methods, the water activity has been set to 0.8 and 1.0 unit in each calculation in order to catch any differences in the results (see Supplementary materials). Our results show that the scatter between the two sets of calculations (i.e. considering the water activity to 1 and 0.8 unit) is lower than the uncertainty of the methods (0.2 GPa and 30°C) and therefore we present the data with the higher water activity (i.e. 1 unit).

6.2 Structural setting of the coupling between oceanic and continental units

The processes allowing the tectonic coupling of oceanic and continental units during the exhumation of high grade units in the subduction setting have been the object of many studies in the last decade (Brun and Faccenna, 2008; Lapen et al., 2007; Angiboust et al., 2012; Agard and Vitale-Brovarone, 2013; Plunder et al., 2012; 2015). Most of these studies provided a detailed reconstruction of the tectono-metamorphic evolution of the continental and oceanic units to decipher how slices of oceanic units, previously subducted and accreted at the base of the orogenic wedge, are then coupled with the continental units that are rising up within the plate interface.

The structural setting of the Corte area at map scale clearly indicates that the oceanic units of the Schistes Lustrés Complex not only occupy the uppermost structural levels of the Alpine Corsica unit stack, but occur also as fragments tectonically sandwiched between the Lower Units, i.e. the units of continental crust that underwent subduction and slicing within the plate interface (Figs. 2, 4). In addition, the structural analysis at meso- and microscale indicate that the oceanic and continental units experienced a polyphase and independent deformation history before their coupling. This polyphase deformation includes two generations of isoclinal folds (D1c/o and D2c/o) showing axial plane foliations developed during the highest metamorphic conditions: none of these sets of folds (F1c/o and F2c/o) deform the tectonic boundaries between oceanic and continental units. The juxtaposition of continental and oceanic units develops through N-S trending top-to-W shear zones (Fig. 4C and section 4.1). These shear zones truncate the F2c fold structures and are in turn deformed by the F3 folds and the associated S3 foliation: therefore they can be consequently considered as occurring at the late stages of the D2 phase (e.g. Molli et al., 2006; Malasoma and Marroni, 2007; Di Rosa et al., 2017a; 2019b). From a structural point of view, the units coupling is therefore defined by the late stage of the D2 phase. In this picture, we can envision the D3 phase as originated from vertical shortening and folding of preexisting non-horizontal layers during the extensional tectonics due to the collapse of the Alpine orogenic wedge, similarly to what recognized in several areas of the Alpine Corsica as, for instance, in the Tenda Massif (e.g., Jolivet et al., 1998; Molli et al., 2006; Maggi et al., 2012; Rossetti et al., 2015) or in the Corte area (e.g. Malasoma et al., 2006; Di Rosa et al., 2017a; 2019a).

Additional constraints to the coupling processes are provided by the metamorphic study of the oceanic and continental units. For the Lower Units, the Chl-Ph couples grown along the S1c foliation recorded the P-peak and T-peak conditions, whereas the same minerals grown along the S2c foliation are in equilibrium at LP-LT conditions. Since no evidence of older foliations occur, and thus no trace of prograde relicts is preserved, we can assume that the P-T history reconstructed in this study is related to the retrograde path of CPU and PPU, recording a multiphase history of exhumation after the P-peak conditions (Di Rosa et al., 2017a; 2017b; 2019b). Moreover, the estimated P-T paths in the two continental units are different: the different absolute P and T values reached during the D1c phase in the CPU and PPU, allowed Di Rosa et al., (2019b) identifying two different paths during exhumation, isothermic for CPU and warmer for PPU. Given a geobaric gradient for a "normal" crust of 27 MPa/km (Best, 2003) and considering that the lithostatic pressure exerted on the Lower Units is given by metamorphic rocks of both oceanic and continental affinities, we have used an average crustal geobaric gradient of 30 MPa/km for every calculation The P–T estimates related to the P-peak suggest a steady thermal regime of 5-6 °C/km for these units, lower than what suggested by Agard and Vitale-Brovarone (2013) for the continental subduction in Oman and New Caledonia, and for other continental units of Alpine Corsica. The proposed lower thermal regime could better fit the subduction of a continental margin after the underthrusting of an old and cool oceanic lithosphere, below an upper plate dominantly made of a continental crust without arc-related magmatism (Marroni et al., 2010 and references therein).

In the Schistes Lustrés Complex, the P-peak conditions are reached during the D2o phase. The P-T differences between the investigated samples indicates that each oceanic tectonic slice moved along independent paths until the end of the D2o phase. The maximum P-T burial conditions for these oceanic slices span roughly between 6 and 11 °C/km, approximately in the range of the subduction gradient estimated for the Schistes Lustrés in the Western Alps (5-10 °C/km, Agard et al., 2001; Plunder et al., 2012).

On the whole, the P-T data confirm these observations. Oceanic and continental units followed different P-T paths until the end of the D2 phase, when they were coupled along what we have defined the late-D2 N-S trending top-to-W shear zones at ~10 km of depth, before being deformed by the F3 folds during the final stages of exhumation. The reconstructed P-T paths for the subduction evolution of the continental units can be compared to what proposed for other sectors of Alpine Corsica by Agard and Vitale-Brovarone (2013) in their “scenario 3” model of burial and slicing of continental units. In this scenario the authors depict early slicing and continued underthrusting of the continental units with HP conditions reached late in the burial evolution. Most importantly, they suggest that this scenario, might be representative of a mechanical coupling concentrated at the bottom of the upper plate. Similar reconstructions of the evolution of both continental and oceanic units of Alpine Corsica have been proposed in literature by Molli et al. (2006), Molli (2008), Maggi et al. (2012) and Rossetti et al. (2015).

A similar P-T evolution has been observed in the Alps by Berger and Bousquet, (2008), which described exhumation of oceanic units occurring through cold geothermic gradients, while that of the continental units as requiring an increasing in temperature during their retrograde path. In the case of Corsica, in particular, the continental units show between them relevant differences during their exhumation, being subjected to isothermic as well as warm paths.

6.3 Timing of the exhumation for the oceanic and continental units

The convergence between the Europe and Adria plates induced the closure of the Ligure-Piemontese oceanic basin during Upper Cretaceous-Early Eocene that was followed in the Middle to Late Eocene by the continental subduction of the European margin (Schmid et al., 1996; Malavieille et al., 1998; Handy et al., 2010; Malusà et al., 2015; Marroni et al., 2017). Coherently with this picture, a progressive younging trend of the deformation and metamorphism from the oceanic and ocean/continent transition (i.e. the Schistes Lustrés Complex) to the continental margin (i.e. the Lower Units) is expected, in accordance with what proposed in literature (Strerzynski et al., 2012, Lanari et al., 2012; 2014a).

For the Lower Units of the study area, no recent and reliable radiogenic data about the metamorphism are available. The age of the deformation and the related metamorphism can be constrained only by stratigraphic relations between the youngest rocks involved in the deformation and the oldest sediments that unconformably seal the stack of the tectonic units. The depositional age of the youngest deformed rocks is attributed to the Late Eocene (Bartonian) for the occurrence of *Nummulites sp.* in the Metabreccia and Metasandstone Fms. of CPU (Bezert and Caby, 1988). The deposits unconformably found at the top of the stack of the Lower Units are represented by the continental sedimentary succession of the Francardo Basin (Ferrandini et al., 2003), whose base has been assigned to the Burdigalian (Alessandri et al., 1977). Therefore, the progressive, multiphase deformation recorded in the Lower Units can be bracketed between 37.8, i.e. the age of the Metabreccia and Metasandstone Fms., and 20.4 Ma, i.e. the age of the base of the Francardo Basin. More accurate constraints are provided by Rossetti et al. (2015) that have studied the East Tenda Shear Zone located at the eastern side of the Tenda Massif (Fig. 1), an European-derived continental crust slice correlated with the Lower Units (Bezert and Caby, 1988; Malasoma and Marroni, 2007; Di Rosa et al., 2017a). The Rb–Sr geochronological data provided by Rossetti et al. (2015) documented that the deformations related to the continental subduction in Alpine Corsica, including our D1c and D2c phase, occurred during the ~27-32 Ma time span, corresponding to Rupelian (Early Oligocene; Walker et al. 2018). In addition, these authors suggested that the extensional tectonic connected to the orogenic collapse occurred after ~27 Ma, with a final exhumation of the continental units of Alpine Corsica during the Early Miocene (~20-21 Ma). These constraints are in agreement with the $^{40}Ar/^{39}Ar$ dating of the Alpine deformations performed in the Hercynian Corsica by Di Vincenzo et al. (2016). These authors have provided the evidence of the syn-kinematic growth of white micas in the strike-slip shear zones between 37-35 Ma and 33-32 Ma, i.e. in the Late Eocene–Early Oligocene time span.

As for the Lower Units, no radiogenic data are available for the metamorphism of the slices Schistes Lustrés Complex cropping out around Corte. Elsewhere in the Alpine Corsica, the ages of the prograde and retrogarde metamorphism in the oceanic and transitional units span a wide range from Upper Cretaceous (Lahondére and Guerrot, 1997) to Late Eocene (Lahondère, 1996; Brunet et al., 2000; Martin et al., 2011; Vitale Brovarone et al., 2012). For the oceanic units correlated with the Lento Unit (e.g. Levi et al., 2007) i.e. the unit to which the slices of the studied area can be correlated, Vitale Brovarone and Hewartz (2013) provided an age for the peak metamorphism of 37.5 Ma. Considering the time span necessary for the subducted oceanic crust to reach the depths of 33 and 28 km, i.e. the estimated depth of peak metamorphism (e.g. Levi et al. 2007 and this study), the inception of subduction of these units must have occurred before the Middle Eocene.

To summarize, the oceanic units of the study area where already subducted and incorporated in the accretionary wedge in the Late Eocene, when the continental margin, represented by the Lower Units of the study area, was still undeformed and characterized by the foredeep sedimentation of the Bartonian Metabreccia and Metasandstone Fms. (CPU unit). This picture is therefore coherent with the progressive younging trend of the deformation and metamorphism from the oceanic and transitional units to the continental units mentioned above (Strerzynski et al., 2012, Lanari et al., 2012; 2014a), and provides further evidence that the continental and oceanic units of the study area have followed an independent tectono-metamorphic history before their coupling.

6.4 In search for a possible model for the coupling

Even if the exhumation record is incomplete, the available data provide evidence that the continental and oceanic rocks of the study area have been exhumed as tectonic units that have followed an independent tectono-metamorphic history before their mechanical coupling. According to what suggested by several tectono-metamorphic studies and thermo-mechanical modeling, these independent histories have in common a multiphased evolution made of several, distinct deformation phases (Raimbourg et al., 2007; Yamato et al. 2007; 2008; Li and Gerya, 2009; Beaumont et al., 2009; Guillot et al., 2009; Burov et al., 2012; 2014; Strerzynski et al., 2012; Agard and Vitale-Brovarone, 2013; Vitale-Brovarone et al., 2013; Plunder et al., 2015; Di Rosa et al., 2019a; 2019b). The structural data indicate that the coupling has occurred in the late stage of the D2o-c deformation phases, so that after this stage, the two groups of units all share the same deformation history, recorded by the D3 structures which also deform all the previous structures in all units. The P-T data about the metamorphism confirm this observation showing that the oceanic and continental units followed different P-T paths until the end of the D2 phase. All these data indicate that coupling occurred at about 10 km of depth. Afterwards, during post-D3, latest stage of exhumation along the plate interface, a possible brittle re-activation of these shear zones responsible for coupling can be hypothesized on the base of the meso-scale observation. However, not much can be said about these tardive, brittle phases, because of the poor-constrained activity of the CCSZ system in the area.

The mechanical coupling thus produced an association of continental and oceanic units, with the latter located both at the top and tectonically sliced inside the continental units. This evidence indicates that the continental units during their exhumation are able to drag slices of the orogenic wedge that are subsequently displaced upward inside the continental rocks (Fig. 8). Therefore, the tectonic erosion of the orogenic wedge, i.e. the removal of materials at the roof of the plate interface, might be envisioned as an effective process active also during the continental subduction.

The contrasting P-T paths recorded in the Lower Units indicate that the CPU and PPU were exhumed at different metamorphic gradients. Whereas the CPU is characterized by isothermal decompression, the PPU is affected during the exhumation by a warming with a small increase of temperature, not higher than 200°C (Fig. 7). Variable factors may influence the thermal structure of plate interface during the oceanic and continental subduction, including not only the effects of shear heating and radioactive heating but also the thermal conditions of the subducting and the overriding plates as well as the plate convergence rate (e.g. Faccenna et al., 2008; Gerya et al., 2008; Maierová et al., 2012; Syracuse et al., 2010; Warren et al., 2008; Zheng and Chen, 2016). Particularly, Gerya et al. (2008) have proposed possible transient episodes of anomalously high temperature along the plate interface during incipient continental collision. These episodes seem to be primarily controlled by changes in the intensity of viscous and radioactive heating in subducted crustal rocks, and are generally associated with partial melting (Burg and Gerya, 2005). In addition, focused pulses of dehydration during subduction have been proposed in literature as contributing to the rapid heating during the early stages of exhumation within the plate interface (Camacho et al., 2005; John et al., 2012; Dragovic et al., 2015). Therefore, we could postulate the occurrence of transient episodes of anomalously high temperature during the exhumation of the Lower Units, to explain the difference in temperature observed in the exhumation paths of CPU and PPU. A possible explanation to these episodes for the PPU case can derive from the P-T path estimated for this unit, where the warming during the exhumation seems to be connected with a break or a slowing in the exhumation process resulting in a stationing at a depth of ca. 17-25 km.

We could simply comment that in the reported study we see no evidence of the melting described by Burg and Gerya, (2005) because the supposed increase of temperature during the exhumation of the PPU was not so relevant to produce the partial melting of subducted crustal rocks. However, this hypothesis is at present only a speculation and will deserve more attention in future investigations on the subducted continental rocks in Alpine Corsica.

In the proposed model we envision a flow of material that is dragged and translated upward through a mechanism that can be regarded as similar to the basal tectonic erosion, when fragments of the wedge are dragged and translated downward during the oceanic subduction (von Huene and Scholl, 1991; Clift and Vannucchi, 2004; Sallares and Ranero, 2005, see also re-definition by Agard et al., 2018). Analogously to what described for basal erosion, specific weak lithological horizons within the orogenic wedge, characterized by rheological contrasts, can be re-activated as shear zones during exhumation, allowing mass dragging along the plate interface/orogenic wedge boundary. Then, the oceanic fragments detached from the base of the orogenic wedge are subsequently incorporated within the continental units and translated upward along the roof of the plate interface. In their model of burial of continental units suggested for Corsica, Agard and Vitale-Brovarone (2013) propose a correlation between the proposed model and a mechanical coupling (i.e. strain) preferentially concentrated at the base of the upper plate. Accordingly, this could facilitate the possibility of removing previously underplated material from the bottom of the wedge as tectonic slices to be incorporated in the rising continental units. Moreover, if we take into account the large volumes of the studied continental units, compared to the small volumes of the Schistes Lustrés slices, we could speculate, in accordance with what observed and proposed for the continental subduction in W. Turkey (Plunder et al., 2015), and in the Western Alps (Angiboust et al., 2009; Plunder et al., 2012), that the buoyancy-driven exhumation of the large Lower Units units may have contributed to scrapping off the slices of oceanic units on its way up the plate interface.

A similar occurrence of oceanic fragments intimately associated with and deformed within the continental rocks has been described by Molli et al. (2006) at the eastern border of the Tenda Massif. The Tenda Massif is regarded as a fragment of the European continental margin involved into subduction during Middle Eocene. As a consequence, the Tenda Massif is strongly deformed and is affected by HP/LT metamorphism and bounded at its roof by the Schistes Lustrés Complex (Waters, 1990; Daniel et al., 1996; Gueydan et al., 2003; Molli et al., 2006; Maggi et al., 2012). In the area studied by Molli et al. (2006), slices of oceanic rocks are recognized inside the orthogneisses of the Tenda Massif, at the core of strongly non-cylindric recumbent F1 fold developed in association with epidote-blueschist facies metamorphism (peak metamorphism at about 1.0 GPa and 450°C). The oceanic and continental rocks show a common retrograde structural and metamorphic history during exhumation that is recorded by the D2 ductile fabrics described in the Tenda Massif and developed under greenschist facies P-T metamorphic conditions. On the whole, the eastern border of the Tenda Massif provides the evidence that the slices of the orogenic wedge are dragged in a ductile way and exhumed with the continental rocks also at a depth of 30-35 km.

If we integrate the information derived from the study area with those from the Tenda Massif, the mechanical coupling between continental and oceanic rocks seems to be effective at two different depths, i.e. at 30-35 km and at about 10 km, where small volumes of rocks are eroded at the roof of the subduction channel and incorporated within. According to Agard et al. (2009), the buoyant continental crust seems to be exhumed during continental subduction with velocities comparable with those of plate tectonics at mantle depths (1–5 cm/yr) and later decelerates (ca. 1 mm/yr) in the upper crust. As a first approximation, the available data for the Lower Units seems to be coherent with this picture, indicating a mean velocity of ~ 1 cm/yr for their burial and exhumation.

The presented data are insufficient to assess whether the coupling between continental and oceanic rocks and their basal erosion occur along the entire plate interface, or if they show a punctuated character and/or a connection with large-scale, lithospheric-scale geodynamic events (Agard et al., 2009; Penniston-Dorland et al., 2015). However, we could tentatively favor a more punctuated process, according to several studies of rock recovery from literature, that point to a mechanical coupling effective only at precise depths (for an exhaustive review, see Agard et al., 2018). The hypothesized stationing at ca. 17-25 km of the PPU during exhumation could support this option. Thus, if the exhumation is punctuated, also the coupling between continental and oceanic fragments can be hypothesized as punctuated and connected with main geodynamic events. Assuming a correlation between the D2c phase in the Lower Units with the D2-phase in the Tenda Massif dated by Rossetti et al. (2015), we can constrain the D2c phase between ~27 and 32 Ma. In this time span also the activation of the shear zones that developed in the Lower Units at the late stage of the D2c phase occurred. This age is highly critical for the geodynamics of the Alpine-Apennine system (e.g. Malusà et al., 2015) since it records: 1) the inception of rifting phase leading to the opening of the Ligure-Provençal oceanic basin (e.g. Chamot-Rooke et al., 1999); 2) the slab-break off of the alpine subducted slab (Handy et al., 2010) and 3) development of the strike slip tectonics connected to the indenter of the Adria plate within the Alpine-Apennine collisional system (Marroni et al. 2019). According to Vignaroli et al (2010) and Agard et al. (2002), all these geodynamic events occurred during the switch from syn-to-post-orogenic extensional deformation in the Alpine-Apennine system. A direct link between these geodynamic events with the erosion at the roof of the plate interface and the final exhumation of the continental and oceanic units requires, however, more data to be assessed.

7. Conclusions

The study of the Corte area (Corsica) presented in his work has revealed a complex tectonic setting with intimately associated oceanic and continental units, both affected by HP metamorphism. In this area the oceanic units, belonging to the Schistes Lustrés Complex, not only occupy the uppermost structural levels of the tectonic stack as in the other areas of the Alpine Corsica, but occur also as thin slices tectonically sandwiched between the Lower Units, i.e. the units of European continental margin that underwent to subduction. This area enables studying the mechanisms of coupling between oceanic and continental units during their exhumation along the plate interface in the frame of continental subduction.

The data collected show that the units experienced different tectono-metamorphic histories, occurred at different time, that represent the oceanic (D1o and D2o) and continental (D1c and D2c) subduction stages until their coupling (late D2o and D2c), after which they were deformed together (D3). The tectono-metamorphic study highlighted that (i) each tectonic unit has a different P-T history, which implies that they followed independent exhumation path until their coupling and (ii) the coupling of the tectonic units occurred at about 10 km of depth through top-to-W ductile shear zones and thus in a still compressive tectonic regime.

Considering the different time in which the oceanic and the continental units were exhumed, we provided the evidence that the processes of exhumation of the continental units were able to drag oceanic slices from the orogenic wedge and displace them upward in intimate association with the continental rocks. This picture suggests that the tectonic erosion of the orogenic wedge, i.e. the removal of materials at the roof of the subduction channel, might be an effective process also during the continental subduction. Moreover, if we take into account the large volumes of the studied continental units, compared to the small volumes of the Schistes Lustrés slices, we could speculate that the buoyancy-driven exhumation of the large Lower Units may have contributed to the scrapping off the slices of oceanic units on its way up the plate interface.

Even if the exhumation record is incomplete, all the available data for the continental units from Alpine Corsica tentatively favor a punctuated process, where the mechanical coupling is effective only at specific depths. The possible link between the main geodynamic events of the Alpine-Apennine system with the erosion at the roof of the plate interface and the final exhumation of the continental and oceanic units should be investigated in the future.

ACKNOWLEDGMENTS

We are thankful to the editor Philippe Agard and the reviewers Gianluca Vignaroli and Pierre Lanari for the critical, stimulating and constructive reviews that allowed us to improve this work. Olivier Vidal, Valentina Batanova and Valerie Magnin (IsTerre, Grenoble) are also thanked for the EPMA analysis. This work was possible thanks to the financial support from Italian societies SIMP, SGI, SOGEI and AIV, and the PRA grant from University of Pisa.

REFERENCES CITED

Agard, P., Vitale Brovarone, A., 2013. Thermal regime of continental subduction: the record from exhumed HP-LT terranes (New Caledonia, Oman, Corsica). Tectonophysics 601, 206-215.

Agard, P., Plunder, A., Angiboust, S., Bonnet, G., Ruh, J., 2018. The subduction plate interference: rock record and mechanical coupling (from long to short timescales). Lithos 320-321, 537-566.

Agard, P., Jolivet, L., Goffé, B., 2001. Tectonometamorphic evolution of the Schistes Lustrés complex: implications for the exhumation of HP and UHP rocks in the Western Alps. Bulletin de la Société Géologique de France 175(5), 617-636.

Agard, P., Monié, P., Jolivet, L., Goffé, B., 2002. In situ laser probe 40Ar/39Ar dating of the Schistes Lustrés complex: implications for the exhumation of the Western Alps. Journal of Metamorphic Geology 20, 599-618.

Agard, P., Yamato, P., Jolivet, L., Burov, E., 2009. Exhumation of oceanic blueschists and eclogites in the subduction channel: timing and mechanisms. Earth Science Reviews 92, 53-79.

Airaghi, L., Lanari, P., de Sigoyer, J., Guillot, S., 2017. Microstructural vs compositional preservation and pseudomorphic replacement of muscovite in deformed metapelites from the Longmen Shan (Sichuan, China). Lithos 282-283, 262-280.

Alessandri, J.A., Magné, J., Pilot, M.D., Samuel, E., 1977. Le Miocène de la région de Corte-Francardo. Bulletin Société Sciences Historiques Naturelles Corse 622, 51-54.

Angiboust, S., Agard, P., Jolivet, L., Beyssac, O., 2009. The Zermatt–Saas ophiolite: the largest (60-km wide) and deepest (c. 70–80 km) continuous slice of oceanic lithosphere detached from a subduction zone? Terra Nova 21, 171–180.

Angiboust, S., Wolf, S., Burov, E., Agard, P., Yamato, P., 2012. Effect of fluid circulation on subduction interface tectonic processes: insights from thermo-mechanical numerical modelling. Earth and Planetary Science Letters 357-358, 238-248.

Beaumont, C., Jamieson, R.A., Butler, J.P., Warren, C.J., 2009. Crustal structure: a key constraint on the mechanism of ultra-high-pressure rock exhumation. Earth and Planetary Science Letters 287, 116-129.

Berger, A., Bousquet, R., 2008. Subduction-related metamorphism in the Alps: review of isotopic ages based on petrology and their geodynamic consequences, in: Sigesmund, S., Fugenschuh, B., Froitzheim, N. (Eds.), Tectonic Aspects of the Alpine-Dinaride-Carpathian system. Geological Society, London, Special Publications 298, pp. 117-144.

Best, M.G. 2003. Igneous and metamorphic petrology. Brigham Young University, Blackwell Publishing, 2nd edition, 758 p.

Bezert P., Caby R., 1988. Sur l’age post-bartonien des événements tectonométamorphiques alpins en bordure orientale de la Corse cristalline (Nord de Corte). Bulletin de la Société Géologique de France 4(6), 965-971.

Boccaletti M., Elter P., Guazzone, G., 1971. Plate tectonic models for the development of the western Alps and northern Apennines. Nature 234, 108-111.

Brun, J.P., Faccenna, C., 2008. Exhumation of high-pressure rocks driven by slab rollback. Earth and Planetary Science Letters 272(1), 1-7.

Brunet, C., Monié, P., Jolivet, L., Cadet J.P. 2000. Migration of compression and extension in the Tyrrhenian Sea, insights from 40Ar/39Ar ages on micas along a transect from Corsica to Tuscany. Tectonophysics 321, 127-155.

Burg, J.P., Gerya, T.V., 2005. The role of viscous heating in Barrovian metamorphism of collisional orogens: thermomechanical models and application to the Lepontine Dome in Central Alps. Journal of Metamorphic Geology 23, 75-95.

Burov, E., Francois, T., Yamato, P., Wolf, S., 2012. Mechanisms of continental subduction and exhumation of HP and UHP rocks. Gondwana Research 25, 464-493.

Burov, E., Francois, T., Agard, P., Le Pourhiet, L., Meyer, B., Tirel, C., Lebedev, S., Yamato, P., Brun, J-P., 2014. Rheological and geodynamic controls on the mechanisms of subduction and HP/UHP exhumation of crustal rocks during continental collision: Insights from numerical models. Tectonophysics 631, 212-250.

Camacho, A., Lee, J.K., Hensen, B.J. and Braun, J., 2005. Short-lived orogenic cycles and the eclogitization of cold crust by spasmodic hot fluids. Nature, 435(7046), p.1191.

Cathelineau, M., 1988. Cation site occupancy in chlorites and illites as a function of temperature. Clay Minerals 23, 471-485.

Cathelineau, M., Nieva, D., 1985. A chlorite solid solution geothermometer. The Los Azufres (Mexico) geothermal system. Contributions to Mineralogy and Petrology 91, 235-224.

Chamot-Rooke, N., Gaulier, J.M., Jestin, F., 1999. Constraints on Moho depth and crustal thickness in the Liguro-Provencal basin from a 3D gravity inversion: geodynamic implications, in: Durand, B., Jolivet, L., Horvath, F., Sérranne, M., (Eds.), The Mediterranean basin: Tertiary extenson within the Alpine Orogen. Geological Society, London, Special Publications 156, pp. 37-61.

Clift, P., Vannucchi, P., 2004. Controls on tectonic accretion versus erosion in subduction zones: implications for the origin and recycling of the continental crust. Reviews of Geophysics 42, RG2001.

Daniel, J.M., Jolivet, L., Goffé, B., Poinssot, C., 1996. Crustal-scale strain partitioning: footwall deformation below the Alpine Oligo-Miocene detachment of Corsica. Journal of Structural Geology 18(1), 41–59.

De Andrade, V., Vidal, O., Lewin, E., O'Brien, P., Agard, P., 2006. Quantification of electron microprobe compositional maps of rock thin sections: an optimized method and examples. Journal of metamorphic Geology 24, 655-668.

Di Rosa, M., De Giorgi, A., Marroni, M., Vidal, O., 2017a. Syn-convergence exhumation of continental crust: evidence from structural and metamorphic analysis of the Monte Cecu area, Alpine Corsica (Northern Corsica, France). Geological Journal 52, 919-937.

Di Rosa, M., De Giorgi, A., Marroni, M., Pandolfi, L., 2017b. Geology of the area between Golo and Tavignano Valleys (Central Corsica): a snapshot of the continental metamorphic units of Alpine Corsica. Journal of Maps 13, 644-653.

Di Rosa, M., Meneghini, F., Marroni, M., Hobbs, N., Vidal, O., (2019a). The exhumation of continental crust in collisional belts: insights from the deep structure of Alpine Corsica in the Cima Pedani area. The Journal of Geology (in press).

Di Rosa, M., Frassi, C., Meneghini, F., Marroni, M., Pandolfi, L., De Giorgi, A., (2019b). Tectono-metamorphic evolution in the European continental margin involved in the Alpine subduction: new insights from the Alpine Corsica, France. Comptes Rendus – Geosciences (in press).

Di Vincenzo, G., Grande, A., Prosser, G., Cavazza, W., DeCelles, P.G., 2016. 40Ar/39Ar laser dating of ductile shear zones from central Corsica (France): Evidence of Alpine (middle to late Eocene) syn-burial shearing in Variscan granitoids. Lithos 262, 369-383.

Dragovic, B., Baxter, E.F., Caddick, M.J., 2015. Pulsed dehydratation and garnet growth during subduction revealed by zoned garnet geochronology and thermodynamic modeling, Sifnos, Greece. Earth and Planetary Science Letters 413, 111-122.

Dubacq, B., Vidal, O., De Andrade, V., 2010. Dehydration of dioctahedral aluminous phyllosilicates: thermodynamic modelling and implications for thermobarometric estimates. Contributions to Mineralogy and Petrology 159, 159–174.

Dunnet, D., 1969. A technique of finite strain analysis using particles. Tectonophysics 7, 117-136.

Durand-Delga, M., 1984. Principaux traits de la Corse Alpine et correlations avec les Alpes Ligures. Memorie della Società Geologica Italiana 28, 285-329.

Faccenna, C., Priomallo, C., Crespo-Blanc, L., Jolivet, L., Rossetti, F., 2004. Lateral slab deformation and the origin of Western Mediterranean arcs. Tectonics 23, TC1012.

Ferrandini, J., Gattacceca, J., Ferrandini, M., Deino, A., Janin, M.C., 2003. Chronostratigraphie et paléomagnétisme des dépots oligo-miocènes de Corse: implications géodynamiques pour l'ouverture du bassin liguro-provencal, Bulletin de la Société Géologique de France 174 (4), 357–371.

Gattacceca, J., Deino, A., Rizzo, R., Jones, D.S., Henry, B., Beaudoin, B., Vedeboin, F., 2007. Miocene rotation of Sardinia: new paleomagnetic and geochronological constraints and geodynamic implications. Earth and Planetary Science Letters 258, 359-377.

Gerya, T.V., Perchuk, L.L., Burg J.P., 2008. Transient hot channels: perpetrating and regurgitating ultrahigh-pressure, high temperature crust-mantle associations in collision belts. Lithos 103, 236-256.

Gibbons, W., Horak, J., 1984. Alpine metamorphism of Hercynian hornblende granodiorite beneath the blueschist facies Schistes Lustrés nappe of NE Corsica. Journal of Metamorphic Geology 2, 95-113.

Gueguen, E., Doglioni, C., Fernandez, M., 1998. On the post-25 Ma geodynamic evolution of the western Mediterranean. Tectonophysics 298, 259–269.

Gueydan, F., Leroy, Y.M., Jolivet, L., Agard, P., 2003. Analyses of continental midcrustal strain localization induced by microfaultinf and reactionsoftening. Journal of Geophysical Research 108, 2064-2081.

Guidotti, C.V., Sassi, F.P. 1998. Miscellaneous isomorphus substitution in Na-K white mica: a review, with special emphasis to metamorphic micas. Rendiconti Lincei. Scienze Fisiche e Naturali 9(9), 57-78.

Guillot S., Hattori K., Agard P., Schwartz S., Vidal O., 2009. Exhumation Processes in Oceanic and Continental Subduction Contexts: A Review, in: Lallemand, S., Funiciello, F., (Eds.), Subduction Zone Geodynamics. Springer-Verlag, Berlin, pp. 175-205.

Handy, M.R., Schmid, S.M., Bousquet, R., Kissling, E., Bernoulli, D., 2010. Reconciling plate–tectonic reconstructions of Alpine Tethys with the geological–geophysical record of spreading and subduction in the Alps. Earth Science Reviews 102, 121–158.

John, T., Gussone, N., Podladchikov, Y.Y., Bebout, G.E., Dohmen, R., Halama, R., Klemd, R., Magna, T. and Seitz, H.M., 2012. Volcanic arcs fed by rapid pulsed fluid flow through subducting slabs. Nature Geoscience, 5(7), p.489.Jolivet, L., Dubois, R., Fournier, M., Goffé, B., Michard, A., Jourdan, C., 1990. Ductile extension in alpine Corsica. Geology, 18, 1007-1010.

Jolivet, L., Dubois, R., Fournier, M., Goffé, B., Michard, A., Jourdan, C., 1990. Ductile extension in alpine Corsica. Geology, 18, 1007-1010.

Jolivet, L., Faccenna, C., Goffé, B., Mattei, M., Rossetti, F., Brunet, C., Parra, T., 1998. Midcrustal shear zones in postorogenic extension: example from the northern Tyrrhenian Sea. Journal of Geophysical Research: Solid Earth, 103, 12123-12160.

Jourdan, C., 1988. Balagne orientale et massif du Tenda (Corse septentrionale): etude structural, interpretation des accidents et des deformation reconstructions géodynamiques. Ph.D. thesis, Paris, Université Paris-Sud.

Lacombe, O., Jolivet, L., 2005. Structural and kinematic relationships between Corsica and the Pyrenees–Provence domain at the time of the Pyrenean orogeny. Tectonics 24, TC1003. doi:10.1029/2004TC001673.

Lahondère, D., Guerrot, C., 1997. Datation Sm-Nd du métamorphisme éclogitique en Corse alpine: un argument pour l'existence au Crétacé supérieur d'une zone de subduction active localisée sous le bloc corso-sarde. Géologie de la France 3, 3-11.

Lahondère, D., 1996. Les schistes blues et les éclogites à lawsonite des unités continentals et océanique de la Corse alpine: Nouvelles donnée pétrologique et structurales (Corse). Documents du BRGM, 240.

Lanari, P., Duesterhoeft, E., 2019. Modeling Metamorphic Rocks using Equilibrium Thermodynamics and Internally Consistent Databases: Past Achievements, Problems and Perspectives. Journal of Petrology 60, 19-56.

Lanari, P., 2012. Micro-cartgraphie P-T-‘d’ dans les roches métamorphiques. Applications aux Alpes et à l’Himalaya. Thèse de doctorat Sciences de la Terre, Université de Grenoble.

Lanari, P., Wagner, T., Vidal, O., 2014a. A thermodynamic model for di-trioctahedral chlorite from experimental and natural data in the system MgO-FeO-Al2O3-SiO2-H2O: applications to P-T sections and geothermometry. Contributions to Mineralogy and Petrology 167. doi:10.1007/s00410-014-0968-8.

Lanari, P., Vidal, O., De Andrade, V., Dubacq, B., Lewin, E., Grosch, E., Schwartz, S., 2014b. XMAPTOOLS: a MATLAB c -based program for electron microprobe X-ray image processing and geothermobarometry. Computers and Geosciences 62, 227-240.

Lapen, T.J., Johnson, C.M., Baumgartner, L.P., Dal Piaz, G.V., Skora, S., Beard, B., 2007. Coupling of oceanic and continental crust during Eocene eclogite-facies metamorphism: evidence from Monte Rosa nappe, Western Alps. Contributions to Mineralogy and Petrology 153, 139-157.

Levi, N., Malasoma, A., Marroni, M., Pandolfi, L., Paperini, M., 2007. Tectono-metamorphic history of the ophiolitic Lento unit (northern Corsica): evidences for the complexity of accretion-exhumation processes in a fossil subduction system. Geodinamica Acta 20(1), 99-118.

Li, Z., Gerya, T.V., 2009. Polyphase formation and exhumation of HP-UHP rocks in continental subduction zone: numerical modelling and application to the Sulu UHP terrane in eastern Cina. Journal of Geophysical Research 114, B09406.

Maggi, M., Rossetti, F., Corfu, F., Theye, T., Andersen, T.B., Faccenna, C., 2012. Clinopyroxene-rutile phyllonites from East Tenda Shear Zone (Alpine Corsica, France): pressure-temperature-time constraints to the Alpine reworking of Variscan Corsica. Journal of the Geological Society of London 169, 723–732.

Maierová, P., Schulmann, K., Lexa, O., Guillot, S., Štípská, P., Janoušek, V. and Čadek, O., 2016. European Variscan orogenic evolution as an analogue of Tibetan- Himalayan orogen: Insights from petrology and numerical modeling. Tectonics, 35(7), pp.1760-1780.

Malasoma, A., Marroni, M., 2007. HP/LT metamorphism in the Volparone Breccia (Northern Corsica, France): evidence for involvement of the Europe/Corsica continental margin in the Alpine subduction zone. Journal of Metamorphic Geology 25, 529-545.

Malasoma, A., Marroni, M., Musumeci, G., Pandolfi, L., 2006. High pressure mineral assemblage in granitic rocks from continental units, Alpine Corsica, France. Geological Journal 41, 49-59.

Malavieille, J., Chemenda, A., Larroque, C., 1998. Evolutionary model for the Alpine Corsica: mechanism for ophiolite emplacement and exhumation of high-pressure rocks. Terra Nova 10, 317–322.

Malusà, M.G., Faccenna, C., Baldwin, S.L., Fitzgerald, P.G., Rossetti, F., Balestrieri, M.L., Danisik., M., Ellero, A., Ottria, G., Piromallo, C., 2015. Contrasting styles of (U)HP rock exhumation along the Cenozoic Adria-europe plate boundary (Western Alps, Calabria, Corsica). Geochemistry, Geophysics, Geosystems 16, 1786-1824.

Maluski, H., Mattauer, M., Matte, P.H., 1973. Sur la presence de decrochement alpins en Corse: Comptes Rendue de l'Académie Science 276, 709-712.

Marroni, M., Meneghini, F., Pandolfi, L., Hobbs, N., Luvisi, E., 2019. The Ottone-Levanto Line of Eastern Liguria (Italy) uncovered: a Late Eocene-Early Oligocene snapshot of Northern Apennine geodynamics at the Alps/Apennines Junction. Episodes (In press)

Marroni, M., Meneghini, F., Pandolfi, L., 2010. Anatomy of the Ligure-Piemontese subduction system: evidence from Late Cretaceous-Middle Eocene convergent margin deposits from Northern Apennines (Italy). International Geological Reviews 10-12, 1160-1192.

Marroni, M., Meneghini, F., Pandolfi, L., 2017. A revised subduction inception model to explain the Late Cretaceous, double-vergent orogen in the pre-collisional Western Tethys: evidence from the Northern Apennines. Tectonics 36, 2227-2249.

Martin, A.J., Rubatto, D., Vitale Brovarone, A., Hermann, J., 2011. Late Eocene lawsonite-eclogite facies metasomatism of a granulite sliver associated to ophiolites in Alpine Corsica. Lithos 125, 620-640.

Massonne, H.J., Schreyer, W., 1987. Phengite geobarometry based on the limiting assemblage with K-feldspar, phlogopite, and quartz. Contributions to Mineralogy and Petrology 96, 212–224.

Michard, A., Martinotti, G., 2002. The Eocene unconformity of the Brianconnais domain in the French-Italian Alps, revisited (Marguareis massif, Cuneo); a hint for a Late Cretaceous-Middle Eocene frontal bulge setting. Geodinamica Acta 15, 289-301.

Molli, G., Tribuzio, R., 2004. Shear zones and metamorphic signature of subducted continental crust as tracers of the evolution of the Corsica/Northern Apennine orogenic system, in: Alsop, G.I., Holdsworth, R.E., McCaffrey, K.J.W., Handy, M., (Eds.) Flow processes in faults and shear zones. Geological Society, London, Special Publications 224, pp. 321-335.

Molli, G., Tribuzio, R., Marquer, D., 2006. Deformation and metamorphism at the eastern border of Tenda Massif (NE Corsica): a record of subduction and exhumation of continental crust. Journal of Structural Geology 28, 1748–1766.

Molli, G., Menegon, L., Malasoma, A., 2017. Switching deformation mode and mechanisms during subduction of continental crust: a case study from Alpine Corsica. Solid Earth Discussions doi:10.5194/se-2017-11.

Molli, G., 2008. Northern Apennine-Corsica orogenic system: an updated overview, in: Siegesmund S., Fugenschuh B., Froitzheim N., (Eds.), Tectonic Aspects of the Alpine-Dinaride-Carpathian System, Geological Society, London, Special Publications 298, 413–442.

Penniston-Dorland, S.C., Kohn, M.J., Manning, C.E., 2015. The global range of subduction zone thermal structures from exhumed blueschists and eclogites: rocks are hotter than models. Earth and Planetary Science Letters 428, 243-254.

Plunder, A., Agard, P., Dubacq, B., Chopin, C., Bellanger, M., 2012. How continuous and precise is the record of P-T paths? Insights from combined thermobarometry and thermodynamic modelling into subduction dynamics (Schistes Lustrés, Western Alps). Journal of Metamorphic Geology 30(3), 323-346.

Plunder, A., Agard, P., Chopin, C., Pourteau, A., Okay, A.I., 2015. Accretion, underplating and exhumation along subduction interface: from subduction initiation to continental subuction (Tavsanli zone, W Turkey). Lithos 226, 233-254.

Raimbourg, H., Jolivet, L., Leroy, Y., 2007. Consequences of progressive eclogitization on crustal exhumation, a mechanical study. Geophysical Journal International 168, 379-401.

Ramsay, J.G., 1967. Folding and fracturing of rocks. New York: McGraw-Hill.

Rossetti, F., Glodny, J., Theye, T., Maggi, M., 2015. Pressure temperature deformation-time of the ductile Alpine shearing in Corsica from orogenic construction to collapse. Lithos 218-219, 99-116.

Rossi, P., Durand-Delga, M., Caron, J.M., Guieu, G., Conchon, O., Libourel, G., Loye-Pilot, M., 1994. Carte Geologique de la France (1/50,000), feuille Corte (1110). BRGM, Orléans.

Sallares, V., Ranero, C.R., 2005. Structure and tectonics of the erosional convergent margin of Antofagasta, north Chile (23°30'S). Journal of Geophysical Research 110, B06101.

Schmid, S.M., Pfiffner, O.A., Froitzheim, N., Schönborn, G., Kissling, E., 1996. Geophysical–geological transect and tectonic evolution of the Swiss–Italian Alps. Tectonics 15(5), 1036–1064.

Sheffer, C., Vanderhaeghe, O., Lanari, P., Tarantola, A., Ponthus, L., Photiades, A., France, L., 2016. Syn- to post-orogenic exhumation of metamorphic nappes: Structure and thermobarometry of the western Attic-Cycladic metamorphic complex (Lavrion, Greece). Journal of Geodynamics 96, 174-193.

Strzerzynski, P., Guillot, S., Leloup, P.H., Arnaud, N., Vidal, O., Ledru, P., Corrioux, G., Darmendrail, X., 2012. Tectono-metamorphic evolution of Brianconnains zone (Modane-Aussois and Southern Vanoise units, Lyon Turin transect, Western Alps). Journal of Geodynamics 56-57, 55-75.

Syracuse, E.M., van Keken, P.E. and Abers, G.A., 2010. The global range of subduction zone thermal models. Physics of the Earth and Planetary Interiors, 183(1-2), pp.73-90.

Tribuzio, R., Giacomini, F., 2002. Blueschist facies metamorphism of peralkaline rhyolites from Tenda crystalline massif (northern Corsica): evidence for involvement in the Alpine subduction event? Journal of Metamorphic Geology 20, 513-526.

Trincal, V., Lanari, P., 2016. Evidence of Al-free di-trioctahedral substitution in chlorite and a ferri-sudoite end-member. Clay Minerals 51, 675-689.

Vidal, O., Parra, T., 2000. Exhumation paths of high-pressure metapelites obtained from local equilibria for chlorite–phengite assemblage. Geological Journal 35, 139–161.

Vidal, O., De Andrade, V., Lewin, E., Munoz, M., Parra, T., Pascarelli, S., 2006. P–T-deformation-Fe2+/Fe3+ mapping at the thin section scale and comparison with XANES mapping: application to a garnet-bearing metapelite from the Sambagawa metamorphic belt (Japan). Journal of Metamorphic Geology 24, 669-683.

Vignaroli, G., Rossetti, F., Rubatto, D., Theye, T., Lisker, F., Phillips, D., 2010. Pressure-temperature-deformation-time (P-T-d-t) exhumation history of the Voltri Massif HP complex, Ligurian Alps, Italy. Tectonics 29(6), TC6009.

Vitale Brovarone, A., Herwartz, D., 2013. Timing of HP metamorphism in the Schistes Lustrés of Alpine Corsica: new Lu-Hf garnet and lawsonite ages. Lithos 172-173, 175–191.

Vitale Brovarone, A., Beyssac, O., Malavieille, J., Molli, G., Beltrando, M., Compagnoni, R., 2012. Stacking and metamorphism of continuous segments of subducted lithosphere in a high-pressure wedge: The example of Alpine Corsica (France). Earth Science Reviews 116, 35-56.

von Huene R, Scholl DW., 1991. Observations at convergent margins concerning sediment subduction, subduction erosion, and the growth of continental crust. Review of Geophysics 29, 279–316.

Walker, J.D., Geissman, J.W., Bowring, S.A., and Babcock, L.E., compilers, 2018, Geologic Time Scale v. 5.0: Geological Society of America, https://doi.org/10.1130/2018.CTS005R3C.

Warren, C.J., Beaumont, C., Jamieson, R.A., 2008. Modelling tectonic styles and ultra-high pressure (UHP) rock exhumation during the transition from oceanic subduction to continental collision. Earth and Planetary Science Letters 267, 129-145.

Waters, C.N., 1990. The Cenozoic tectonic evolution of Alpine Corsica. Journal of Geological Society of London 147, 811-824.

Whitney, D. L., Evans, B. W., 2010. Abbreviations for names of rock-forming minerals. American Mineralogist 95, 185-187.

Yamato, P., Agard, P., Burov, E., Le Pourhiet, L., Jolivet, L., Tiberi, C., 2007. Burial and exhumation in a subducting wedge: mutual constraints from thermomechanical modeling and natural P-T-t data (Sch.Lustrés, W. Alps). Journal of Geophysical Research 112, B07410.

Yamato, P., Burov, E., Agard, P., Le Pourhiet, L., Jolivet, L., 2008. HP-UHP exhumation during slow continental subduction: self-consistent thermodynamically and thermomechanically coupled model with application to the Western Alps. Earth and Planetary Science Letters 271, 63-74.

Zheng, Y., Chen, R., Xu, Z. and Zhang, S., 2016. The transport of water in subduction zones. Science China Earth Sciences, 59(4), pp.651-682.

FIGURE CAPTIONS

Figure 1. (A) Tectonic map of the north-eastern Corsica (modified after Vitale Brovarone et al., 2012) and schematic cross section (not to scale, after Di Rosa et al., 2017a). QtD: Quaternary deposits, SfB: Saint-Florent Basin, FcB: Francardo Basin, AlP: Aleria Plain, MaU: Macinaggio Unit, BoU: Bas-Ostriconi Unit, BaU: Balagne Unit, NeU: Nebbio Unit, SpU: Serra Debbione and Pineto Units, SlU: Santa Lucia Unit, CsU: Castagniccia Unit, MfU: Morteda-Farinole-Volpajola Unit, SoU: Serra di Pigno and Oletta Units, IZU: Inzecca and Lento Units, BrU: Bagliacone-Riventosa Unit, CeU: Centuri Unit, TeM: Tenda Massif, AnU: Annunciata Unit, EcU: External Continental Units, PdU: Cima Pedani Units, CoU: Caporalino Unit, HcY: Hercynian Corsica; the position of the Fig. 1B is marked in blue. (B) Tectonic sketch of the study area; the positions of the Fig. 2A, B are marked in black.

Figure 2. Geological map, cross section and stereographic projections of (A) Buttinacce (modified after Di Rosa et al., 2017b) and (B) IZU- Botro, where the relationships between the continental and oceanic units are highlighted. In the stereographic projections related to the D3 phase different colours are used for the data measured in the Lower Units (A3: blue, S3: red) and in the Schistes Lustrés Complex (A3: green; S3: yellow), to highlight that this deformation event affected uniformly the entire stack of units

Figure 3. D1-D2 phases (A-E) in the continental units and (F-H) in the oceanic units. (A) F1c sheath fold in the Metasandstone Fm., Piedigriggio-Prato Unit. (B) F2c isoclinal folds and related S2c axial plane foliation, Detritic Metalimestone Fm., Piedigriggio-Prato Unit. (C) S-C fabric in the Detritic Metalimestone Fm. in the Lower Units (CPU). (D) Relict of chlorite crystal grown during the D1c phase in the Metasandstone Fm., Castiglione-Popolasca Unit

(sample CM29A, parallel nicols); the S1c foliation is also shown. (E) S1c-S2c foliations interference pattern in the Metasandstone Fm., Castiglione-Popolasca Unit (sample CM29A, crossed nicols). (F) F2o subisoclinal folds in the calc-schists, Inzecca Unit; a subtle S3 foliation is also shown. (G) Relicts of S1o foliation within the S2o foliation in a pelitic layer in the calc-schists, Inzecca Unit (sample CMD121A, parallel nicols); the late S2o foliation is also shown. (H) Subgrain rotation (SR) recrystallization parallel to the S2 foliation in the F2o hinges zones, quartz veins in metabasalts, Inzecca Unit (sample CMD123A', crossed nicols).

Figure 4. Map-, meso and microphotographs of the D3 phase. (A) Landscape of Pietra Piana (NE of Monte Cecu): a slice of the Schistes Lustrés Complex (IZU) is sandwiched between the Lower Units (two subunits of PPU). Both the tectonic contacts are folded by the D3 phase. (B) Folded tectonic contact between the Lower Units (PPU) and the Schistes Lustrés Complex (IZU) in San Quilico hill, NE of Monte Cecu; the contact is cut by two post-D3 faults (CCSZ). (C) S2c-S3 foliations interference pattern in the Metasandstone Fm., PPU (sample CM23B, parallel nicols).

Figure 5. Binary and ternary diagrams showing the compositions of the Chl and Ph of the samples studied. The position of each colored rhombus in the diagrams is that of the average value calculated on 15 spot analysis. The position of the DT (di-trioctahedral) and TK (Tschermak) substitutions in the Al/Si diagram are calculated by Trincal and Lanari, 2016. Blue spots in the small ternary diagrams indicate the distribution of all the spot analysis acquired from the compositional map. Yellow triangles and DT and TK substitutions reported in the ternary diagrams are taken from Vidal and Parra, 2000.

Figure 6. Chemical analysis, compositional maps and the results of the analytical methods employed (Chl-Qz-wt, Ph-Qz-wt and Chl-Ph-Qz-wt multiequilibrium methods) for the study of the sample CM22B related to the Lower Units (A-B) and the sample CM121B related to the Schistes Lustrés Complex (C-D). In the binary plots and in the compositional maps (Si- and Al-content for Ph, Mg- and Al-content for Chl) of the samples (A) CM22B and (C) CMD121B, the Chl and the Ph types discussed in the text are noted by black arrows. The colored boxes in the P/T diagram represent the P-T equilibrium stability of the Chl-Ph couples (in (B): Early D1c, Late D1c and D2c; in (D): D1o, D2o and late D2o), tracked using the results of the Chl-Qz-wt method of Vidal et al., 2006 (histograms) and of the Ph-Qz-wt method of Dubacq et al., 2010 (blue, red and yellow lines). Black circles along the colored lines indicate the activity of the water (aH_2O). Stars indicate the P-T equilibria conditions of a single representative Chl-Ph couple (blue star for the early D1c and D1o, red star for the late D1c and D2o and yellow star for the D2c and late D2o) estimated with the Chl-Ph-Qz-wt multiequilibrium approach (Vidal and Parra, 2000). Details about the reactions related to these Chl-Ph couples are reported in the small P-T diagrams.

Figure 7. P-T paths of the samples studied. Colored boxes indicate the P-T ranges calculated with the Chl-Qz-wt and Ph-Qz-wt methods (average ranges were calculated in the case of more than one sample for the same unit). The paths (colored arrows) were drawn considering the best fit between the boxes and the P-T estimates obtained with the Chl-Ph-Qz-wt multiequilibrium method (average values were considered in the case of more than one sample for the same unit).

Figure 8. 2D sketch (not to scale) of a snapshot of the Corsica system at Late Eocene/Lower Oligocene time, showing the model proposed in this work for the mechanical coupling of the

Lower Units with the Schistes Lustrés Complex in the Corte area. In the main sketch the position the blue box evidences the position of the Lower Units as well as the Tenda massif at the plate interface; thick white and thin black arrows represent the last extensional event, thick black arrows indicate the kinematics at the boundaries of the plate interface and the blue box indicates the position of the zoom. The zoom shows a schematic representation of the path (i.e. the dotted orange line) made by the Lower Units at the plate interface and the geometry of the zone of mechanical coupling between the Lower Units and the slices of the Schistes Lustrés Complex (in the dotted box); black arrow indicates the subduction of the European crust. In the PT path, the three thick arrows represent three different stages of the unit deformation. Blue arrow indicates the underplating of the Lower Units up to the p-peak (i.e. early D1c). Green arrow indicates the first stage of exhumation from the early D1c phase to the D2c phase. During a later stage of exhumation (i.e. the late D2c phase), top-to-W shear zones are activated within the plate interface and along the roof decollement and produced the basal erosion of the Schistes Lustrés Complex that is exhumed as thin slices together with the Lower Units (yellow arrow). At the end of the D2 phase the Lower Units are located at the base of the Schistes Lustrés Complex (the tectonic contact is indicated by a thick black line in the zoom). The last stage of exhumation deformed this unit pile in an extensional regime (i.e. the D3 phase). In the PT diagram, the path of CPU (orange), PPU (red), IZU-Botro (green) and IZU-Buttinacce (blue) is drown (simplified version of Fig. 7).

Tab. 1 Chemical ranges and end-members proportions of Chl and Ph related to each metamorphic assemblage.

Tab. 2 Representative electron microprobe analysis of the Chl-Ph pairs selected in the samples of metapelites.

Tab. 3 P-T estimates for the three generations of Chl-Ph pairs in the 5 studied units. P-T estimates of CPU and PPU are after Di Rosa et al. (2019a). The results (Chl-Ph 1st, 2nd and 3rd generation) obtained with the Chl-Ph-Qz-wt multiequilibrium approach (Vidal and Parra, 2000) are compared with those calculated with the Chl-Qz-wt (Vidal et al., 2006) and Ph-Qz-wt (Dubacq et al., 2010) methods (T and P range, respectively) and with classical geothermometers and geobarometers (P and T max).

Figure 1

Click here to download high resolution image

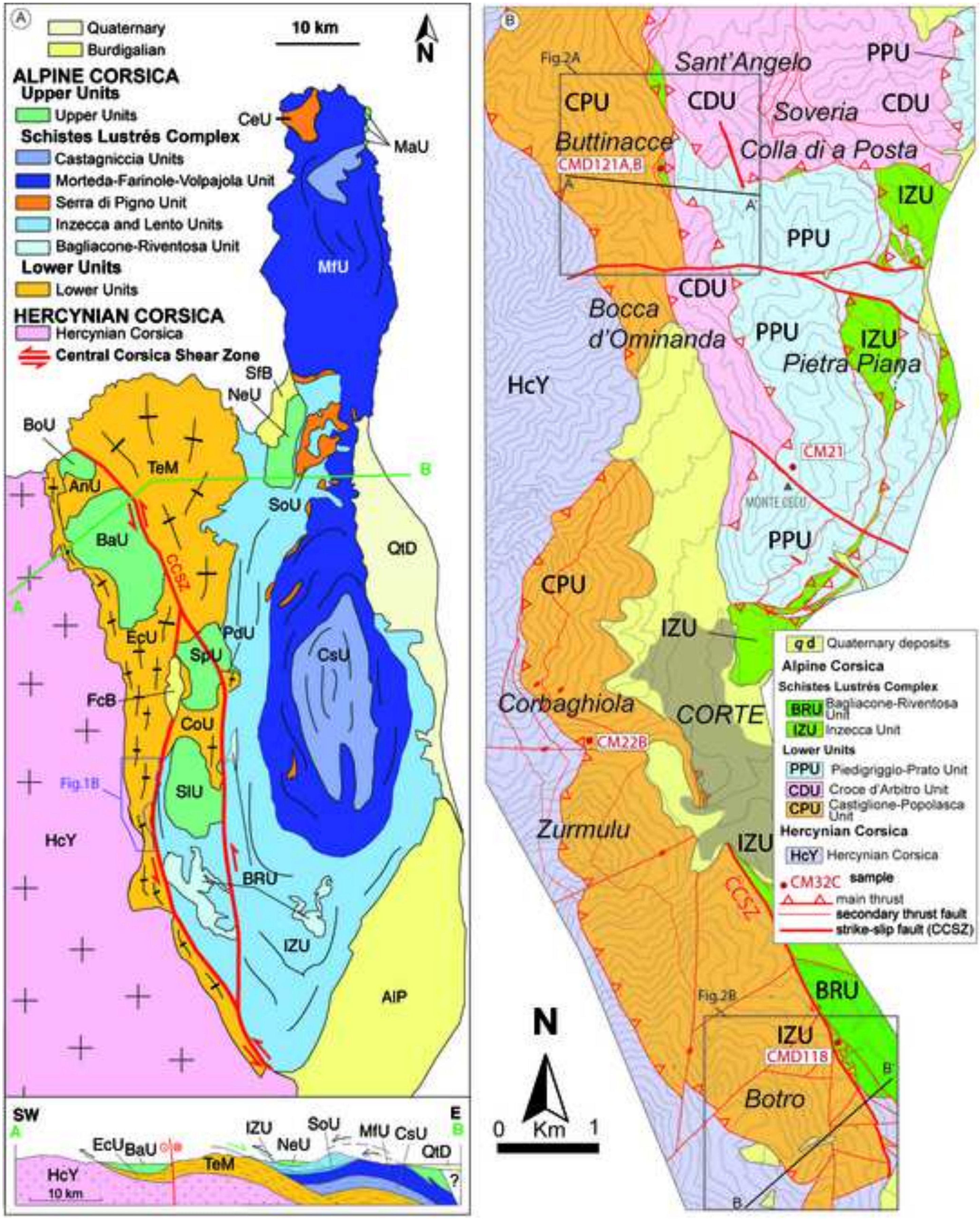

Figure 2A

Click here to download high resolution image

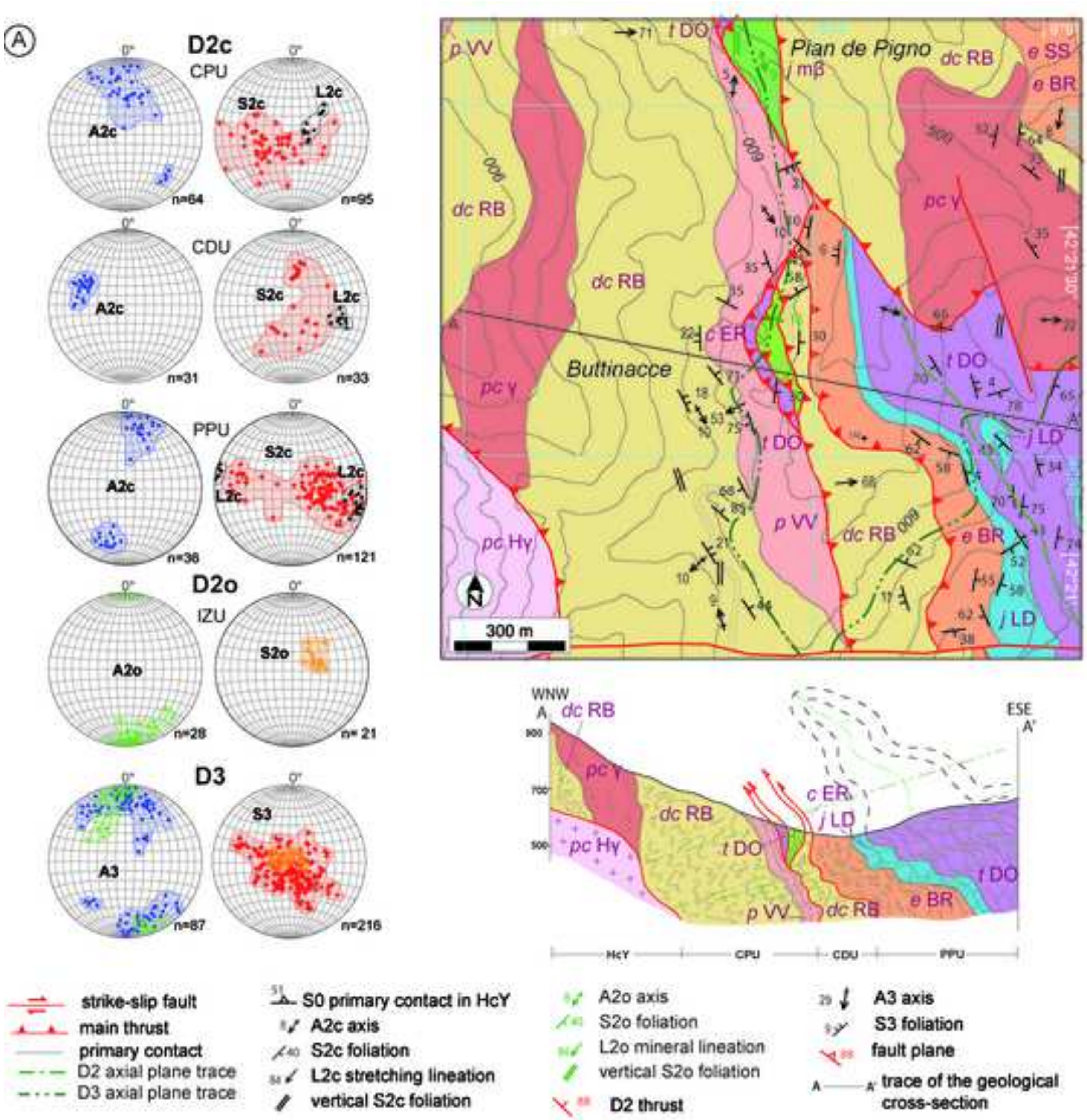

Figure 2B
Click here to download high resolution image

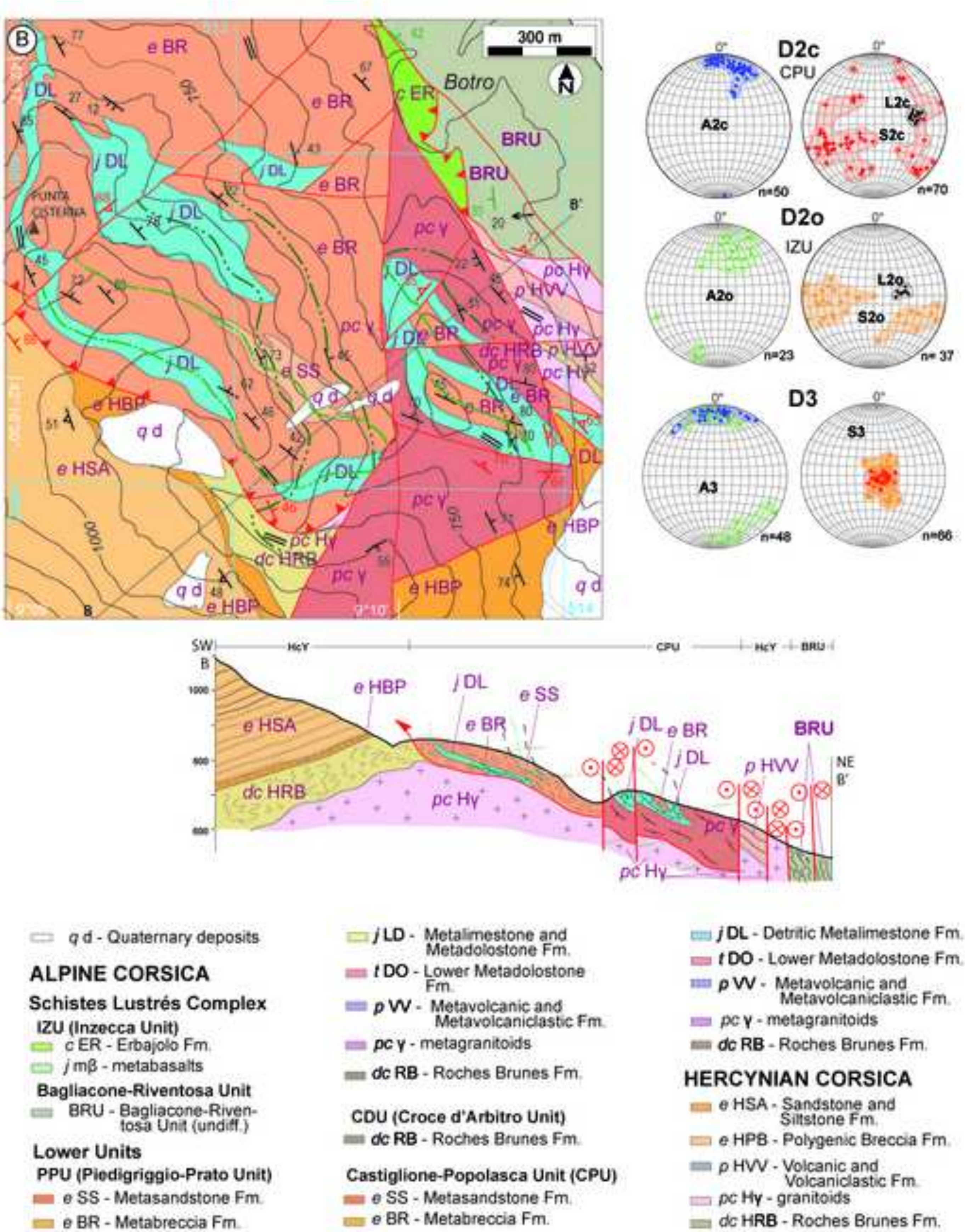

Figure 3

Click here to download high resolution image

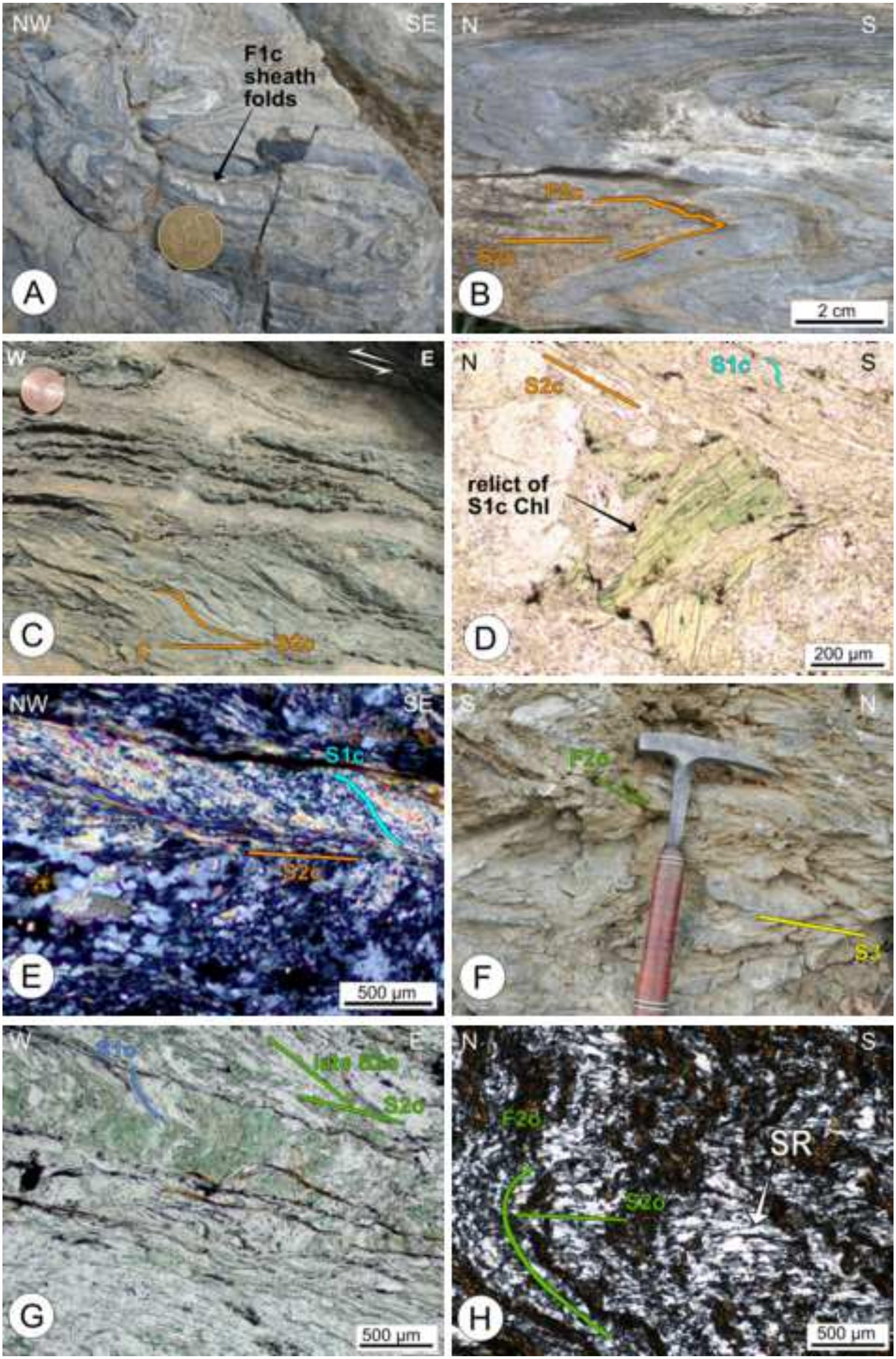

Figure 4
Click here to download high resolution image

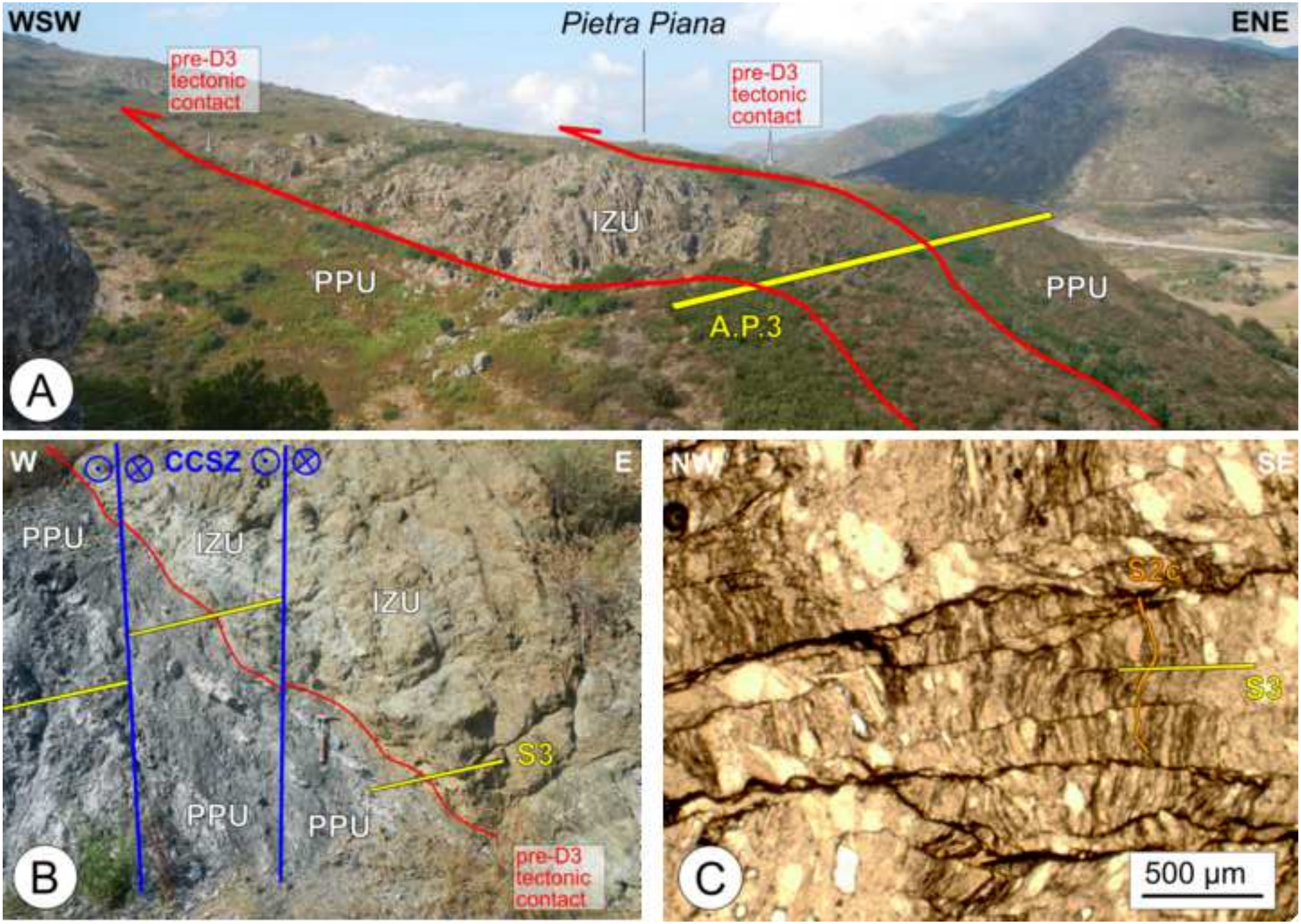

Figure 5

Click here to download high resolution image

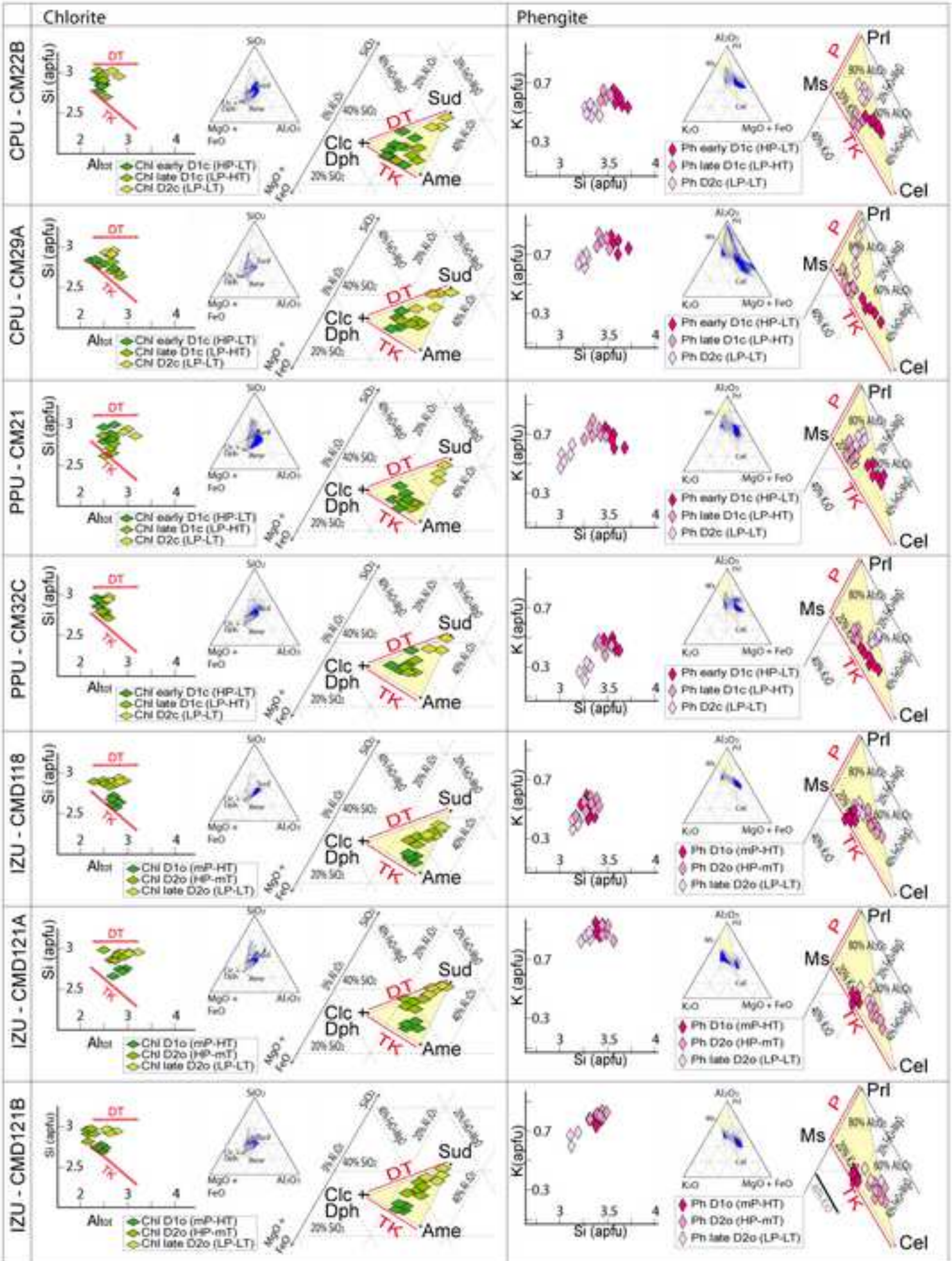

Figure 6AB

Click here to download high resolution image

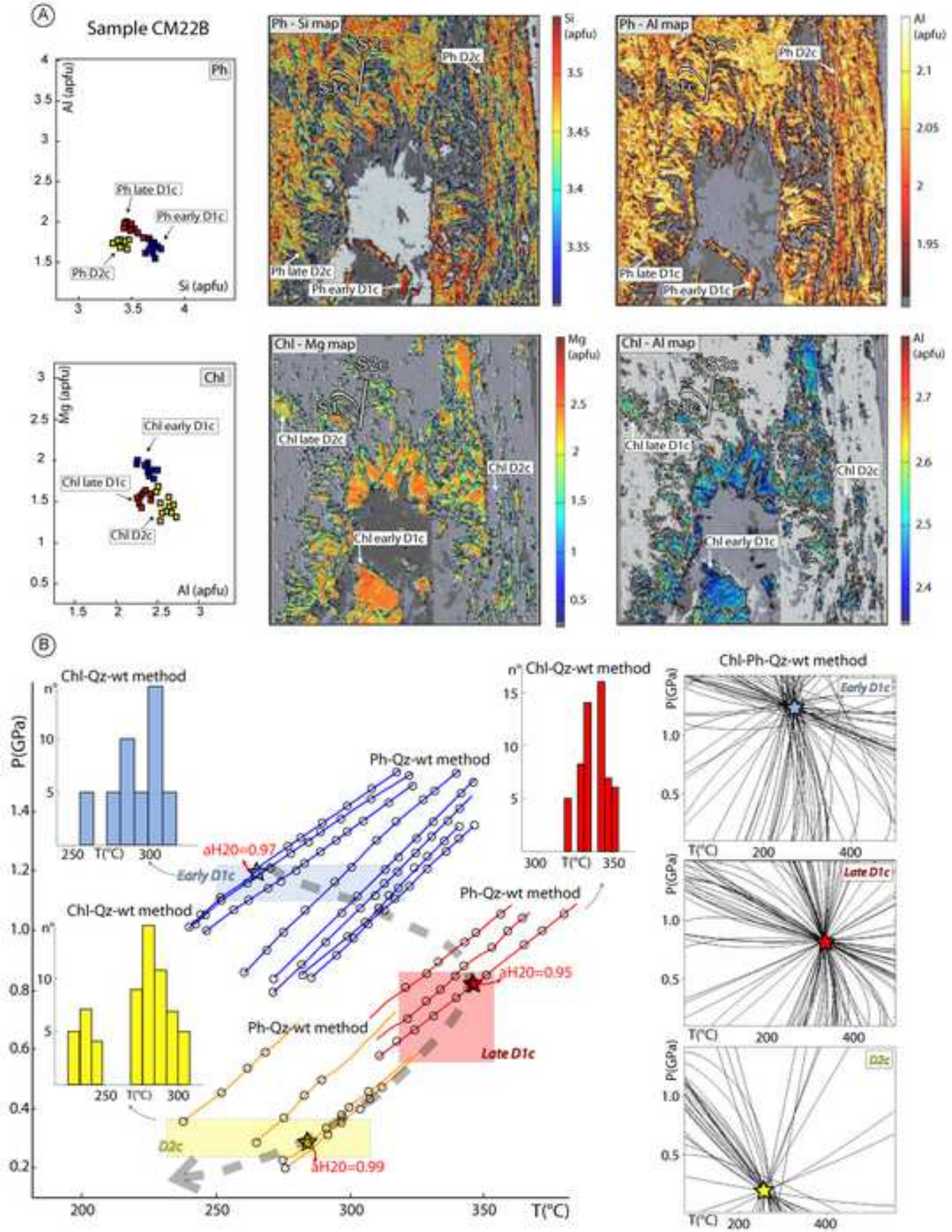

Figure 6CD

Click here to download high resolution image

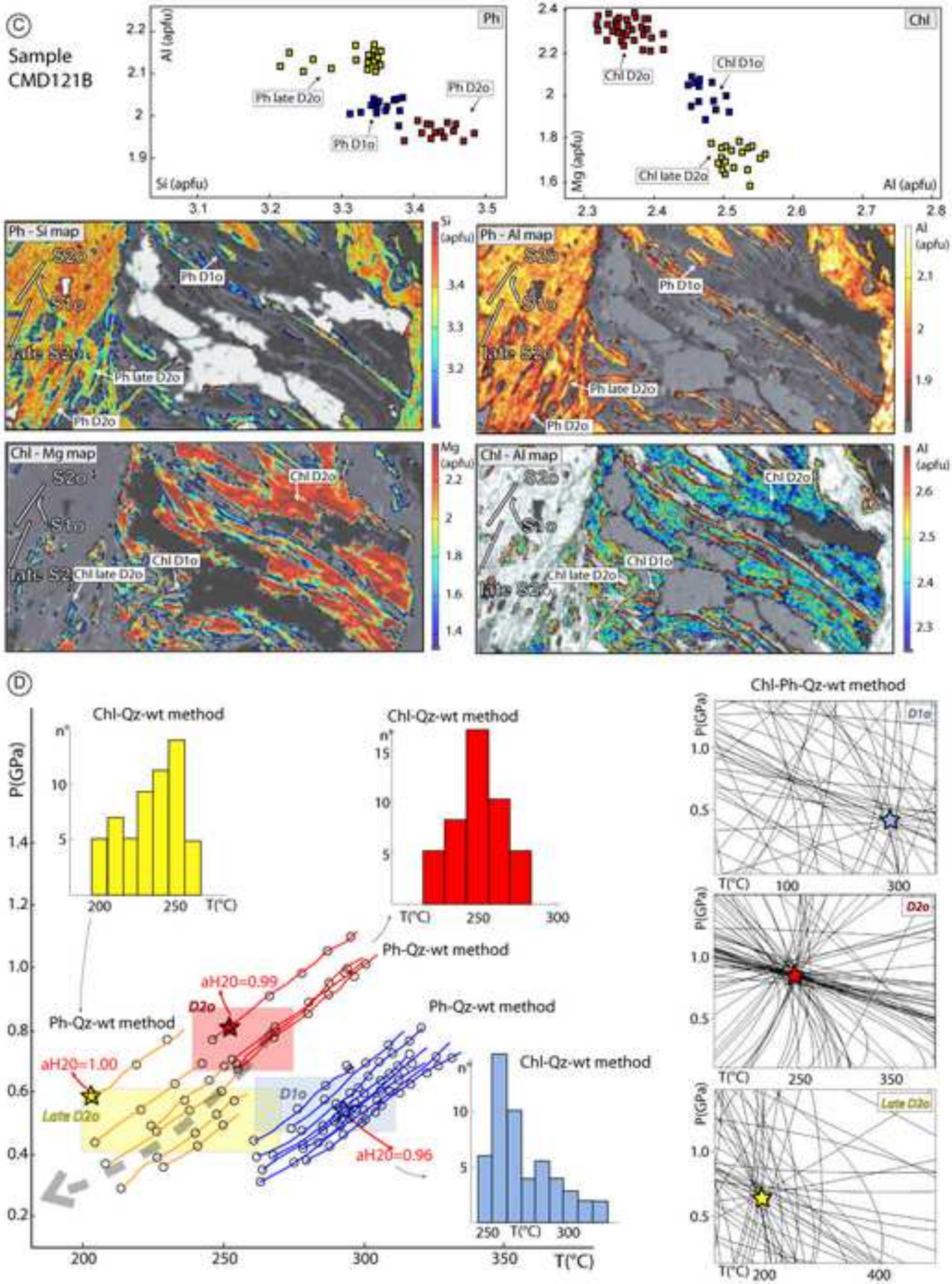

Figure 7
Click here to download high resolution image

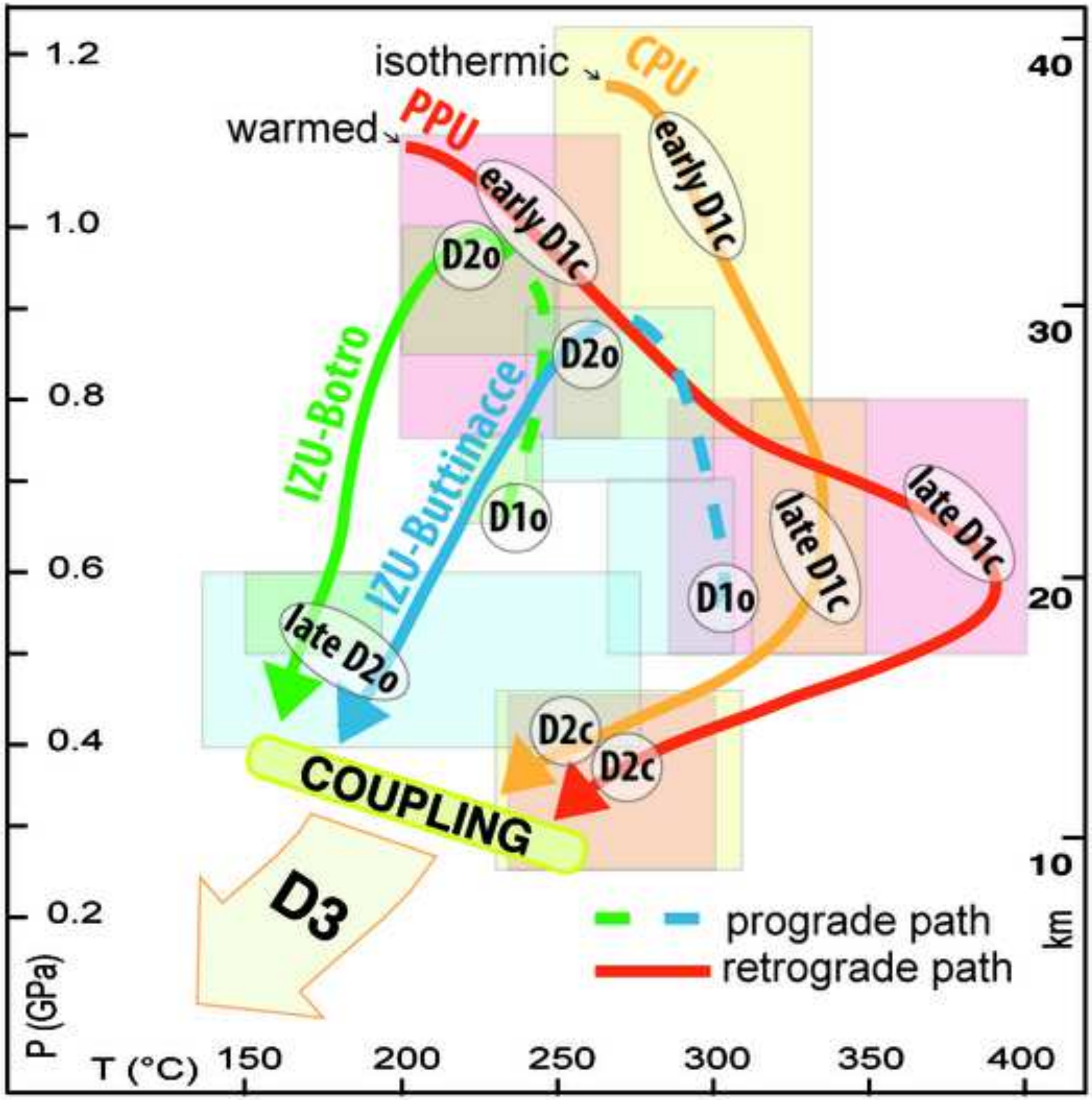

Figure 8
Click here to download high resolution image

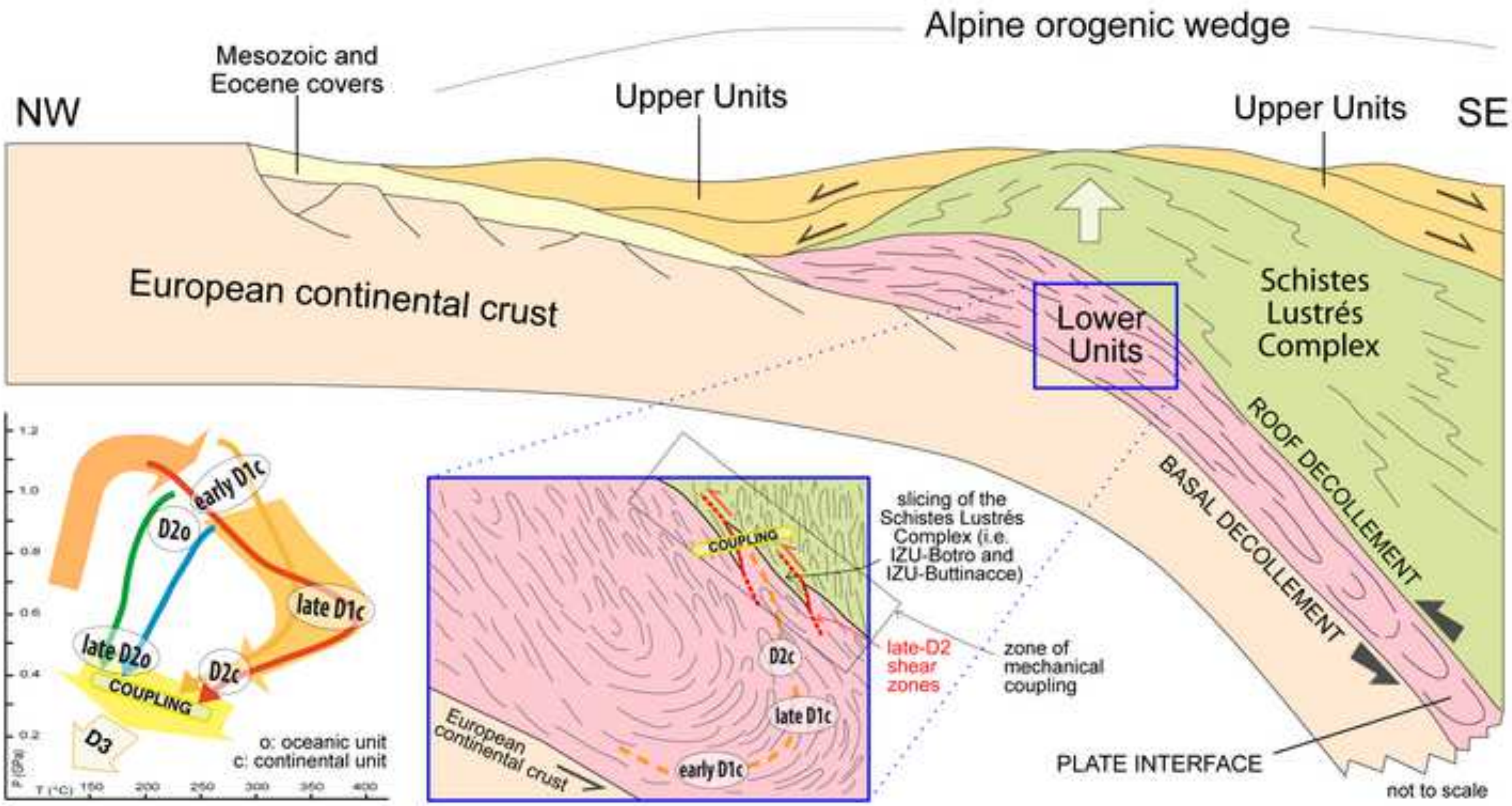

Tables

Click here to download Table: TabLITHOSREV28ago19.docx

Tab. 1 Chemical ranges and end-members proportions of Chl and Ph related to each metamorphic assemblage.

Chlorite							
Sample		**Si (apfu)**	**Al_{tot} (apfu)**	**XMg**	**Ame (%)**	**Clc+Dph (%)**	**Sud (%)**
CM22B	**early D1c**	2.72-3.00	2.25-2.51	0.35-0,43	0%-25%	75%-85%	0%-20%
	late D1c	2.65-2.92	2.35-2.78	0.37-0.40	20%-30%	65%-80%	0%-20%
	D2c	2.88-3.00	2.15-2.80	0.39-0.42	0%-10%	60%-70%	35%-40%
CM29A	**early D1c**	2.66-2.80	2.22-2.73	0.20-0.42	5%-25%	80%-95%	10%-35%
	late D1c	2.59-2.77	2.51-2.86	0.18-0.34	20%-35%	70%-80%	0%-20%
	D2c	2.79-2.95	2.55-2.69	0.15-0.32	0%-15%	60%-75%	0%-20%
CM21	**early D1c**	2.75-2.92	2.38-2.76	0.29-0.42	5%-25%	70%-80%	0%-20%
	late D1c	2.58-2.93	2.38-2.75	0.35-0.43	20%-30%	70%-75%	5%-15%
	D2c	2.76-3.06	2.50-3.05	0.33-0.40	0%-10%	65%-75%	15%-35%
CM32C	**early D1c**	2.78-2.96	2.35-2.49	0.48-0.54	0%-15%	80%-90%	10%-25%
	late D1c	2.60-2.88	2.45-2.56	0.41-0.45	10%-30%	75%-85%	15%-20%
	D2c	2.90-2.96	2.55-2.59	0.32-0.46	0%-10%	70%-80%	25%-30%
CMD118	**D1o**	2.53-2.92	2.30-2.84	0.44-0.47	10%-40%	65%-70%	0%-15%
	D2o	2.80-2.92	2.25-2.90	0.43-0.44	0%-25%	60%-70%	20%-35%
	late D2o	2.83-2.95	2.58-2.98	0.43-0.45	0%-20%	55%-60%	30%-40%
CMD121A	**D1o**	2.60-2.76	2.51-2.98	0.50-0.52	15%-25%	75%-85%	0%-10%
	D2o	2.84-2.98	2.46-2.97	0.48-0.50	0%-10%	80%-85%	10%-20%
	late D2o	2.88-2.93	2.70-3.10	0.47-0.51	0%-5%	70%-75%	20%-30%
CMD121B	**D1o**	2.61-2.78	2.46-2.55	0.52-0.55	0%-10%	75%-90%	0%-10%
	D2o	2.76-2.98	2.33-2.48	0.48-0.52	5%-25%	70%-90%	10%-20%
	late D2o	2.80-2.96	2.45-2.56	0.47-0.52	10%-30%	65%-80%	20%-30%

Phengite							
Sample		**Si (apfu)**	**K (apfu)**	**Al_{tot} (apfu)**	**Cel (%)**	**Ms (%)**	**Prl (%)**
CM22B	**early D1c**	3.62-3.80	0.49-0.68	1.55-1.80	40%-50%	30%-45%	15%-30%
	late D1c	3.41-3.68	0.52-0.70	1.72-2.20	40%-45%	50%-60%	10%-15%
	D2c	3.36-3.77	0.43-0.79	1.68-2.10	30%-40%	35%-55%	20%-40%
CM29A	**early D1c**	3.53-3.71	0.70-0.81	1.90-2-04	45%-60%	30%-35%	15%-20%
	late D1c	3.32-3.55	0.77-0.85	1.95-2.14	35%-45%	35%-50%	10%-20%
	D2c	3.24-3.38	0.62-0.72	2.02-2.12	30%-40%	30%-40%	20%-25%
CM21	**early D1c**	3.25-3.70	0.59-0.80	2.05-2.53	30%-40%	40%-50%	15%-25%
	late D1c	3.30-3.62	0.66-0.82	1.97-2.45	25%-30%	45%-60%	10%-20%
	D2c	3.40-3.72	0.48-0.69	2.08-2.20	25%-30%	50%-65%	20%-30%
CM32C	**early D1c**	3.45-3.61	0.42-0.50	2.00-2.14	40%-55%	30%-50%	10%-30%
	late D1c	3.30-3.47	0.36-0.48	1.95-2.15	30%-35%	45%-55%	15%-35%
	D2c	3.20-3.29	0.22-0.38	1.95-2.03	35%-45%	25%-35%	10%-40%
CMD118	**D1o**	3.23-3.42	0.42-0.92	2.18-2.27	25%-35%	55%-65%	5%-15%
	D2o	3.15-3.48	0.48-0.70	2.12-2.24	30%-45%	40%-50%	15%-25%
	late D2o	3.18-3.24	0.34-0.76	2.30-2.35	25%-35%	50%-60%	10%-20%
CMD121A	**D1o**	3.38-3.49	0.76-0.84	1.85-2.05	30%-40%	60%-65%	0%-10%
	D2o	3.40-3.53	0.74-0.82	1.80-1.94	45%-55%	50%-55%	10%-20%
	late D2o	3.23-3.28	0.75-0.78	2.01-2.14	30%-45%	50%-60%	10%-25%
CMD121B	**D1o**	3.20-3.38	0.71-0.84	1.97-2.03	35%-40%	45%-60%	5%-10%
	D2o	3.29-3.49	0.73-0.86	1.95-1.99	40%-60%	35%-45%	10%-20%
	late D2o	3.22-3.36	0.62-0.89	2.10-2.16	35%-55%	35%-50%	10%-20%

Tab.2 Representative electron microprobe analysis of the Chl-Ph pairs selected in the samples of metapelites.

Sample	**Schistes Lustrés Complex - Botro (CMD118)**						**Schistes Lustrés Complex - Buttinacce (CMD121B)**					
Domain	S1o		S2o		Late S2o		S1o		S2o		Late S2o	
Analyse	*Chl27*	*Ph20*	*Chl65*	*Ph10*	*Chl64*	*Ph23*	*Chl38*	*Ph2*	*Chl8*	*Ph6*	*Chl12*	*Ph1*
Wt%												
SiO_2	27.95	50.07	28.05	44.02	28.65	46.87	25.91	48.29	26.20	48.08	26.41	48.09
TiO_2	0.02	0.09	0.02	0.08	0.02	0.09	0.02	0.14	0.01	0.14	0.02	0.16
Al_2O_3	18.80	29.92	23.95	26.70	22.87	27.75	19.57	31.32	19.38	28.65	19.45	29.89
FeO	25.99	2.10	25.91	6.64	25.22	5.60	25.28	2.40	25.71	2.96	25.64	2.95
MnO	0.15	0.02	0.09	0.02	0.09	0.01	0.70	0.04	0.72	0.06	0.70	0.04
MgO	16.13	2.91	11.11	4.43	11.49	4.00	15.05	2.71	13.71	2.97	13.83	2.92
CaO	0.03	0.02	0.03	0.02	0.03	0.02	0.07	0.05	0.09	0.05	0.09	0.07
Na_2O	0.03	0.09	0.03	0.09	0.04	0.11	0.04	0.13	0.08	0.12	0.07	0.14
K_2O	0.06	10.31	0.22	7.90	0.21	8.24	0.33	9.66	0.27	9.73	0.27	9.59
tot.	89.16	95.54	89.41	89.34	88.62	92.69	86.99	94.74	86.17	92.76	86.48	93.85
Cations												
Si	2.90	3.32	2.87	3.18	2.94	3.24	2.77	3.23	2.83	3.30	2.84	3.27
Ti	-	-	-	-	-	0.01	-	0.01	-	0.01	-	0.01
Al	2.30	2.34	2.89	2.27	2.77	2.26	2.47	2.47	2.47	2.32	2.46	2.39
Fe^{2+}	2.25	0.12	2.22	0.40	2.17	0.32	2.26	0.13	2.32	0.17	2.31	0.17
Mn	0.01	-	0.01	-	0.01	-	0.06	-	0.07	-	0.06	-
Mg	2.49	0.29	1.69	0.48	1.76	0.41	2.40	0.27	2.21	0.30	2.22	0.30
Ca	-	-	-	-	-	-	0.01	-	0.01	-	0.01	0,01
Na	0.01	0.01	0.01	0.01	0,01	0.02	0,01	0.02	0.02	0.02	0.02	0.02
K	0.01	0.87	0.03	0.67	0.03	0.73	0.05	0.82	0.04	0.85	0.04	0.83
sum ox	14	11	14	11	14	11	14	11	14	11	14	11

Sample	**Lower Units - CPU (CM22B)**						**Lower Units - PPU (CM21)**					
Domain	S1c (P-peak)		S1c (T-peak)		S2c		S1c (P-peak)		S1c (T-peak)		S2c	
Analyse	*Chl 757*	*Ph 269*	*Chl 856*	*Ph 55*	*Chl 26*	*Ph 136*	*Chl 31*	*Ph 18*	*Chl 18*	*Ph 13*	*Chl 12*	*Ph 5*
Wt%												
SiO_2	25.77	50.81	27.22	52.92	28.14	45.36	28.27	48.40	25.58	50.22	30.67	55.27
TiO_2	0.03	0,27	0.03	0.18	0.03	0.23	0.02	0.11	0.03	0.12	0.03	0.21
Al_2O_3	19.68	20.86	22.35	28.77	19.51	22.06	22.61	30.56	20.98	29.77	23.67	28.36
FeO	24.47	4.30	23.58	3.48	24.85	4.19	22.54	3.31	26.91	3.06	19.87	3.48
MnO	0.42	0.02	0.36	0.03	0.36	0.04	0.04	2.29	0.03	2.27	0.03	0.03
MgO	14.94	3.17	13.21	3.65	15.15	2.69	13.99	0.03	13.36	0.03	13.19	3.62
CaO	0.01	0.04	0.01	0.01	0.01	0.03	0.04	0.01	0.04	0.01	0.03	0.02
Na_2O	0.02	0.17	0.02	0.03	0.02	0.07	0.05	0.14	0.05	0.15	0.05	0.04
K_2O	0.05	7.13	0.02	8.21	0.02	7.90	0.68	8.98	0.06	9.01	1.12	8.29
tot.	85.39	86.77	86.8	97.28	88.09	82.57	88.24	93.83	87.04	94.64	88.66	99.32
Cations												
Si	2.79	3.68	2.85	3.41	2.93	3.50	2.89	3.29	2.73	3.38	3.06	3.48
Ti	-	0.02	-	0,01	-	0.01	-	-	-	0.01	-	0.01
Al	2.51	1,78	2.76	2.19	2.39	2.00	2.73	2.45	2.65	2.36	2.78	2.11
Fe^{2+}	2.21	0.26	2.06	0.19	2.16	0.27	1.93	0.19	2.41	0.17	1.66	0.18
Mn	0.04	-	0.03	-	0.03	-	-	0.13	-	0.13	-	-
Mg	2.41	0.34	2.06	0.35	2.35	0.31	2.13	-	2.13	-	1.96	0,34
Ca	-	-	-	-	-	-	-	0.01	0.01	-	-	-
Na	-	0,02	-	-	-	-	0.01	0.02	0.01	0.02	0.01	0.01
K	0.01	0.66	-	0,68	-	0.77	0.09	0.78	0.01	0.77	0.14	0,66
sum ox	14	11	14	11	14	11	14	11	14	11	14	11

- : below deection limit

Tab. 3 P-T estimates for the three generations of Chl-Ph pairs in the 5 studied units. P-T estimates of CPU and PPU are after Di Rosa et al. (2019b). The results (Chl-Ph 1st, 2nd and 3rd generation) obtained with the Chl-Ph-Qz-wt method (Vidal and Parra, 2000) are compared with those calculated with the Chl-Qz-wt (Vidal et al., 2006) and Ph-Qz-wt (Dubacq et al., 2010) methods (T and P range, respectively) and with classical geothermometers and geobarometers (T max and Lowest P conditions related to the P-peak).

		P-T estimates (Vidal and Parra, 2000)						**T range** (Vidal et al., 2006)			**P range** (Dubacq et al., 2010)			**T max**	**Lowest P conditions related to the P-peak** (Massonne and Schreyer, 1987)
		D1c PHASE				**D2c PHASE**									
		Early D1c Chl-Ph		Late D1c Chl-Ph		D2c Chl-Ph		Early D1c Chl	Late D1c Chl	D2c Chl	Early D1c Ph	Late D1c Ph	D2c Ph		
		T (°C)	**P (GPa)**	**T (°C)**	**P (GPa)**	**T (°C)**	**P (GPa)**	**T (°C)**	**T (°C)**	**T (°C)**	**P (GPa)**	**P (GPa)**	**P (GPa)**	**T (°C)**	**P (GPa)**
Lower Units	CM22B (CPU)	250-330	1.20-1.10	320-350	0.80-0.55	230-310	0.35-0.25	250-310	320-350	230-310	1.20-1.05	0.85-0.50	0.35-0.25	350 (Lanari et al., 2014a)	1.25
	CM29A (CPU)	250-330	1.10-0.75	320-345	0.65-0.50	250-310	0.45-0.25	250-300	315-340	260-320	1.10-0.80	0.5-0.65	0.30-0.50	320 (Cathelineau and Nieva, 1985)	1.30
	CM21 (PPU)	200-240	1.05-0.75	340-400	0.80-0.50	240-300	0.40-0.25	200-235	350-385	195-230	1.00-0.80	0.55-0.80	0.35-0.40	345 (Lanari et al., 2014a)	1.20
	CM32 (PPU)	250-270	1.10-1.00	280-390	0.80-0.65	230-270	0.45-0.25	250-300	300-370	225-270	1.10-1.00	0.70-0.85	0.30-0.45	320 (Cathelineau, 1988)	1.26
		D1o PHASE		**D2o PHASE**				**T range** (Vidal et al., 2006)			**P range** (Dubacq et al., 2010)			**T max**	**Lowest P conditions related to the P-peak** (Massonne and Schreyer, 1987)
		D1o Chl-Ph		D2o Chl-Ph		Late D2o Chl-Ph		D1o Chl-	D2o Chl-	Late D2o Chl	D1o Ph	D2o Ph	Late D2o Ph		
		T (°C)	**P (GPa)**	**T (°C)**	**P (GPa)**	**T (°C)**	**P (GPa)**	**T (°C)**	**T (°C)**	**T (°C)**	**P (GPa)**	**P (GPa)**	**P (GPa)**	**T (°C)**	**P (GPa)**
Schistes Lustrés Complex	CMD118 (IZU-Botro)	220-245-	0.65-0.75	200-250	1.00-0.85	150-190	0.60-0.50	220-240	205-240	150-175	0.60-0.75	1.00-0.90	0.50-0.60	340 (Cathelineau and Nieva, 1985)	1.10
	CMD121A (IZU-Buttinacce)	270-290	0.50-0.70	245-300	0.90-0.75	140-215	0.50-0.45	275-305	250-310	160-200	0.55-0.70	0.75-0.90	0.45-0.65	335 (Lanari et al., 2014a)	1.15
	CMD121B (IZU-Buttinacce)	265-310	0.55-0.65	240-275	0.85-0.70	200-275	0.60-0.40	265-320	220-280	200-270	0.45-0.60	0.85-0.65	0.60-0.40	325 (Lanari et al, 2014a)	1.00